GRAPHENE 2011

INDEX: INVITED CONTRIBUTIONS

INDEX: KEYNOTE CONTRIBUTIONS

INDEX: ORAL CONTRIBUTIONS

ALPHABETICAL ORDER

I: Invited / K: Keynote / O: Oral

I: Invited / K: Keynote / O: Oral

I: Invited / K: Keynote / O: Oral

GRAPHENE 2011

ABSTRACTS
ALPHABETICAL ORDER

GRAPHENE-BASED ELECTRONICS AND OPTOELECTRONICS

Phaedon Avouris

T. J. Watson Research Center, Yorktown Heights, NY 10598, USA
avouris@us.ibm.com

Graphene a two-dimensional, single atomic layer material with linear electron dispersion has rather unique electrical and properties [1]. There is currently strong interest in taking advantage of these properties for technological applications [2]. In my talk I will review the key properties of graphene, how these are affected by environmental interactions and how they can be utilized in electronics and optoelectronics.

Specifically, I will discuss high frequency (>100 GHz) graphene transistors [3], their fabrication and operation, as well as related device physics aspects, such as transport mechanisms, contacts, temperature effects, dissipation, etc. Simple integrated graphene circuits will also be presented. I will then discuss key optical properties of graphene and how they can be combined with its excellent electrical properties and used in optoelectronics applications. Specific examples involving ultrafast graphene photodetectors [4] and their applications in optical data detection[5] will be presented.

References:

[1] Geim, A.K. Science 3, 1530 (2009).
[2] Avouris, Ph., Nano Lett. 10, 4285 (2010).
[3] Lin, Y.-M.; Dimitrakopoulos, C.; Jenkins, K.A.; Farmer, D.B., Chiu, H.-Y. ; Grill, A.; Avouris, Ph. Science 327, 662 (2010); Wu , Y. et al., to be published.
[4] Xia, F.; Mueller, T.; Lin, Y.-M.; Valdes-Garcia, A.; Avouris, Ph. Nature Nano 4, 839 (2009).
[5] Mueller, T.; Xia, F.; Avouris, Ph. Nature Photon. 4, 297 (2010).

NANOELECTROMECHANICAL RESONATORS BASED ON GRAPHENE

Adrian Bachtold

ICN, CIN2, Campus UABarcelona, Bellaterra, Spain
adrian.bachtold@cin2.es

The theory of damping finds its roots in Newton's Principia and has been exhaustively tested in objects as disparate as the Foucault pendulum, mirrors used in gravitational-wave detectors, and submicron mechanical resonators. Owing to recent advances in nanotechnology it is now possible to explore damping in systems with transverse dimensions on the atomic scale. Here, we study the damping of mechanical resonators based on a graphene sheet, the ultimate two-dimensional nanoelectromechanical systems (NEMS). The damping is found to strongly depend on the amplitude of the motion; it is well described by a nonlinear force $\eta x^2 \dot{x}$ (with x the deflection and $\dot{x}$ its time derivative). This is in stark contrast to the linear damping paradigm valid for larger mechanical resonators. Besides, we exploit the nonlinear nature of the damping to improve the figure of merit of graphene resonators.

TWO-DIMENSIONAL THERMAL TRANSPORT IN GRAPHENE: INTRINSIC VS. EXTRINSIC EFFECTS

Alexander A. Balandin

Nano-Device Laboratory, Department of Electrical Engineering and Materials Science and Engineering Program, Bourns College of Engineering, Univ. of California, Riverside, CA 92521 USA
balandin@ee.ucr.edu

Recent years witnessed a rapid growth of interest of the scientific and engineering communities to thermal properties of materials. The increasing importance of thermal properties is explained both by practical needs and fundamental science. Heat removal has become a crucial issue for continuing progress in electronic industry [1]. The knowledge of how well and how fast the material conducts heat becomes essential for design of the next generation of integrated circuits. From another side, efficient thermoelectric energy conversion requires finding materials, which simultaneously have high electrical conductivity but strongly suppressed thermal conductivity *K*. Material's ability to conduct heat is deeply rooted in its atomic structure, and knowledge of thermal properties can shed light on many other materials' characteristics. Thermal conductivity of materials changes when they are structured on a nanometer scale. The latter can happen because of the intrinsic effects, e.g. phonon dispersion and velocities of the low-dimensional crystal differ from those in bulk [2], or extrinsic effects such as increased phonon - rough boundary scattering when the feature size of nanostructure becomes comparable to that of the phonon mean free path (MFP) in a given material [3]. Other extrinsic effects on thermal conductivity include strain in the lattice and phonon scattering on lattice defects or impurities.

The discovery of graphene [4-5] further stimulated the interest to thermal properties because, for the first time, it became possible to study experimentally heat conduction in strictly 2D crystals. The heat conduction in 2D crystals is particularly intriguing because of the theoretically predicted logarithmic divergence of thermal conductivity *K* with the size of 2D crystal [6-7]. The *K* divergence in 2D crystals means that unlike in 3D bulk, the crystal lattice anharmonicity along is not sufficient for restoring thermal equilibrium, and one needs to either limit the system size or introduce disorder to have the physically meaningful finite value of *K*. To elucidate the physics of heat conduction in graphene, it is important to determine whether thermal transport is mostly limited by the *intrinsic* properties, e.g. by the dimensionality of the lattice and its dynamics, or by the *extrinsic* effects, e.g. phonon scattering from rough interfaces, edges, defects and impurities or graphene – substrate interactions. Heat conduction in the suspended graphene will be closer to the intrinsic phonon transport regime while that in the encased graphene will be closer to the extrinsic transport regime. The first experimental study of the evolution of heat conduction in few-layer graphene (FLG), found that *K* of suspended uncapped FLG, which is the highest in the single-layer graphene (SLG), decreases with increasing number of the atomic planes *n*, and approaches the bulk graphite limit (see Figure 1a) [8]. For comparison, the thickness dependence of thermal conductivity of the encased disordered carbon films is also shown [9].

Recent years witnessed a rapid growth of interest of the scientific and engineering communities to thermal properties of materials. The increasing importance of thermal properties is explained both by practical needs and fundamental science. Heat removal has become a crucial issue for continuing progress in electronic industry [1]. The knowledge of how well and how fast the material conducts heat becomes essential for design of the next generation of integrated circuits. From another side, efficient thermoelectric energy conversion requires finding materials, which simultaneously have high electrical conductivity but strongly suppressed thermal conductivity *K*. Material's ability to conduct heat is deeply rooted in its atomic structure, and knowledge of thermal properties can shed light on many other materials' characteristics. Thermal conductivity of materials changes when they are structured on a nanometer scale. The latter can happen because of the intrinsic effects, e.g. phonon dispersion and velocities of the low-dimensional crystal differ from those in bulk [2], or extrinsic effects such as increased phonon - rough boundary scattering when the feature size of nanostructure becomes comparable to that of the phonon mean free path (MFP) in a given material [3]. Other extrinsic effects on thermal conductivity include strain in the lattice and phonon scattering on lattice defects or impurities.

The discovery of graphene [4-5] further stimulated the interest to thermal properties because, for the first time, it became possible to study experimentally heat conduction in strictly 2D crystals. The heat conduction in 2D crystals is particularly intriguing because of the theoretically predicted logarithmic divergence of thermal conductivity *K* with the size of 2D crystal [6-7]. The *K* divergence in 2D crystals means that unlike in 3D bulk, the crystal lattice anharmonicity along is not sufficient for restoring thermal equilibrium, and one needs to either limit the system size or introduce disorder to have the physically meaningful finite value of *K*. To elucidate the physics of heat conduction in graphene, it is important to determine whether thermal transport is mostly limited by the *intrinsic* properties, e.g. by the dimensionality of the lattice and its dynamics, or by the *extrinsic* effects, e.g. phonon scattering from rough interfaces, edges, defects and impurities or graphene – substrate interactions. Heat conduction in the suspended graphene will be closer to the intrinsic phonon transport regime while that in the encased graphene will be closer to the extrinsic transport regime. The first experimental study of the evolution of heat conduction in few-layer graphene (FLG), found that *K* of suspended uncapped FLG, which is the highest in the single-layer graphene (SLG), decreases with increasing number of the atomic planes *n*, and approaches the bulk graphite limit (see Figure 1a) [8]. For comparison, the thickness dependence of thermal conductivity of the encased disordered carbon films is also shown [9].

Acknowledgements:

This work was supported, in part, by U.S. ONR award N00014-10-1-0224, SRC-DARPA FCRP Center on Functional Engineered Nano Architectonics (FENA) and DARPA Defense Microelectronics Activity (DMEA) award H94003-10-2-1003. The author thanks S. Roche, A. Geim and K. Novoselov for useful discussions.

References:

[1] C. Lin and K. Banerjee, IEEE Trans. Electron Dev., 55, 245 (2008).
[2] A. Balandin and K.L. Wang, Phys. Rev. B, 58, 1544 (1998).
[3] T. Borca-Tasciuc, *et al*., Microscale Thermophys. Eng., 5, 225 (2001).
[4] K.S. Novoselov, A.K. Geim, *et al*., Science, 306, 666 (2004).
[5] A.K. Geim and K.S. Novoselov, Nature Mater., 6, 183 (2007).
[6] For a review, see S. Lepri, *et al*., Phys. Rep. 377, 1 (2003) and references therein.
[7] K. Saito and A. Dhar, Phys. Rev. Lett., 104, 040601 (2010).
[8] S. Ghosh, *et al*., Nature Materials, 9, 555 (2010).
[9] A.A. Balandin, *et al*., Appl. Phys. Lett., 93, 043115 (2008).
[10] W. Jang, *et al*., Nano Lett., 10, 3909 (2010).

Figures:

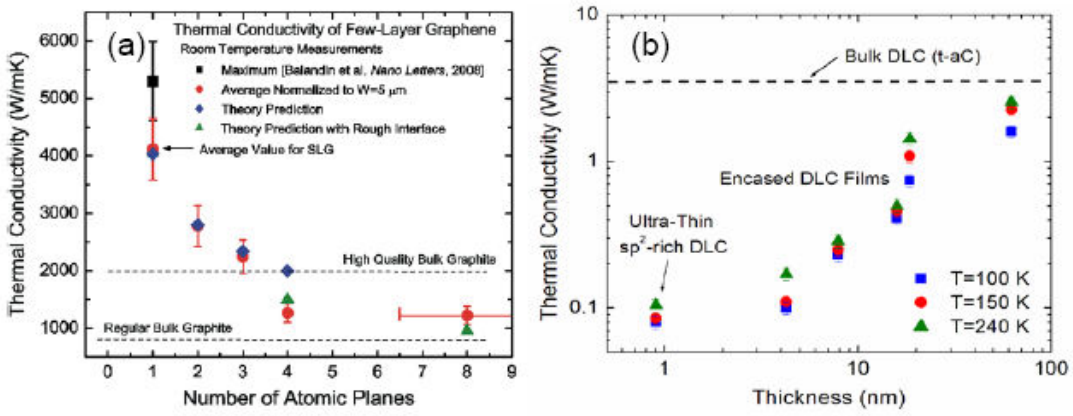

Figure 1: *Thermal conductivity of the suspended FLG (a) and in the encased ultra-thin diamond-like carbon films (b) as function of thickness. The figure (a) is adapted from Ref. [8] while the figure (b) is based on the data reported in Ref. [9].*

THE INTERACTION OF GRAPHENE WITH METALS STUDIED BY IN-SITU ELECTRON MICROSCOPY

F. Banhart[1], J. A. Rodríguez-Manzo[1], O. Cretu[1], A. Krasheninnikov[2,3]

[1] Institut de Physique et Chimie des Matériaux, UMR 7504, Université de Strasbourg, 23 rue du Loess, 67034 Strasbourg, France
[2] Materials Physics Division, University of Helsinki, P.O. Box 43, FI-00014 Helsinki, Finland
[3] Department of Applied Physics, Aalto University, P.O. Box 1100, FI-00076 Aalto, Finland
Banhart@ipcms.u-strasbg.fr

The interaction between graphene and metals is of high importance in the understanding of the growth of graphene from catalytically active metals but also from the viewpoint of doping graphene with foreign atoms. *In-situ* electron microscopy allows the atomic-scale observation of this interaction in a wide temperature range. Dissolution or precipitation phenomena, where carbon atoms are taken up by or extruded from metallic crystals, can be observed as well as the interaction between the graphenic lattice and individual metal atoms [1]. Of particular importance in this context are structural defects in graphene [2] due to the possibility of trapping dopant atoms and thus changing the electronic properties of graphene locally. Since the formation energy of single or multiple vacancies in graphene is above 7 eV, the replacement of carbon by other atoms needs an energetic process such as the ballistic atom displacement by electron beams [3]. Therefore, both defect formation and interaction of defective graphene with metal atoms can be observed in the same experiment in an electron microscope.

The mechanism of trapping metal atoms in graphene was studied by creating defects in the graphene lattice under electron irradiation while metal atoms were migrating on the surface of graphene [4, 5]. In a certain temperature range, tungsten atoms were seen to be trapped in localized defects but can also escape from the defects at sufficiently high temperature. A detailed analysis in a combination of experiments and computation shows that reconstructed divacancies (figure 1) such as the 555-777 type (3 pentagons and 3 heptagons) act as traps, binding the metal atom with an energy of 2 eV [4]. A direct replacement of carbon by metal atoms was excluded, showing the instability of single vacancies in graphene at elevated temperatures. The diffusive migration of trapped Au and Pt atoms was also studied by *in-situ* observation of the metal atoms. Activation energies of the order 2.5 eV were obtained [6].

Trapping of metal atoms at defects in graphene can also be induced selectively with atomic precision. In an electron microscope with aberration-corrected condenser, the electron beam spot with a diameter of 1 Å was focused on pre-selected positions of the graphene lattice, leading to subsequent trapping of metal atoms in these locations [5]. This was used to create a pattern of dots, decorated with foreign atoms, on a graphene sheet.

The interaction between graphene and catalytically active bulk crystals was studied by heating a bilayer system, consisting of an amorphous carbon film covered with a polycrystalline layer of Fe, Ni, or Co. Above approximately 600°C, the dissolution of carbon in the metal layer was observed, followed by the segregation of single- or multi-layer graphene on the metal surface (figure 2) [6]. Ostwald ripening of the metal crystals at increasing temperature allowed us to liberate the graphene areas and thus to observe the growth of graphene in-situ. This is a solid-state growth process (no gases are involved) which is induced by the lowering of the energy of the carbon system from the energetically higher amorphous phase to graphene by using a catalytically active metal. At the same time, the metal crystals act as a diffusion channel for carbon atoms.

References:

[1] F. Banhart, Nanoscale 1 (2009), 201
[2] F. Banhart, J. Kotakoski, A. Krasheninnikov, ACS Nano, DOI 10.1021/nn102598m.
[3] A. Krasheninnikov, F. Banhart, Nature Materials 6 (2007), 723.
[4] O. Cretu, A. V. Krasheninnikov, J. A. Rodríguez-Manzo, R. Nieminen, F. Banhart, Phys. Rev. Lett. 105 (2010) 196102.
[5] J. A. Rodríguez-Manzo, O. Cretu, F. Banhart, ACS Nano 4 (2010) 3422.
[6] Y. Gan, L. Sun, F. Banhart, Small, 4 (2008), 587.
[7] J. A. Rodríguez-Manzo, C. Pham-Huu, F. Banhart, ACS Nano, in the press.

Figures:

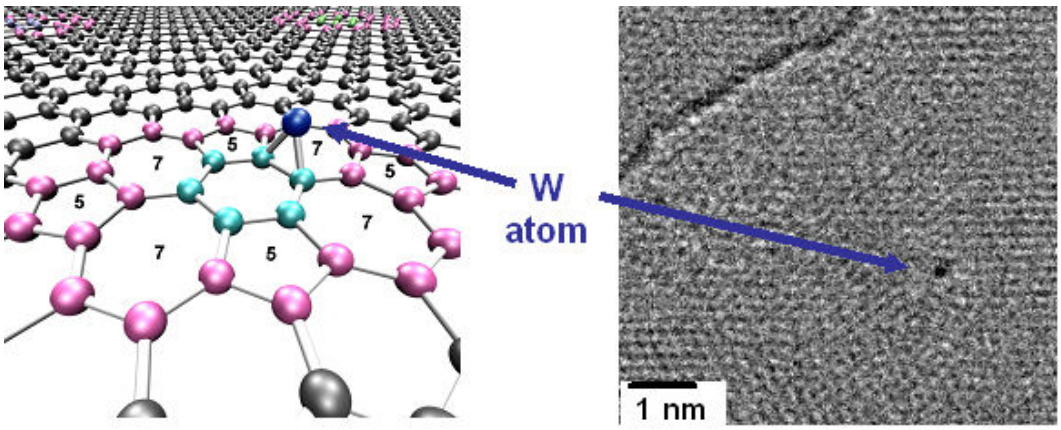

Figure 1: *Trapping of a W atom on a reconstructed divacancy such as the (5555-6-7777)-defect as shown in the model on the left hand side. The Electron microscopy image shows a W atom trapped on such a defect in the uppermost layer of a multi-layer graphene sheet [4].*

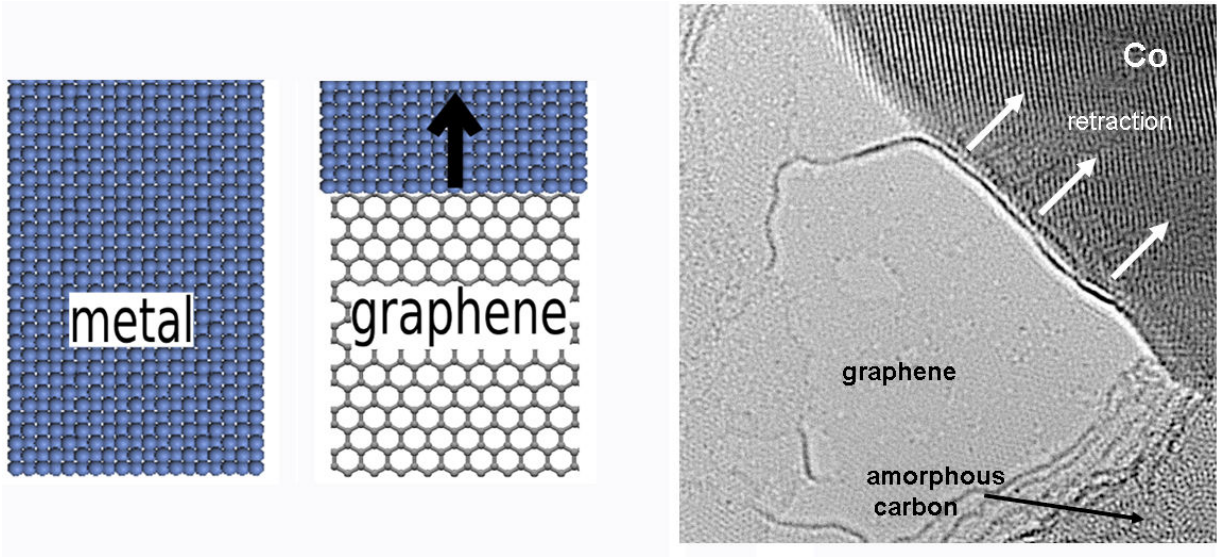

Figure 2: *Solid-state transformation of amorphous carbon to graphene in the presence of a catalytically active transition metal. The metal initially covers the amorphous carbon film. After heating, the amorphous carbon is taken up by the metal. Subsequently, graphene nucleates on the metal surface which can be seen as the metal retracts by a ripening effect (model image on the left hand side). The TEM image shows a retracting Co crystal, leaving a graphene layer in its trace [7].*

GRAPHENE-BASED NATURAL DYE-SENSITIZED SOLAR CELLS

Francesco Bonaccorso[a], Giuseppe Calogero[b], Giulia Privitera[a], Onofrio M. Maragò[b], Pietro G. Gucciardi[b], Gaetano Di Marco[b] and Andrea C. Ferrari[a]

[a] Engineering Department, Cambridge University, 9 JJ Thomson Avenue, Cambridge, UK
[b] Istituto per i Processi Chimico-Fisici, via Ferdinando Stagno-D'Alcontres 37, 98158 Faro Superiore, Messina, Italy
fb296@cam.ac.uk

Dye-sensitized solar cells (DSSCs) [1] have attracted much attention due to their good light-to-electricity conversion efficiency and simple fabrication. The counter electrode (CE) employed for the regeneration of electrolyte is commonly constituted of a catalytic Platinum (Pt) film deposited on TCOs. TCOs, usually Indium Tin-oxide (ITO) and Fluorine-doped Tin-oxide (FTO), require high temperature processing, hindering the deposition on some substrates (e.g., polymeric substrates). Moreover, they are brittle, limiting their use in applications where flexibility is required. On the other hand, Pt tends to degrade over time when in contact with the (I^-/I_3^-) liquid electrolyte, reducing the overall efficiency of DSSCs [2]. Thus, the replacement of such elements with low-cost and/or more versatile materials is at the centre of an ongoing research effort. In this context carbonaceous materials feature good catalytic properties, electronic conductivity, corrosion resistance towards iodine, high reactivity, abundance, and low cost [3,4]. Another fundamental part of a DSSC is the dye. Generally, transition metal coordination compound complexes [5] and synthetic organic dyes [6] are used as effective sensitizers in DSSCs. However, the preparation routes for these dyes are based on tedious and expensive chromatographic purification procedures. Natural dyes and their organic derivatives are non toxic, biodegradable, low in cost, renewable and abundant, so they are the ideal candidate for environmentally friendly solar cells [7].

Here we show that the combination of graphene and natural sensitizers opens up new scenarios for totally green, natural, environmentally friendly and low cost DSSCs, Figure 1. In particular, its unique electronic [8] and optical properties [9] make graphene an attractive material for CEs in DSSCs. Indeed, graphene matches all the key requirements needed for CE materials such as high specific surface area, high exchange current density and low charge-transfer resistance.

Graphene thin films were produced by liquid phase exfoliation of graphite [10], and spin-casted on stainless steel, FTO and glass. We show that graphene CEs have promising activity, similar to the Pt one. Indeed, DSSCs assembled with CE made of graphene deposited onto FTO (1.42%) outperform the total conversion efficiency of those based on Pt (1.21%). Moreover, we show that graphene, contrary to Pt, can both catalyses the reduction of tri-Iodide and back transfers the electrons arriving from the external circuit to the redox system. DSSCs assembled with graphene deposited onto glass as CE show efficiency ~0.8%. This demonstrates the potential of graphene to simultaneously replace both the Pt catalyst and the conductive glass. We also demonstrate an environmentally friendly DSSC assembled using natural dyes, which show high Internal Photocurrent Efficiency (Figure 2), and graphene as CE with efficiency of ~ 0.40%.

References:

[1] B. O'Regan, M. Gratzel, Nature, 353, (1991), 737.
[2] B.K. Koo, et al. Journal of Electroceramics, 17, (2006), 79.
[3] G. Calogero, et al. Dalton Transaction, 39, (2010), 2903.
[4] A.Kay and M. Gratzel, Solar.Ener. Mater. Solar Cells, 44, (1996), 99.
[5] M. K. Nazeeruddin, et. al. J. Am. Chem. Soc., 115, (1993), 6382.
[6] J. H. Yum, et. al. J. Am. Chem. Soc., 129, (2007), 10320.
[7] G. Calogero, G. Di Marco, Solar Energy Material & Solar Cells, 92, (2008), 1341.
[8] A. K. Geim and K. S. Novoselov, Nat. Mater., 6, (2007), 183.
[9] F. Bonaccorso et al. Nat. Photon., 4, (2010), 611.
[10] Y. Hernandez et al. Nat. Nano., 3, (2008), 563.

Figures:

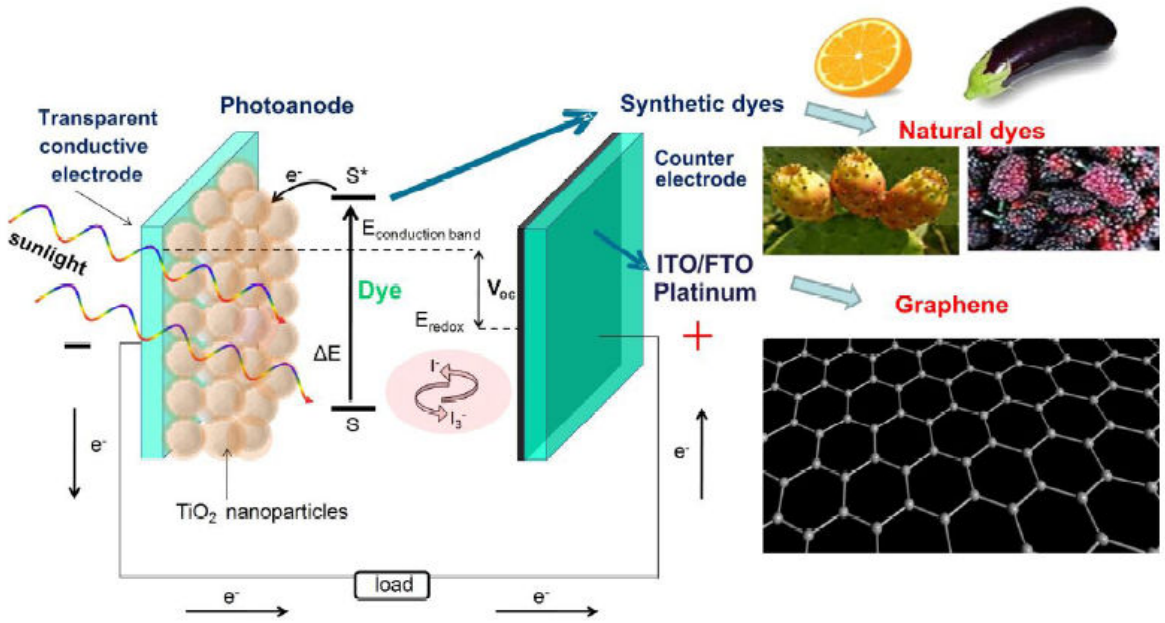

Figure 1: *Schematic representation of the where the synthetic dyes are replaced by the natural dyes and graphene is used at the CE to simultaneously replace TCO films and Pt.*

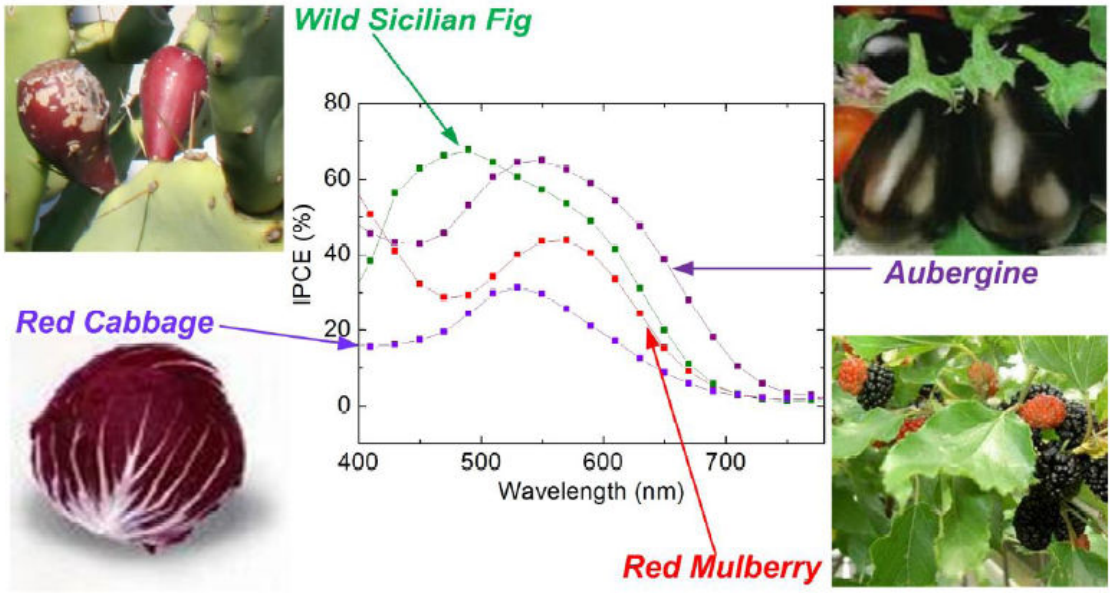

Figure 2: *Internal Photocurrent Efficiency spectra of: Wild Sicilian Fig (green line), Aubergine (purple line), Red Mulberry (red line) and Red Cabbage (violet line).*

HYSTERESIS LOOPS OF THE MAGNETOCONDUCTANCE IN GRAPHENE DEVICES

Andrea Candini[a], Christian Alvino[a,b], Wolfgang Wernsdorfer[c] and Marco Affronte[a,b]

[a] Istituto Nanoscienze – CNR Centro S3, Modena. Via Campi 213/a 41125 Modena. Italy
[b] Dipartimento di Fisica, Università di Modena e Reggio Emilia, Via Campi 213/a 41125 Modena. Italy
[c] Institut Néel, CNRS, BP166, 25 Av des Martyrs, 38042 Grenoble, France
andrea.candini@unimore.it

We report a systematic study of the low temperature magnetoconductance of various graphene devices with the field applied in the plane of graphene. At temperatures below 1K, the magnetoconductance signal depends on the gate and its sign is related to universal conductance fluctuations. When the field is swept at high enough rates (dB/dt > 10mT/s) a hysteresis is observed in the signal. We have systematically measured different devices of various sizes, form unpatterned large flakes down to narrow ribbons (50nm large) and constrictions (30nm in width), finding that the magnetic signal does not depend on the size nor on the transport regime of the device. We attribute the origin of the signal to the magnetization reversal of paramagnetic centers in graphene, which might originate from structural defects in the graphene layer, most probably vacancies [1]. Based on the field and temperature dependencies of the hysteresis, we conclude that the spin of the localized moments is higher than S = 1/2, in agreement with recent works[2,3].

References:

[1] A. Candini et al. accepted for publication in Phys Rev. B (2011) and selected as an Edotor's Suggestion. Available online at: arXiv:1101.3030v1
[2] M. Sepioni et al., Phys. Rev. Lett. 105, (2010) 207205
[3] D.W. Boukhvalov et al., arXiv:1012.3828v1 (2010)

Figures:

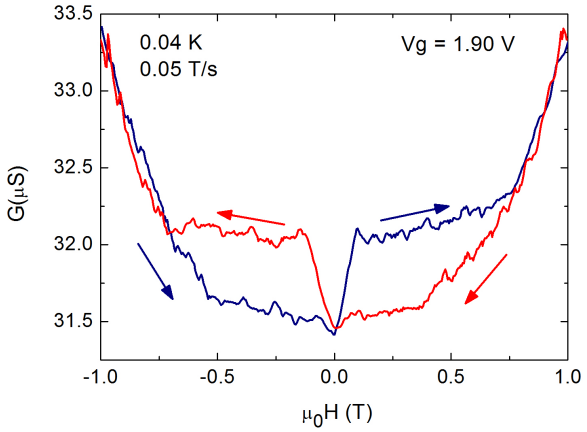

Figure 1: *Parallel magnetoconductance of a graphene device for a fixed gate voltage, taken at 0.04 K and at a field sweep rate of 0.05 T/s. The hysteresis is clearly visible. Figure taken from reference [1].*

MOBILITY OF SUSPENDED BILAYER GRAPHENE AT FINITE TEMPERATURE

Eduardo V. Castro[1], Héctor Ochoa[1], M. I. Katsnelson[2], F. Guinea[1]

[1]Instituto de Ciencia de Materiales de Madrid, CSIC, Cantoblanco, E-28049 Madrid, Spain
[2]Radboud Univ Nijmegen, Inst for Molecules and Materials, NL-6525 AJ Nijmegen, The Netherlands
evcastro @icmm.csic.es

Recent realization of suspended monolayer [1, 2] and bilayer [3] graphene samples made possible a direct probe of the intrinsic, unusual properties of these systems. In particular, intrinsic scattering mechanisms limiting mobility may now be unveiled [4]. In a recent publication we have shown [5] that in suspended, non-strained monolayer graphene room temperature mobility is limited to values observed for samples on substrate due to scattering by out of plane – flexural – acoustic phonons. This limitation can, however, be avoided by applying tension. Bilayer graphene has a different low energy electronic behavior as well as different electron-phonon coupling. It is then natural to wonder what is the situation in the bilayer regarding electron scattering by acoustic phonons, and in particular by flexural phonons.

In the present contribution, after reviewing the single layer graphene case, we will present our recent results for scattering by both acoustic in-plane phonons and flexural phonons in doped, suspended bilayer graphene. We have found the bilayer membrane to follow the qualitative behavior of the monolayer cousin [5]. Different electronic structure combine with different electron-phonon coupling to give the same parametric dependence in resistivity, and in particular the same temperature behavior. In parallel with the single layer, flexural phonons dominate the phonon contribution to resistivity in the absence of strain, where a density independent mobility is obtained. This contribution is strongly suppressed by tension, similarly to monolayer graphene [5]. However, an interesting quantitative difference with respect to suspended monolayer has been found. In the latter, as shown in [5], flexural phonons limit room temperature mobility to values obtained for samples on substrate,.~1 $m^2/(Vs)$, when tension is absent. In bilayer, quantitative differences in electron-phonon coupling and elastic constants lead to a room temperature mobility enhanced by one order of magnitude, ~10–20 $m^2/(Vs)$, even in nonstrained samples. This finding has obvious advantages for electronic applications.

References:

[1] K. I. Bolotin, K. J. Sikes, Z. Jiang, G. Fudenberg, J. Hone, P. Kim, and H. L. Stormer, Solid State Commun., 146 (2008) 351.
[2] X. Du, I. Skachko, A. Barker, and E. Y. Andrei, Nature Nanotech., 3 (2008) 491.
[3] B. E. Feldman, J. Martin, and A. Yacoby, Nature Phys., 5 (2009) 889.
[4] S. V. Morozov, K. S. Novoselov, M. I. Katsnelson, F. Schedin, D. Elias, J. A. Jaszczak, and A. K. Geim, Phys. Rev. Lett. 100 (2008) 016602.
[5] Eduardo V. Castro, H. Ochoa, M. I. Katsnelson, R. V. Gorbachev, D. C. Elias, K. S. Novoselov, A. K. Geim, and F. Guinea, Phys. Rev. Lett. 105 (2010) 266601.

STRAIN ENGINEERING IN GRAPHENE

Antonio Castro Neto

Department of Physics, Boston University, USA
Graphene Research Centre, National University of Singapore

Graphene is a unique example of a one atom thick metallic membrane. Hence, graphene brings together properties of soft and hard condensed matter systems. The elementary electronic excitations in graphene, the Dirac quasiparticles, couple in a singular way to structural distortions in the form of scalar and vector potentials. Therefore, graphene has an effective electrodynamics where structural deformations couple to the Dirac particles at equal footing to electric and magnetic fields. This so-called strain engineering of the electronic properties of graphene opens doors for a new paradigm in terms of electronic devices, where electronic properties can be manipulated at will using its membrane-like properties.

GRAPHENE: PROPERTIES, PREPARATION AND APPLICATION PERSPECTIVE

Yongsheng Chen

State Key Laboratory for Functional Polymer Materials and Center for Nanoscale Science & Technology, Institute of Polymer Chemistry, College of Chemistry, Nankai University, Tianjin 300071, China

The large scale preparation and characterization of graphene materials and their hybrid and composite materials, together with their various device applications will be presented. These include the results for organic photovoltaic device, light emission device, transparent electrode and memory device, room-temperature ferromagnetism, nonlinear optical limiting, electromagnetic interference shielding and absorbing and photoconducting applications and so on.

References:

[1] "Organic Photovoltaic Devices Based on a Novel Acceptor Material: Graphene", Zunfeng Liu, Qian Liu, Xiaoyan Zhang, Yi Huang, Yanfeng Ma, Shougen Yin* and Yongsheng Chen* Adv Mater. 2008. 20, 3924.

[2] "Evaluation of Solution-Processed Reduced Graphene Oxide Films as Transparent Conductors", Hector A. Becerril, Jie Mao, Zunfeng Liu, Randall M. Stoltenberg, Zhenan Bao, and Yongsheng Chen*, ACS Nano, 2008, 2, 463.

[3] "A Graphene Hybrid Material Covalently Functionalized with Porphyrin: Synthesis and Optical Limiting Property", Yanfei Xu, Zhibo Liu, Xiaoliang Zhang, Yan Wang, Jianguo Tian, Yi Huang, Yanfeng Ma, Xiaoyan Zhang, Yongsheng Chen* Adv Mater. 2009. 21, 1275.

[4] "Molecular-level Dispersion of Graphene into Poly(vinyl alcohol), and Effective Reinforcement of Their Nanocomposites", Jiajie Liang, Yi Huang, Long Zhang, Yan Wang, Yanfeng Ma, Tianyin Guo and Yongsheng Chen*, Adv Funct Mater, 2009,19, 2297

[5] "Polymer photovoltaic cell based on a solution processable graphene and P3HT", Qian Liu, Zunfeng Liu, Xiaoyan Zhang, LiyingYang, Nan Zhang, Guiling Pan, Shougen Yin,* Yongsheng Chen*, and Jun Wei, Adv Funct Mater, 2009, 19, 894

[6] "Photoconductivity of Bulk Films Based on Graphene Sheets", Xin Lv, Yi Huang, Zhibo Liu, Jianguo Tian, Yan Wang, Yanfeng Ma, Jiajie Liang, Shipeng Fu, Xiangjian Wan, Yongsheng Chen*, Small, 2009, 5,1682.

[7] "Room temperature ferromagnetism of graphene", Yan Wang, Yi Huang, You Song, Xiaoyan Zhang, Yanfeng Ma, Jiajie Liang, Yongsheng Chen*, Nano Lett, 2009, 9, 220

[8] "Size-controlled synthesis of graphene oxide sheets on a large scale using chemical exfoliation", Long Zhang, Jiajie Liang, Yi Huang, Yanfeng Ma, Yan Wang, Yongsheng Chen*, Carbon, 2009, 47, 3365

[9] "Supercapacitor devices based on graphene materials",Yan Wang, Zhiqiang Shi, Yi Huang, Yanfeng Ma, Chengyang Wang, Mingming Chen, Yongsheng Chen*; J Phys Chem C, 2009, 113, 13103.

[10] "Infrared-triggered actuators from graphene-based nanocomposites", Jiajie Liang, Yanfei Xu, Yi Huang*, Long Zhang, Yan Wang, Yanfeng Ma, Feifei Li, Tianying Guo, Yongsheng Chen*, J Phys Chem C, 2009, 113, 9921.

[11] "Toward All-Carbon Electronics: Fabrication of Graphene-Based Flexible Electronic Circuits and Memory Cards Using Maskless Laser Direct Writing",Jiajie Liang, Yongsheng Chen, Yanfei Xu, Zhibo Liu, Long Zhang, Xin Zhao, Xiaoliang Zhang, Jianguo Tian, Yi Huang, Yanfeng Ma, Feifei Li; ACS Appl. Mater. Interfaces, 2010, 2, 3310.

[12] "Fabrication and Evaluation of Solution-Processed Reduced Graphene Oxide Electrodes for p- and n-Channel Bottom-Contact Organic Thin-Film Transistors",Hector A. Becerril, Randall M. Stoltenberg,Ming Lee Tang, Mark E. Roberts, Zunfeng Liu,Yongsheng Chen, Do Hwan Kim, Bang-Lin Lee, Sangyoon Lee, and Zhenan Bao ACS Nano, 2010, 4, 6343.

[13] "Flexible, Magnetic and Electrically Conductive Graphene/Fe3O4 Paper and Its Application for Magnetic-Controlled Switches",Jiajie Liang, Yanfei Xu, Dong Sui, Long Zhang, Yi Huang, Yanfeng Ma, Feifei Li, Yongsheng Chen J Phys Chem C, 2010, 114, 17465.

[14] "Towards Flexible All-Carbon Electronics: Flexible Organic Field-Effect Transistors and Inverter Circuits Using Solution-Processed All Graphene Source/Drain/Gate Electrodes",Yongsheng Chen, Yanfei Xu, Kai Zhao, Xiangjian Wan, Jiachun Deng, Weibo Yan Nano Res, 2010, 10, 714.
[15] "Solution-processed bulk heterojunction organic solar cells based on an oligothiophene derivative", Bin Yin, Liying Yang, Yongsheng Liu, Yongsheng Chen, Qingjin Qi, Fengling Zhang, and Shougen Yin Appl. Phys. Lett., 2010, 97, 023303.

THERMAL EXPANSION COEFFICIENT OF SINGLE-LAYER GRAPHENE MEASURED BY RAMAN SPECTROSCOPY

Duhee Yoon,[1] Young-Woo Son,[2] and **Hyeonsik Cheong**[1*]

[1]Department of Physics, Sogang University, Seoul 121-742, Korea,
[2]School of Computational Sciences, Korea Institute for Advanced Study, Seoul 130-722, Korea
hcheong@sogang.ac.kr

Graphene is attracting much interest due to potential application as next generation electronic material as well as its unique physical properties. In particular, its superior thermal and mechanical properties, including high thermal conductivity and extremely high mechanical strength that exceeds 100 GPa, make it a prime candidate material for heat control in high-density, high-speed integrated electronic devices. For such applications, knowledge of the thermal expansion coefficient (TEC) as a function of temperature is crucial, but so far few reliable measurements on the TEC have been reported [1]. Several authors have calculated the TEC using various models [2-6]. Mounet *et al*. estimated the TEC of graphene as a function of temperature by using a first-principles calculation and predicted that graphene has a negative TEC at least up to 2500 K [6]. Bao *et al*. experimentally estimated the thermal coefficient in the temperature range of 300 – 400 K by monitoring the miniscule change in the sagging of a graphene piece suspended over a trench and found that it is negative only up to ~350 K [1]. It is not yet clear whether this discrepancy between theory and experimental data is caused by uncertainties in the accuracy of the experimental measurements or limitations in the theoretical calculation. Since precise knowledge of the TEC in the temperature range around room temperature is crucial in designing graphene-based devices and heat management systems, more precise measurements are needed. In this work, we analyze the temperature-dependent shift of the Raman *G* band of monolayer graphene on SiO_2 to estimate the TEC of graphene. We find that the data can be explained in the temperature range of 200 – 400 K with the help of the calculated temperature dependence of the Raman *G* band of free standing graphene.

When the temperature of a graphene sample fabricated on a SiO_2/Si substrate is raised, two effects should be considered: the temperature dependence of the phonon frequencies and the modification of the phonon dispersion due to strain caused by mismatch of the TEC'ss of the substrate and graphene. The Raman frequency shift of the *G* band of free standing graphene as a function of temperature has been estimated by first-principles calculations [7]. Since most graphene samples are fabricated on SiO_2 substrates or over a trench held at the edges, the pure effect of temperature change on the Raman spectrum cannot be measured directly and compared with the theory. The discrepancy between the experimentally measured Raman frequency shift and the theoretical prediction can be reconciled by accounting for the TEC mismatch between the substrate and graphene.

Graphene samples used in this work were prepared on silicon substrates covered with a 300-nm-thick SiO_2 layer by mechanical exfoliation of natural graphite flakes. The number of graphene layers was determined by inspecting the line shape of the Raman 2*D* band. Temperature-dependent Raman spectra of graphene and graphite were obtained while cooling and heating the samples in a microscope cryostat where the temperature could be controlled between 4.2 K and 475 K. The 514.5-nm line of an Ar ion laser was used as the excitation source, and low power (< 0.3 mW) was used to avoid unintentional heating. A long-working-distance microscope objective (40x, 0.6 N.A.) was used to focus the laser beam onto the sample and collect the scattered light. The Raman scattered light signal was dispersed by a Jobin-Yvon Triax 550 spectrometer (1800 grooves/mm) and detected with a liquid-nitrogen-cooled CCD detector. The spectral resolution was ~0.7 cm^{-1}.

Figure (a) shows the frequency shifts of the Raman *G* band of single-layer graphene (SLG), bilayer graphene (BLG), and graphite samples as functions of temperature. The Raman peaks redshift as temperature rises and blueshift as temperature falls from room temperature. The Raman peak shift of SLG as a function of temperature is largest. Temperature-dependent Raman shift is commonly attributed to thermal expansion of the lattice and an anharmonic effect which changes the phonon self-energy. As the temperature rises, the SiO_2 layer expands whereas the graphene sheet contracts. This TEC mismatch would induce a biaxial tensile strain on the graphene sample. When the sample is cooled, a compressive strain is induced instead. In order to interpret our data correctly, we should

consider the effect of stain on graphene induced by the TEC mismatch between the SiO_2 layer and the graphene sheet.

We estimated the TEC by fitting our data to the theoretical prediction [7] of temperature dependence of the Raman *G* band of *free standing* graphene. Figure (b) shows the temperature dependent TEC obtained from the fitting. TEC at room temperature is estimated to be -9×10^{-6} K^{-1}, which is similar to the previous experimental value of -7×10^{-6} K^{-1} [1].

References:

[1] W. Z. Bao et al., Nat. Nanotechnol. 4 (2009) 562.
[2] P. K. Schelling, and R. Keblinski, Phys. Rev. B 68 (2003) 035425.
[3] Y. K. Kwon, S. Berber, and D. Tomanek, Phys. Rev. Lett. 92 (2004) 015901.
[4] K. V. Zakharchenko, M. I. Katsnelson, and A. Fasolino, Phys. Rev. Lett. 102 (2009) 046808.
[5] J. W. Jiang, J. S. Wang, and B. W. Li, Phys. Rev. B 80 (2009) 205429.
[6] N. Mounet, and N. Marzari, Phys. Rev. B 71 (2005) 205214.
[7] N. Bonini, M. Lazzeri, N. Marzari, and F. Mauri, Phys. Rev. Lett. 99 (2007) 176802.

Figures:

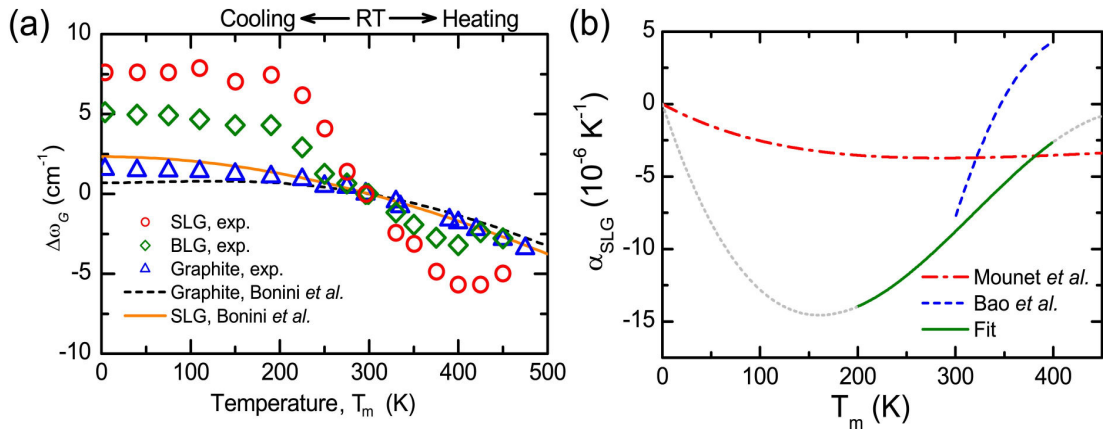

Figure 1: *(a) Raman frequency shifts of graphene and graphite as functions of temperature. (b) Thermal expansion coefficient of single layer graphene that gives the best fit between data and theoretical estimate.*

OPTO-ELECTRONIC PROPERTIES OF GRAPHENE OXIDE

Manish Chhowalla

Rutgers - The State University of New Jersey; Department of Materials Science and Engineering;
607 Taylor Road, Piscataway, NJ 08854, USA

The In this presentation, a solution based method that allows uniform and controllable deposition of reduced graphene oxide (GO) thin films with thicknesses ranging from a single monolayer up to several layers over large areas will be described. The oxidation treatment during synthesis of GO creates sp^3 C-O sites where oxygen atoms are bonded in the form of various functional groups. GO is therefore a two dimensional network of sp^2 and sp^3 bonded atoms, in contrast to an ideal graphene sheet which consists of 100% sp^2 carbon atoms. The most notable difference between GO and graphene is that photoluminescence from blue to red emission can be observed. The atomic and electronic structure along with tunable photoluminescence of graphene oxide at various degrees of reduction will be described.

High temperatures (~ 1000 ºC) are typically required for efficient removal of oxygen functional groups from GO. Furthermore, the attractive properties of graphene are not fully recovered due to creation of structural defects and the presence of residual oxygen in the reduced material. In the second part of the talk, the synthesis and properties of partially oxidized graphene (POG), a material that exhibits significantly different chemical structure to GO will be described. Due to low initial oxygen content, as-synthesized POG can be reduced in mild annealing conditions (< 300 ºC). Our results suggest that fine-tuning the oxidation chemistry of graphene will allow bulk production of highly soluble graphene without extensively compromising its intrinsic properties. We will demonstrate that partial oxidation approach opens up new promising routes to high-performance graphene-based electronics plastic platforms.

UNIFORM MONOLAYER GRAPHENE IN 6-INCH SCALE: ITS ORIGIN AND APPLICATION

Hyun-Jong Chung, David Seo, Sung-Hoon Lee, Jinseong Heo, Heejun Yang, Hyun Jae Song, Seongjun Park

Samsung Advanced Institute of Technology, San 14, Nongseo-dong, Giheung-gu, Yongin-si, Gyeonggi-do Korea

hyunjong.chung@samsung.com

Monolayer graphene has been grown on Cu thin film in 6-inch scale at low temperature using inductive coupled plasma chemical vapor deposition. More than 99% of the film is single layer according to Raman mapping and optical microscopy. [1] Scanning tunneling microscopy and spectroscopy study reveals line structure and undisturbed spectroscopy of graphene which could be the origin of the thinner layer than thermally grown graphene on Cu foil. [2] More than 2000 Hall bars were fabricated on the 6-inch wafer and measured Id-Vg and Id-Vd curves. Also, screening effect for multi-layer graphene was measured using Kelvin probe force microscopy. [3]

References:

[1] J. Lee et al., IEDM (2011).
[2] Jeon et al., ACS Nano, 3 (2011) 1915.
[3] N.J. Lee et al., Appl. Phys. Lett., 22 (2009) 222107.

GRAPHENE FOR BEYOND CMOS DEVICES

Luigi Colombo[1] and Rodney S. Ruoff[2]

[1]Texas Instruments Incorporated, Dallas, TX 75243, USA
[2]Department of Mechanical Engineering and the Texas Materials Institute, 1 University Station C2200, The University of Texas at Austin, Austin, TX 78712-0292, USA
colombo@ti.com

Electronic devices fabricated on silicon, III-V, and II-VI compounds require the highest quality material that can be achieved in order to meet the performance, uniformity, reliability, and cost requirements. The semiconductor industry has demonstrated the ability to produce and provide high quality and reliable devices to the community for many decades as a result of its ability to produce and integrate the highest quality materials. As we move toward trying to replace the basic electronic device, the transistor, with new materials whether it is using Ge, III-Vs or graphene, the highest quality material will be needed to continue meeting the stringent requirements.

Graphene is being studied as a new switch material for devices beyond CMOS. Assuming that the material has the necessary fundamental properties required to fabricate the new switch, namely a Bose-Einstein condensate (BEC), it is will be necessary to grow large area films with the highest quality in order to fabricate these new devices in a manufacturing environment. Graphene will have to be integrated with dielectrics and metals to fabricate the simplest device structures and thus it may be necessary to grow this material defect free. Graphene can be produced by several techniques: 1) exfoliation from bulk graphite [1-3]; 2) chemical reduction of exfoliated graphite oxide [4]; 3) precipitation from bulk metals [5-7]; 4) growth on SiC by silicon desorption [8,9]; and 5) chemical vapor deposition on copper surface [10] or metal surfaces with extremely C solubility of C diffusivity. Growth on very low carbon solubility substrates like copper occurs by a surface mediated process and can cover extremely large areas. Recently Li et al. [11] have also discovered that large single crystals can be grown without domains or grain. The objective of this presentation is to describe the growth process of graphene on metals and how we can use this process to create high quality large area graphene. Figure 1 shows an SEM image of a single graphene domain that according to LEEM (Li et al) is single crystal across the entire domain (400 to 500 □m) [11].

References:

[1] Lu, X. K.; Yu, M. F.; Huang, H.; Ruoff, R. S. Nanotechnology 1999, 10, 269-272.
[2] Novoselov, K. S.; Geim, A. K.; Morozov, S. V.; Jiang, D.; Zhang, Y.; Dubonos, S. V.; Grigorieva, I. V.; Firsov, A. A. Science 2004, 306, 666-669.
[3] Zhang, Y. B.; Small, J. P.; Pontius, W. V.; Kim, P. Appl. Phys. Lett. 2005, 86.
[4] Stankovich, S.; Dikin, D. A.; Piner, R. D.; Kohlhaas, K. A.; Kleinhammes, A.; Jia, Y.; Wu, Y.; Nguyen, S. T.; Ruoff, R. S. Carbon 2007, 45, 1558-1565.
[5] Eizenberg, M.; Blakely, J. M. Surf. Sci. 1979, 82, 228-236.
[6] Hamilton, J. C.; Blakely, J. M. Surf. Sci. 1980, 91, 199-217.
[7] Reina, A.; Thiele, S.; Jia, X. T.; Bhaviripudi, S.; Dresselhaus, M. S.; Schaefer, J. A.; Kong, J. Nano Res. 2009, 2, 509-516.
[8] Van Bommel, A. J.; Crombeen, J. E.; Van Tooren, A. Surf. Sci. 1975, 48, 463-472.
[9] Berger, C.; Song, Z.; Li, T.; Li, X.; Ogbazghi, A. Y.; Feng, R.; Dai, Z.; Marchenkov, A. N.; Conrad, E. H.; First, P. N.; de Heer, W. A. The Journal of Physical Chemistry B 2004, 108, 19912-19916.
[10] Li, X.; Cai, W.; An, J. H.; Kim, S.; Nah, J.; Yang, D.; Piner, R.; Velamakanni, A.; Jung, I.; Tutuc, E.; Banerjee, S. K.; Colombo, L.; Ruoff, R. S. Science 2009, 324, 1312-1314.
[11] Li, X.; Magnuson, C. W.; Venugopal, A.; Tromp, R. M.; Hannon, J. B.; Vogel, E. M.; Colombo, L.; Ruoff, R. S. J. Am. Chem. Soc., 133, 2816-2819.

Figures:

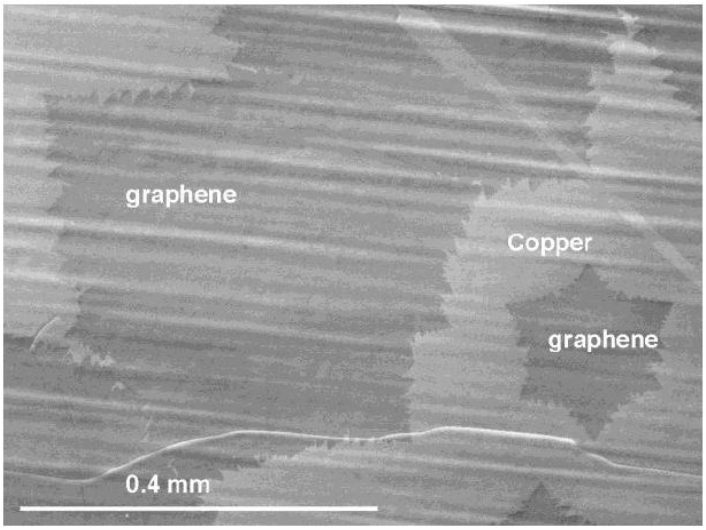

Figure 1: *Large single crystals of graphene grown by low pressure chemical vapor deposition. LEEM analysis has shown that these crystals are mostly single crystals. (Li et al.).*

BAND-GAP ENGINEERING IN GRAPHENE THROUGH FUNCTIONALIZATION WITH FLUORINE

M.F. Craciun[1], F. Withers[2], M. Dubois[3], A. K. Savchenko[2] and S. Russo[2]

[1]Centre for Graphene Science, School of Engineering, University of Exeter, Exeter EX4 4QF, UK
[2]Centre for Graphene Science, School of Physics, University of Exeter, Exeter EX4 4QL, UK
[3]Laboratoire des Matériaux Inorganiques, Clermont Université–UBP, CNRS-UMR 6002, 63177 Aubière, France
M.F.Craciun@exeter.ac.uk

Rece Graphene – a single layer of sp^2 bonded carbon atoms arranged in a honeycomb pattern – is an indefinitely large aromatic molecule, of unique interest in the field of transparent organic electronics. This is a transparent material where charge carriers (relativistic Dirac fermions) exhibit mobilities (>10^6 cm^2/Vs) higher than Si at room temperature. However, the energy dispersion of graphene is gap-less, and this would limit its applications in electronic devices. For instance, in a graphene-based transistor the absence of the gap in the band-structure results in a relatively small resistance difference between the electro-neutrality (Dirac) region and a region with large carrier concentration (i.e., between the "on" and "off" states). Due to this significant limitation in the use of graphene in electronics, intensive research is currently underway aimed at the creation of a (tunable) gap in graphene's energy spectrum.

The ability to chemically functionalize graphene, for instance with fluorine [1] and hydrogen [2] atoms, paved the way towards band-gap engineering. This type of functionalization transforms the graphene planar crystal structure, with sp^2 bonds between the carbon atoms, into a three-dimensional structure with sp^3 bonding between them. Theoretical predictions show that a band gap of 3.8 eV and 4.2 eV is expected for hydrogen and fluorine for 100% functionalization, respectively [3, 4].

Here I will review recent results on fluorinated graphene transistors [1] produced by mechanical exfoliation of natural graphite which is fluorinated to 24% and 100% (as measured by mass uptake). Transport measurements over a wide range of temperatures (from 4.2K to 300K) show a very large and strongly temperature dependent resistance in the electro-neutrality region. The strong temperature dependence of fluorinated graphene is due to the opening of a mobility in gap in the energy spectrum of graphene where electron transport takes place via localised electron states.

Magneto-transport experiments through fluorinated graphene as a function of gate voltage, bias voltage, and temperature show that a magnetic field systematically leads to an increase of the conductance on a scale of a few tesla. This phenomenon is accompanied by a decrease in the energy scales associated to charging effects, and to hopping processes probed by temperature-dependent measurements. All these results demonstrate that disorder induced sub-gap states originate strong localization effects in the transport of charge carriers for energies below the energy-gap of fluorinated graphene.

References:

[1] F. Withers et al., Phys. Rev. B 82 (2010), 073403
[2] D. C. Elias et al., Science 323 (2009), 610
[3] J. O. Sofo, et al., Phys. Rev. B 75 (2007), 153401
[4] D. W. Boukhvalov and M. I. Katsnelson, J. Phys.: Condens. Matter 21 (2009), 344205

EPITAXIAL GRAPHENE GROWN ON SILICON CARBIDE FOR FUNDAMENTAL PHYSICS AND NANOELECTRONICS

Walt de Heer

Georgia Institute of Technology, USA

The invention of graphene based electronics at Georgia Tech (patented in 2003 [1]) was based on carbon nanotube properties of ballistic and coherent transport as well as several other outstanding features of carbon nanotubes, including the possibility of tuning the bandgap in graphene ribbons using the ribbon width. Silicon carbide, with its natural property to produce epitaxial graphene layers after heating in vacuum was considered to be the most promising platform for graphene based electronics.

Considerable advances have since been made in realizing graphene electronics however it is clear that the field is still in its infancy. Graphene devices are not yet competitive with those produced from standard electronic materials. Nevertheless, currently, epitaxial graphene on silicon carbide is still considered to be the most viable platform for high performance graphene based electronics. (In contrast, mechanically transferred CVD graphene is showing potential for low end electronics applications; exfoliated graphene is not scaleable and backgating is not useful for electronics.) There have been demonstrations of extremely high frequency transistors and the possibility of using epitaxial graphene Hall bars as resistance standards. But there remain serious questions whether graphene based nanoelectronics can be realized. The moblities of narrow ribbons produced by standard lithography methods generally show strong localization effects and the apparent band gaps are most likely mobility gaps. Many of these problems can be traced back to edge scattering effects that ultimately result from rough and chemically poorly defined edges.

Recent work at Georgia Tech has demonstrated that many of these problems can be overcome by "growing" graphene on the edges of structures that are directly etched onto the silicon carbide in order to produce interconnected narrow graphene ribbons. These graphene ribbons are demonstrating many of the advantageous properties of carbon nanotubes. Gated ribbons show evidence of single channel ballistic transport, also observed in carbon nanotubes, and PN junctions show evidence of "Klein tunneling" effects. On the other hand, the ribbons produced by this method apparently do not have band gaps. Nevertheless, it is clear that "sidewall" graphene electronics is opening new directions in graphene based electronics, that resembles nanotube based electronics. But this does imply a departure from the standard field effect transistor paradigm of electronics.

This talk will present an overview of these developments as well as providing a survey of the vast fundamental physics that has been accomplished with graphene that it epitaxially grown on silicon carbide.

References:

[1] W.A. de Heer, C. Berger, P.N. First, US Patent No 7015142 (filed 2003, issued 2006)

GRAPHENE PROCESSING FOR ELECTRONICS AND SENSING

Shishir Kumar[1,2], Nikos Peltekis[1], Chan H. Lee[1], KangHo Lee[1], Hye-Young Kim[1],
Georg S. Duesberg[1,2]

[1]Centre for Research in Adaptive Nanostructures and Nanodevices (CRANN), Dublin 2, Irlanda
[2]School of Chemistry, Trinity College Dublin, Dublin 2, Irlanda
duesberg@tcd.ie

The unique electronic properties of graphene of potential applications in future electronic devices. The quality of graphene layers is crucial for those applications, as contamination, impurities, morphology and defects can substantially affect the electronic properties and the performance of these devices. After numerous studies on hand grafted devices CVD growth of graphene yield macroscale samples, opening a pathway to reliably fabricate devices.
Graphene surfaces are ultra sensitive to local chemical environment due to changes in their electrical properties by vicinity doping of adsorbed molecules. Their chemical stability and lithographic manufacturability make them an appealing candidate for next generation biosensors. To exploit the full potential of graphene in sensing, however, selectivity to analytes must be established.
We present a comprehensive study on large scale CVD grown graphene films. Challenges faced in structuring graphene with conventional microfabrication techniques are discussed. Mild plasma treatments for cleaning graphene surfaces and novel hardmasks are introduced, leading reproducible devices with high field effect mobilities. With extensive analysis based on high resolution XPS, Raman spectroscopy and microscopy the metallicity, defect density and contaminations can be clearly identified. This work, therefore, will help high volume processing of graphene using these scalable processes steps, yielding interconnects, FET and sensor device arrays.

ELECTRONIC STRUCTURES OF NANOGRAPHENE WITH ZIGZAG AND ARMCHAIR EDGES

Toshiaki Enoki[1], Ken-ichi Sakai[1], Shintato Fujii[1], Kazuyuki Takai[1], Kenichi Sasaki[2], Katsunori Wakabayashi[2], Takeshi Nakanishi[3], and Ken-ichi Fukui[4]

[1]Chem. Department, Tokyo Institute of Technology, Ookayama, Meguro-ku, Tokyo 152-8551, Japan
[2]International Center for Materials Nanoarchitectonics, NIMS, Namiki, Tsukuba 305-0044, Japan
[3]Nanotube Research Center, AIST, Tsukuba 305-8565, Japan
[4]Dept. of Materials Engineering Science, Osaka University, Toyonaka, Osaka 560-8531, Japan
tenoki@chem.titech.ac.jp

The electronic structure of graphene is described in terms of massless Dirac fermion with two Dirac cones (K and K') in the Brillouin zone, giving unconventional features of zero-gap semiconductor. When a graphene sheet is cut into fractions, the created edges affect seriously the electronic structure depending on the edge shape (zigzag and armchair edges) as observed with the electron wave interference and the creation of non-bonding π-electron state (edge state). We investigated the edgeinherent electronic features by STM/STS observations and Raman spectra. Graphene nanostructures were fabricated using graphene oxide with an AFM tip.

STM/STS observations of hydrogen-terminated graphene edges demonstrate that edge states are created in zigzag edges in spite of the absence of such state in armchair edges [1]. In addition, zigzag edges tend to be short and defective whereas armchair edge is long and continuous in general. These findings suggest that zigzag edge is less energetically stable in comparison with armchair edge, consistent with Clar's aromatic sextet rule. In a finite length zigzag edge embedded between armchair edges, electron confinement is observed in the edge state.

The electron wave scattering takes place differently between zigzag and armchair edges, showing different superlattice patterns in STM lattice images. In the vicinity of an armchair edge, a hexagonal pattern was observed together with a fine structure of three-fold symmetry at the individual superlattice spots [2] (Fig.1), different from the $\sqrt{3}\times\sqrt{3}$ superlattice observed in bulk graphene and also in zigzag edge. At a zigzag edge, the electron wave is subjected to the K-K intra-valley scattering without interference, whereas the K-K' inter-vallery scattering with interference takes place in the scattering event at an armchair edge. Tight binding calculation reproduces the hexagonal superlattice observed in the armchair edge. The three-fold symmetric fine structure is understood as the antibonding coupling between the adjacent spots in the hexagonal superlattice with the mediation of the wave function at the STM tip.

The Raman G-band shows the edge-shape dependence same to that observed in the STM superlattices in relation to the intra-valley/inte-rvalley transition for the scattering at zigzag/armchair edges [3]. The inter-valley scattering at an armchair edge gives specific dependence of the G-band intensity on the polarization direction of the incident beam as expressed by $\cos^2\Theta$ (Θ ; the angle between the polarization and the armchair edge direction). A nanographene ribbon of 8 nm × >1 μm prepared by heat-treatment of graphite step edges shows this angular dependence, being demonstrated to consist of pure armchair edges [4].

Single sheet graphene oxide was found to form a two dimensional arrangement of linear corrugations of oxidized lines running along the zigzag direction with an interline spacing of ca.10 nm [5] (Fig.2). This suggests that zigzag edged nanographene ribbons with a width of ca.5 nm are created between the oxidized lines. Nanofabrication by an AFM tip can allow us to create a nanostructure of graphene sheet intentionally.

References:

[1] T. Enoki, Y. Kobayashi, and K. Fukui, Inter. Rev. Phys. Chem. 26 (2007) 609.
[2] K. Sakai, K. Takai, K. Fukui, T. Nakanishi. and T. Enoki, Phys. Rev. B81 (2010) 235417.
[3] L. G. Cançado, M. A. Pimenta, B. R. A. Neves, G. Medeiros-Ribeiro, T. Enoki, Y. Kobayashi, K. Takai, K. Fukui, M. S. Dresselhaus, R. Saito, and A. Jorio, Phys. Rev. Lett. 93 (2004) 047403.
[4] K. Sasaki, R. Saito, K. Wakabayashi, and T. Enoki, J. Phys. Soc. Jpn.79 (2010) 044603.
[5] S. Fujii and T. Enoki, J. Amer. Chem. Soc. 132 (2010) 10034.

Figures:

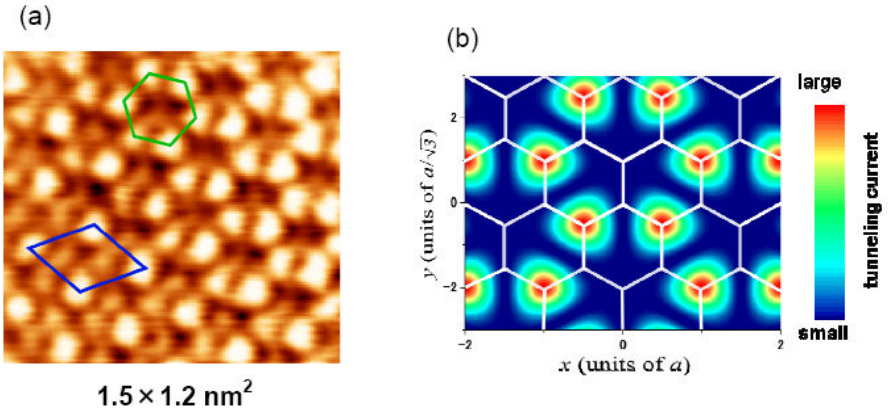

Figure 1: *(a) √3×√3 and hexagonal superlattices near an armchair edge. (b) Calculated current image of the hexagonal superlattice.*

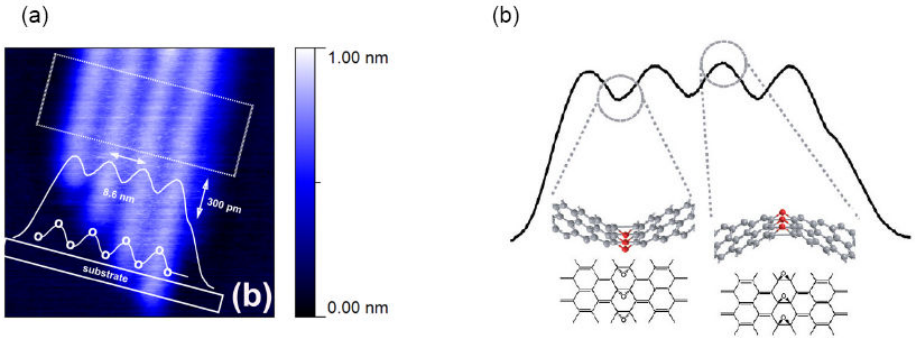

Figure 2: *(a) 1D wrinkles in graphene oxide nanohsheet observed by non-contact AFM. (b) schematic model of graphene oxide consisting of zigzag edged nanographene sheets inter-connected through oxygen bridges.*

GRAPHENE QUANTUM CIRCUITS

F. Molitor, J. Güttinger, S. Schnez, S. Dröscher, A. Jacobsen, C. Stampfer, T. Ihn and **K. Ensslin**

ETH Zurich, Switzerland

Graphene quantum dots and constrictions have been fabricated by mechanical exfoliation of graphene followed by electron beam lithography and dry etching. The single layer quality of graphene has been checked by Raman spectroscopy. The electron hole-crossover can be investigated by linear transport experiments as well as using non-linear effects in three-terminal junctions. A variety of nanostructures such as graphene constrictions, graphene quantum dots and graphene rings have been realized. Of particular interest is the electron hole crossover in graphene quantum dots, spin states as well as the electronic transport through graphene double dots. The goal is to establish the peculiar consequences of the graphene bandstructure with its linear dispersion for the electronic properties of nanostructures.

INTEGER QUANTUM HALL EFFECT IN TRILAYER GRAPHENE

W. Escoffier[1], J.M. Poumirol[1], A. Kumar[1], C. Faugeras[2], D. P. Arovas[3], M. M. Fogler[3], P. Guinea[4], S. Roche[5], M. Goiran[1] and B. Raquet[1]

[1]LNCMI, CNRS, 143 av. de rangueil, 31400 Toulouse, France
[2]LNCMI, CNRS, 25 rue des Martyrs, 38042 Grenoble, France
[3]Department of Physics, Univ. of California - San Diego, 9500 Gilman Drive, California 92093, USA
[4]Instituto de Cienca de Materiales de Madrid, CSIC, Cantoblanco E28049 Madrid, Spain
[5]Centre d'Investigaci en Nanocincia i Nanotecnologia (CSIC-ICN), UAB, 08193 Barcelona, Spain
walter.escoffier@lncmi.cnrs.fr

The Integer Quantum Hall Effect (IQHE) constitutes the hallmark of two-dimensional systems subjected to a strong perpendicular magnetic field. So far, three different realizations of 2D systems displaying distinctive IQHE features have been reported in the literature. These are conventional semiconducting heterostructures, graphene and bi-layer graphene. In the case of graphene-based systems, it has been anticipated that the dynamics of charged carriers drastically change every time an extra graphene layer in added [1,2]. Therefore, the LL spectrum of N-layer graphene systems would display unique IQHE features eventually characterizing their N.π Berry's phase [3]. This property particularly applies to trilayer graphene for which 3π Berry's phase would drastically change the sequence of QH plateaus as compared to mono or bi-layer graphene systems. Making use of both Raman spectroscopy and high field magneto-transport, we report for the first time on a fourth type of IQHE in tri-layer graphene. The sequence of QH resistance plateaus is similar to graphene, however the v=2 QH plateau is missing. The experimental data are supported by a theoretical analysis where both the Bernal and rhombohedral stacking order have been considered. We notice that a nice comparison between theoretical and experimental results is achieved only for the rhombohedral stacking order. At very high magnetic field, the QH resistance tends to vanish as the system is driven close to CNP. We show that the presence of charge puddles is necessary to explain this trend, which is further confirmed by analysing the zero-field temperature and carrier density dependence of the resistance [4].

References:

[1] F. Guinea et. al., Physcal Review B 73 (2006) 245426
[2] Daniel P. Arovas and F. Guinea, Phys. Rev. B 78 (2008) 245416 [3] M. Koshino et. al., Physcal Review B 79 (2009) 125443
[3] J.M. Poumirol et. al., Physical Review B 82 (2010) 121401(R)

Figures:

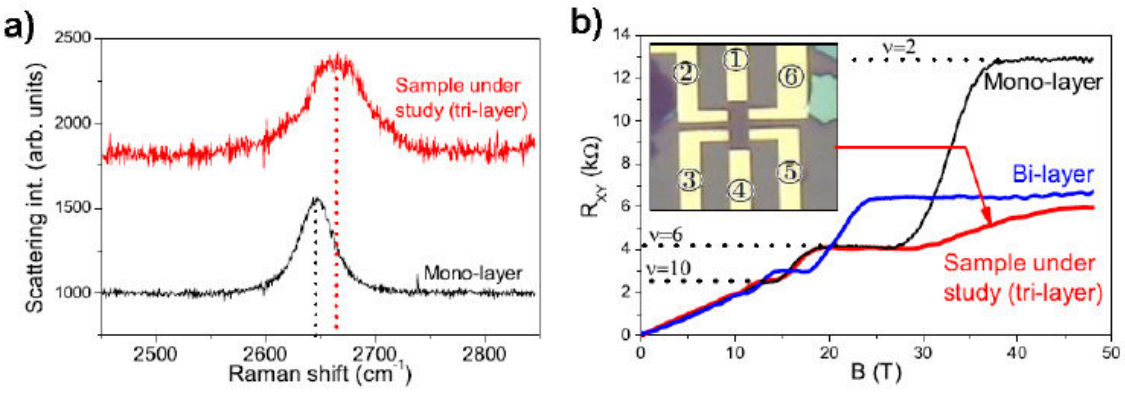

Figure 1: *a) Raman spectra of the sample under study (graphene trilayer) and monolayer graphene for comparison. b) High field Quantum Hall resistance for monolayer, bilayer and trilayer graphene. Inset : optical image of the sample under study.*

POINT DEFECTS ON GRAPHENE ON METALS

D. Fernández-Torre[1], M.M. Ugeda[2], I. Brihuega[2], P. Pou[1], A.J. Martínez-Galera[2], R. Pérez[1], and J.M. Gómez-Rodríguez[2]

[1]Departamento de Física Teórica de la Materia Condensada, Univ Autónoma de Madrid, 28049 Madrid, Spain
[2]Departamento de Física de la Materia Condensada Univ Autónoma de Madrid, 28049 Madrid, Spain
delia.fernandez @ uam.es

Understanding the coupling of graphene with its local environment is absolutely critical to be able to integrate it in tomorrow's electronic devices. Previous studies have shown that highly perfect sheets of graphene can be obtained by epitaxial growth on metal surfaces, and for some transition elements, like Ir or Pt, the interaction is so weak that many characteristic properties of graphene, such as the Dirac cones, are preserved [1,2]. In this work, we show how the presence of a metallic substrate of this kind affects the properties of an atomically tailored graphene layer. After growing a pristine monolayer on a Pt(111) surface, we have deliberately created single carbon vacancies on the graphene sheet, and studied its impact in the electronic, structural and magnetic properties. To this end, we combine low temperature scanning tunneling microscopy (LT-STM) experiments [3] with density functional theory calculations (DFT) and non-equilibrium Green's functions (NEGF) methods to model the electronic transport [4]. The DFT calculations have been performed using the PBE functional empirically corrected to take into account dispersion interactions [5]. Some of our results are displayed in Figure 1. For the non-defective graphene adsorbed on Pt(111), our calculations show that the periodic modulations typically observed by STM on the Moiré patterns can be explained as a purely electronic effect, because the simulated image is anticorrelated with the topmost regions of the corrugated sheet. For the vacancies on graphene/Pt(111), the calculations help us to associate the STM images observed with the positions of the atoms. Our experiments reveal a broad electronic resonance which is shifted above the Fermi energy, and resembles that previously observed near the Fermi level on graphite [6]. Vacancy sites become reactive, leading to an increase of the coupling between the graphene layer and the metal substrate at these points. This gives rise to a rapid decay of the localized state and the quenching of the magnetic moment associated with carbon vacancies in free-standing graphene layers.

References:

[1] Pletikosic et al, Phys. Rev. Lett., 102 (2009) 056808.
[2] P. Sutter et al, Phys. Rev. B, 80 (2009) 245411.
[3] M. M. Ugeda, doctoral thesis, Universidad Autónoma de Madrid (to be published)
[4] J.M. Blanco et al, Prog. Surf. Sci., 81 (2006) 403.
[5] S. Grimme, J. Comp. Chem. 27 (2006) 1787; G. Kresse and J. Furthmüller, Phys. Rev. B 54 (1996) 11169.
[6] M.M. Ugeda et al, Phys. Rev. Lett., 104 (2010) 096804.

Figures:

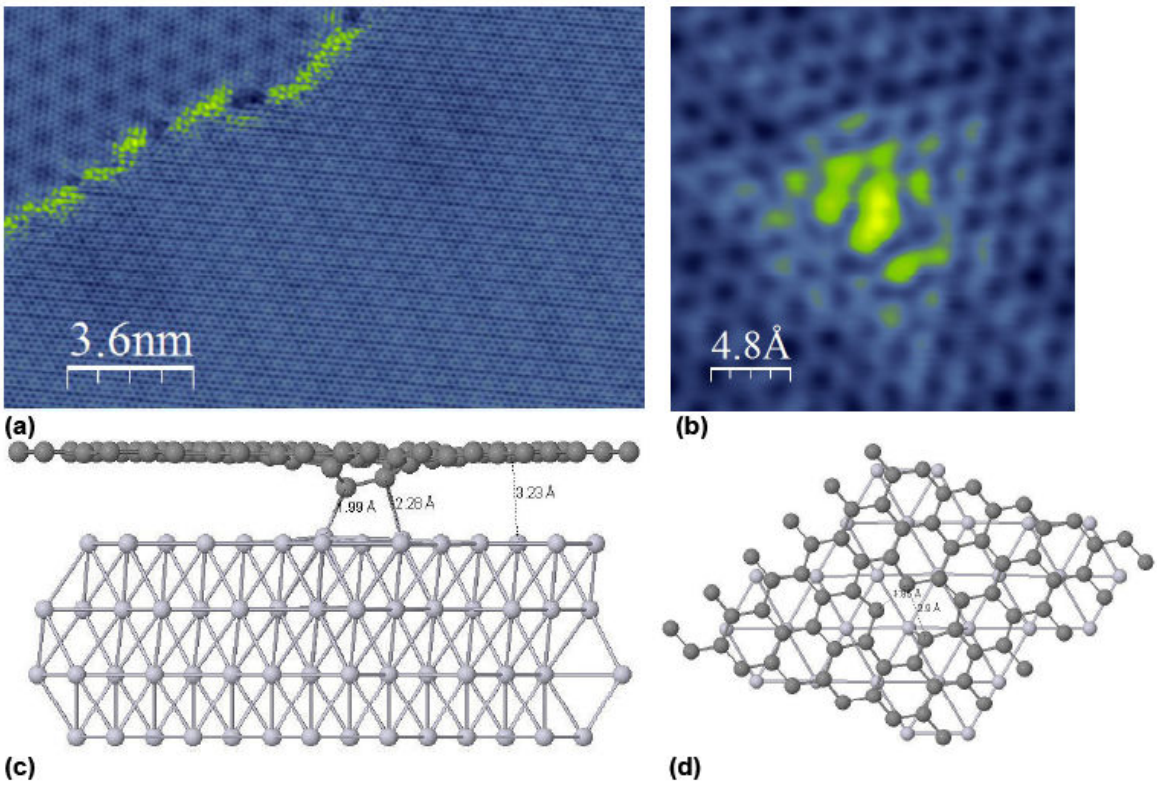

Figure 1: *(a) 14x20 nm2 STM image of the pristine graphene/Pt(111) surface showing two different Moiré structures: an R19xR19 on the upper left side and a 3x3 in the rest of the image. Sample bias: 50 mV, tunneling current: 1.0 nA. (b) STM image of a single vacancy on graphene/Pt(111). Sample bias: -30mV, tunneling current: 0.8 nA. (c) and (d) One of the possible adsorption sites for a single vacancy in graphene on Pt(111). The supercell used is fully displayed in (c). In (d) we show only the topmost Pt layer for clarity.*

RAMAN SPECTROSCOPY OF GRAPHENE: STATE OF THE ART

Andrea C. Ferrari

Department of Engineering, University of Cambridge, Cambridge CB3 OFA, UK
acf26@eng.cam.ac.uk

Raman spectroscopy is the most common and informative characterization technique in graphene science and technology. It is used to determine the number of layers, doping, strain, defects, functional groups, quality and type of edges [1-15]. I will outline the state of the art in this field, the recent developments and future directions of research, focussing on the link between Raman spectra and sample mobility, the quantification and identification of defects, and the role of electron-electron interactions.

References:

[1] A. C. Ferrari et al. Phys. Rev. Lett. 97, 187401 (2006)
[2] C. Casiraghi et al. Nano. Lett. 7, 2711 (2007)
[3] C. Casiraghi et al. Appl. Phys. Lett. , 91, 233108 (2007)
[4] S. Pisana et al. Nat. Mater. 6, 198 (2007)
[5] S. Piscanec et al. Phys. Rev. Lett. 93, 185503 (2004)
[6] C. Casiraghi, et al. Nano Lett. 9, 1433 (2009)
[7] A. C. Ferrari, Solid State Comm. 143, 47 (2007)
[8] A. Das et al. Nature Nano. 3, 210 (2008)
[9] A. Das et al. Phys. Rev. B 79, 155417 (2009)
[10] T. M. G. Mohiuddin et al. Phys. Rev. B 79, 205433 (2009)
[11] J. Yan et al. Phys. Rev. Lett. 98, 166802 (2007)
[12] D Graf et al. Nano Lett. 7, 238 (2007)
[13] A. C Ferrari et al. Phys. Rev. B 61, 14095 (2000); 64, 075414 (2001)
[14] D. M. Basko et al. Phys Rev B 80, 165413 (2009)
[15] F. Schedin et al. ACS Nano (2010)

PHYSICAL CONSEQUENCES OF ELECTRON-ELECTRON INTERACTIONS IN GRAPHENE LANDAU LEVELS

Mark Oliver Goerbig

Laboratoire de Physique des Solides, CNRS, Univ Paris-Sud, Bât. 510, 91405 Orsay cedex, France
goerbig@lps.u-psud.fr

The relative role of electron-electron interactions in graphene can be triggered via the magnetic field. Whereas in the absence of such quantising field, the relative strength of the interactions is given in terms of the "graphene fine-structure constant", the latter is relevant in graphene in a magnetic field only in the integer quantum Hall effect, i.e. when an an integer number of Landau levels is completely filled. In this case, a perturbative treatment of the electron-electron interactions provides valuable insight into the collective excitations of graphene in a magnetic field. In comparison with non-relativistic 2D electron systems, graphene displays a similar upper-hybrid mode (the magnetic-field descendant of the 2D plasmon), but also linear magneto-plasmons (see figure) that are an original feature of Dirac fermions in monolayer graphene [1,2].

However, because of the large Landau-level degeneracy, the situation is drastically different when the levels are only partially filled. In this case, inter-Landau-level excitations constitute high-energy degrees of freedom, due to the level separation, whereas the low-energy physical properties are governed by intra-Landau-level excitations [3]. Since these excitations do not alter the kinetic energy, the latter does not play any dynamical role and may be omitted, such that the remaining energy scale is set by the Coulomb interaction. One therefore obtains the regime of the fractional quantum Hall effect, or generally speaking that of strong electronic correlations. The observed fractional quantum Hall effect in graphene [4] displays the large internal symmetry [SU(4)] due to the fourfold spin-valley degeneracy of the relativistic Landau levels. The SU(4) picture of the fractional quantum Hall effect [5,6] has very recently found an experimental proof in four-terminal measurements on an h-BN substrate [7]. Most saliently, the family of 1/3 states may be stabilised in the case of even very small symmetry-breaking fields, such as the Zeeman effect, and displays novel collective spin-flip excitations beyond the Laughlin state [8].

References:

[1] R. Roldán, J.-N. Fuchs, and M. O. Goerbig, Phys. Rev. B 90 (2009) 085408.
[2] R. Roldán, M. O. Goerbig, and J.-N. Fuchs, Semicond. Sci. Technol. 25 (2010) 034005.
[3] M. O. Goerbig, arXiv:1004.3396 (2010).
[4] X. Du et al., Nature 462 (2009) 192; K. I. Bolotin et al., Nature 462 (2009) 196.
[5] M. O. Goerbig and N. Regnault, Phys. Rev. B 75 (2007) 241405.
[6] C. Töke and J. K. Jain, Phys. Rev. B 75 (2007) 245440.
[7] C. Dean et al., arXiv:1010.1179 (2010).
[8] Z. Papić, M. O. Goerbig, and N. Regnault, Phys. Rev. Lett. 105 (2010) 176802.

Figures:

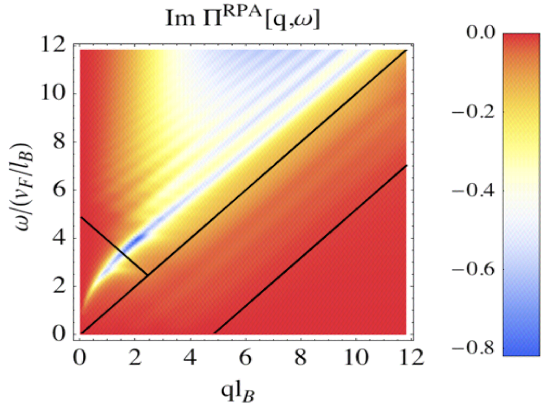

***Figure 1**: Imaginary part of the particle-hole excitation spectrum for graphene in the integer quantum Hall regime, calculated within the random-phase approximation. In addition to the upper-hybrid mode, which disperses as the square root of the wave vector at small values of the latter, one obtains linear magneto-plasmons that disperse roughly linearly parallel to the central diagonal.*

LOW MAGNETIC SIGNALS MEASURED BY A COMBINATION OF MFM AND KPFM

M. Jaafar[1], D. Martínez[1], R. Pérez[2], **J. Gómez – Herrero[1]**, O. Iglesias- Freire[3], L. E. Serrano[4], R. Ibarra[5], J. Mª de Teresa[4] and A. Asenjo[3]

[1] Dpto. Física de la Materia Condensada, Universidad Autónoma de Madrid, Spain
[2]Dpto. Física Teórica de la Materia Condensada, Universidad Autónoma de Madrid, Spain
[3]Instituto de Ciencia de Materiales de Madrid, CSIC, Spain
[4]Instituto de Ciencia de Materiales de Aragón, CSIC, Zaragoza, Spain
[5]Instituto de Nanociencia de Aragón, Zaragoza, Spain
miriam.jaafar@uam.es

The most outstanding feature of the Scanning Force Microscopy (SFM) is the capability to detect different short and long range interactions. In particular, Magnetic Force Microscopy (MFM) is used to characterize the domain configuration in ferromagnetic materials like thin films grown by physical techniques or ferromagnetic nanostructures. It is a usual procedure to separate the topography and the magnetic signal by scanning at a lift distance of 25-50nm so the long range tip –sample interactions dominate. The MFM is nowadays proposed as valuable technique to characterize more complex system such as organic nanomagnets, magnetic oxide nanoislands and carbon based materials [1]. In those cases, the magnetic nanoelements and its substrate present quite different electronic behavior i.e. they exhibit large surface potential differences which causes heterogeneous electrostatic interaction between tip and sample [2] that could be interpreted as magnetic interaction. To distinguish clearly the origin of the tip-sample forces we propose two different methods: (i) by applying *in situ* magnetic field during the MFM operation to detect the variation in the image contrast corresponding to the modification of the magnetic state of the tip or sample [3], (ii) by performing a combination of Kelvin Probe Force Microscopy (KPFM) and MFM to compensate the electrostatic contribution in the frequency shift signal The useful of the KPFM-MFM combination is illustrated by studying Co nanostripes grown by Focused Electron Beam [4] (Figure 1). As another example of this technique we investigate possible ferromagnetic order on the graphite surface [5]. The results show that the tip-sample interaction along the steps is independent of an external magnetic field. By combining KPFM and MFM, we are able to separate the electrostatic and magnetic interactions along the steps obtaining an upper bound for the magnetic force gradient of 16 μN/m (Figure 2). Our experiments suggest the absence of ferromagnetic signal in graphite at room temperature in strong contradiction with [1].

References:

[1] J.Cervenka, M. I. Katsnelson and C. F. J. Flipse, Nature Physics 5, (2009) 840 - 844
[2] R. Schmidt, A. Schwarz and R. Wiesendanger, Nanotechnology 20, (2009) 26400 7
[3] M. Jaafar, J. Gómez-Herrero, A. Gil, P. Ares, M. Vázquez, and A. Asenjo, Ultramicroscopy, 109, (2009) 693
[4] M. Jaafar, O. Iglesias-Freire, L. Serrano-Ramón, M.R. Ibarra J.M. de Teresa and A. Asenjo, in preparation
[5] D. Martínez, M. Jaafar, R. Pérez, J. Gómez - Herrero and A. Asenjo, Phys.Rew.Lett. 105 (2010) 257203

Figures:

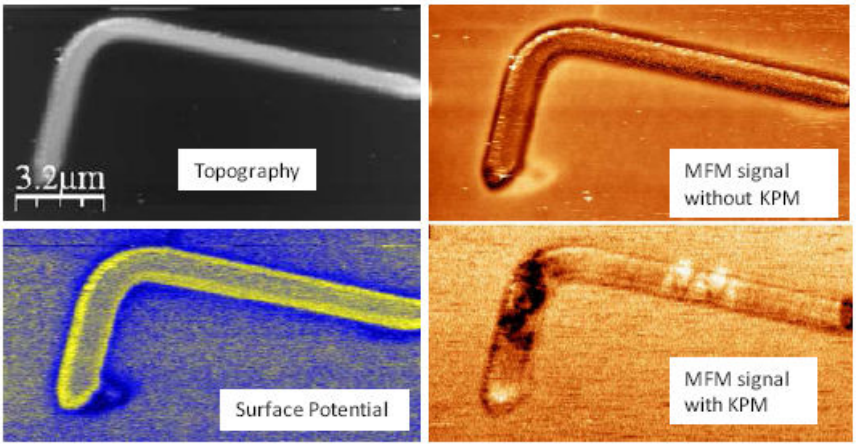

Figure 1: *(a) Topography and (b) MFM signal (frequency shift) of a cobalt nanostripe without electrostatic compensation. The contrast drastically changes when KPM is used simultaneously: (c) Surface potential image and (d) MFM signal with KPFM.*

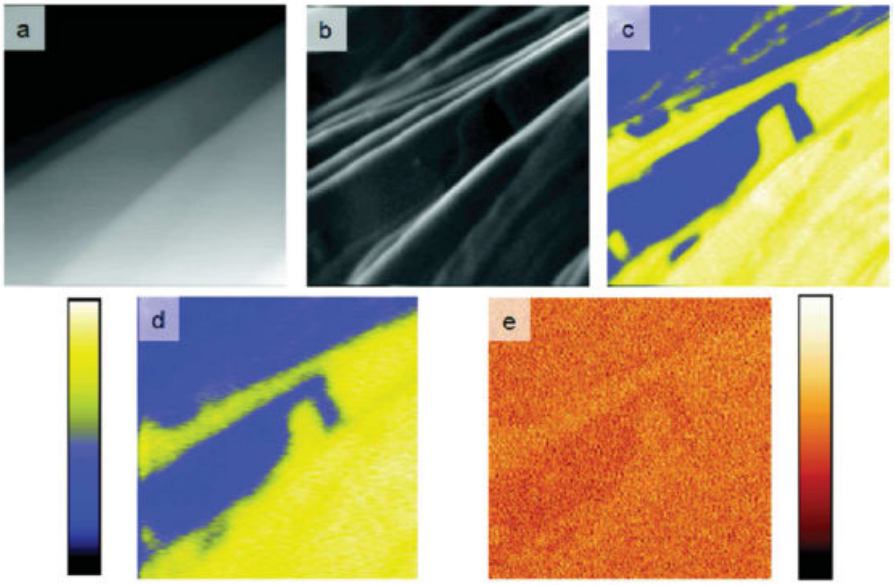

Figure 2: *3 µm x 3 µm AFM, KPFM, and MFM images taken in high vacuum with a cobalt-coated probe on ZYHHOPG. (a) Topography. (b) Edge enhanced image of (a) showing the surface steps. (c) KPFM image simultaneously taken with (a), showing electrostatic domains and steps on the sample surface (the potential difference between bright and dark areas is 200 mV). (d) KPFM image taken in retrace at 50 nm lift distance. (e) Frequency shift image taken simultaneously with (d). The total frequency shift variation in figure (e) is 0.4 Hz.*

IMPURITY SCATTERING IN COHERENT AND INCOHERENT SINGLE AND BILAYER GRAPHENE

Sophie Gueron, M. Monteverde, C. Ojeda Aristizabal, R. Weil, K. Bennaceur, C. Glattli, M. Ferrier, H. Bouchiat, J.N. Fuchs and D. Maslov,

Laboratoire de Physique des Solides, U. Paris Sud Orsay, France
gueron@lps.u-psud.fr

The nature of the scatterers which to this day limit the mobility of graphene, and determine most of its conduction properties, is still highly debated. Some groups attempt to deduce the nature of these scatterers from the effect of the dielectric surrounding the graphene. I will describe our approach in Orsay, which consists in comparing two different scattering times, the elastic scattering time and the transport scattering time, which play different roles in the magnetoresistance of the samples. I will show that the ratio of these two times, as well as their dependence with charge density, point to dominant scattering originating from strong, neutral, short range scatterers, rather than from charged impurities.
I will also present a consequence on quantum transport of the existence of these scatterers, namely, the reproducible conductance fluctuations in these samples at low temperature, when the quantum coherence extends over the entire sample length. We exploit the possibility to control the diffusion constant with gate voltage in monolayer and bilayer graphene to test the theory of mesoscopic fluctuations. We find that the correlation energy is given by the Thouless energy, and that the correlation field corresponds to a magnetic flux quantum threading a coherent area in the sample. But we find that the ergodicity hypothesis is not verified: the gate-voltage dependent fluctuations vary with gate voltage, and are largest near the charge neutrality point, whereas the magnetic field dependent fluctuations do not change with doping. The percolating nature of transport near the charge neutrality point may explain this unexpected result.

In both experiments, we exploit the asset of monolayer and bilayer graphene, namely the fact that the different band structures lead to different gate-voltage dependences of the diffusion coefficients, enabling a quantitative test of heories over broad ranges, impossible to realize with other materials.

References:

[1] C. Ojeda-Aristizabal, R. Weil, M. Ferrier, S. Guéron, H. Bouchiat, J.N. Fuchs, D.Maslov, “Transport and elastic scattering times as probes of the nature of impurity scattering in single and bilayer graphene”, M. Monteverde, Phys. Rev. Lett. 104, 126801 (2010).
[2] C. Ojeda-Aristizabal, M. Monteverde, R.Weil, M. Ferrier, S. Gueron, H. Bouchiat, “Conductance fluctuations and field asymmetry of rectification in graphene”, Phys. Rev. Lett. 104, 186802 (2010).

LARGE INTRINSIC BAND GAPS, FERROMAGNETISM, AND ANOMALOUS MAGNETORESISTANCE OSCILLATIONS DERIVED FROM GRAPHEME EDGE STATES: NANORIBBONS AND ANTIDOT-LATTICE GRAPHENES

Junji Haruyama

Faculty of Science and Engineering, Aoyama Gakuin University, 5-10-1 Fuchinobe, Sagamihara, Kanagawa 252-5258, Japan
J-haru@ee.aoyama.ac.jp

A variety of quantum phenomena observed in graphene is attracting significant attention. In contrast, few works have experimentally reported edge states and related phenomena, although there are so many theoretical reports, which predicted that electrons localize at zigzag edges of graphene due to presence of flat bans and the electron spins strongly polarize. One main reason for lack of experimental reports is high damages at edges introduced by lithographic fabrication.

Here, in the talk, I will present the following two systems fabricated by non-lithographic methods in order to reveal edge-related phenomena; 1. Graphene nanoribbons (GNRs) fabricated by chemical unzipping of carbon nanotubes (CNTs) and 3-stepped annealing [1] and 2. Antidot-lattice graphenes (ADLGs; graphene nano-pore arrays) fabricated using nano-porous alumina templates as etching masks [2, 3].

In the GNRs, we confirm low defects by Raman spectrum, HRTEM, single electron spectroscopy, and also electrical measurements. I present a large an intrinsic energy band gap of 55 meV, which is 7-times larger than those in lithographically fabricated GNRs with defects. It can be understood by calculation for arm-chair edge GNRs.

In the ADLGs, we confirm high electronic density of states at antidot (nano pore) edges by STM. I will show appearance of room-temperature ferromagnetism and anomalous magnetoresistance oscillations derived from edge-localized spins in hydrogen-terminated ADLGs. They can be qualitatively understood by theories for zigzag edges. These results must open a new door to all-carbon (rare-metal free) magnets and also spintronic devices based on spin Hall effects by inducing spin-orbit interaction.

References:

[1] T.Shimizu, J.Haruyama, et al, “Large intrinsic energy bandgaps in annealed nanotube-derived graphene nanoribbons” Nature Nanotech. 6, 45-50 (2011) (Selected for Latest Highlights, News&Views, and Cover index)
[2] T.Shimizu, J.Haruyama, et al, “Edge-state-derived ferromagnetism and anomalous magnetoresistance in antidot-lattice graphenes” To be published on Phys.Rev.Lett.
[3] K. Tada, J.Haruyama, et al, “All-carbon ferromagnetism derived from edges states in graphene nano-pore arrays” Nature Nanotrch. In-depth Review

SUBSTRATE DEPENDENCE IN HYDROGEN-GRAPHENE INTERACTION

L. Hornekær, L. Nilsson, M. Andersen, R. Balog, J. Bjerre, B. Jørgensen, J. Thrower, E. Friis, E. Lægsgaard, F. Besenbacher, I. Stensgaard, P. Hoffman and B. Hammer

Dept. Physics and Astronomy and Interdisciplinary nano-science center, iNANO, Aarhus University, Ny Munkegade Bygn. 1520, Aarhus C, Denmark
liv@phys.au.dk

Theoretical and experimental studies have revealed that the properties of graphene can be changed substantially by hydrogenation. Theoretical calculations show that fully hydrogenated graphene, referred to as graphane, is an insulator [1] and that hydrogen line structures can induce graphene nanoribbon – like band gaps in graphene [2]. Experimental investigations reveal a change of electronic properties of graphene upon hydrogenation [3-6]. The experiments also show that graphene hydrogenation is substrate dependent [6-9]. Here we report on the substrate dependence of hydrogen adsorbate structures on graphene on SiC, Ir(111), Pt(100) and graphite.

Combined STM, TPD, DFT and XPS investigations of the interaction of graphene with atomic hydrogen reveal the formation of different types of hydrogen adsorbate structures on the graphene surface, depending on the degree and type of interaction between graphene and the underlying substrate. In the case of low substrate interaction, dimer like structures, similar to those displayed in figure 1.a. are observed, while in the case of a higher degree of interaction with the substrate, cluster structures with higher stability, similar to those displayed in figure 1.b. are observed. Furthermore, in some systems hydrogenation is observed to lead to increased graphene-substrate interaction.

In e.g. the graphene-Pt(100) system the graphene-substrate interaction is observed to be coverage dependent. At low coverage, hydrogen atoms are observed to form dimer structures similar to those observed previously on graphite, while, at higher coverage the reconstruction of the platinum substrate is lifted and more stable hydrogen adsorbate structures are observed. The experimental data indicate that the Pt substrate plays an active role in stabilizing these adsorbate structures on graphene.

References:

[1] Sofo, J.O., Chaudhari, A.S., & Barber, G.D., Phys. Rev. B, 75 (2007) 153401
[2] Chernozatonskiĭ, L., Sorokin, P., Belova, E., Brüning, J., & Fedorov, A., Jetp. Lett. 85 (2007) 77
[3] Bostwick, A. McChesney, J.L. Emtsev, K.V. Seyller, T. Horn, K. Kevan, S.D. & Rotenberg, E., Phys. Rev. Lett. 103 (2009) 1
[4] Elias, D., Nair, R.R., Mohiuddin, T.M.G., Morozov, S.V., Blake, P., Halsall, M.P., Ferrari, A.C., Boukhvalov, D.W., Katsnelson, M.I., Geim, A.K., & Novoselov, K.S., Science 323 (2009) 610
[5] Guisinger, N., Rutter, G., Crain, J., First, P., & Stroscio, J., Nano Lett. 9 (2009) 1462
[6] Balog, R.; Jorgensen, B.; Nilsson, L.; Andersen, M.; Rienks, E.; Bianchi, M.; Fanetti, M.; Laegsgaard, E.; Baraldi, A.; Lizzit, S.; Sljivancanin, Z.; Besenbacher, F.; Hammer, B.; Pedersen, T. G.; Hofmann, P.; & Hornekaer, L., Nature Materials, 9 (2010) 315
[7] Hornekaer, L.; Sljivancanin, Z.; Xu, W.; Otero, R.; Rauls, E.; Stensgaard, I.; Laegsgaard, E.; Hammer, B.; & Besenbacher, F., Physical Review Letters 96 (2006) 156104
[8] Balog, R., Jørgensen, B., Wells, J., Lægsgaard, E., Hofmann, P., Besenbacher, F., & Hornekær, L., J. Am. Chem. Soc. 131 (2009) 8744
[9] Ng, M. L., Balog, R., Hornekaer, L., Preobrajenski, A. B., Vinogradov, N. A., Martensson, & N., Schulte, K., Journal Of Physical Chemistry C, 114 (2010) 18559

Figures:

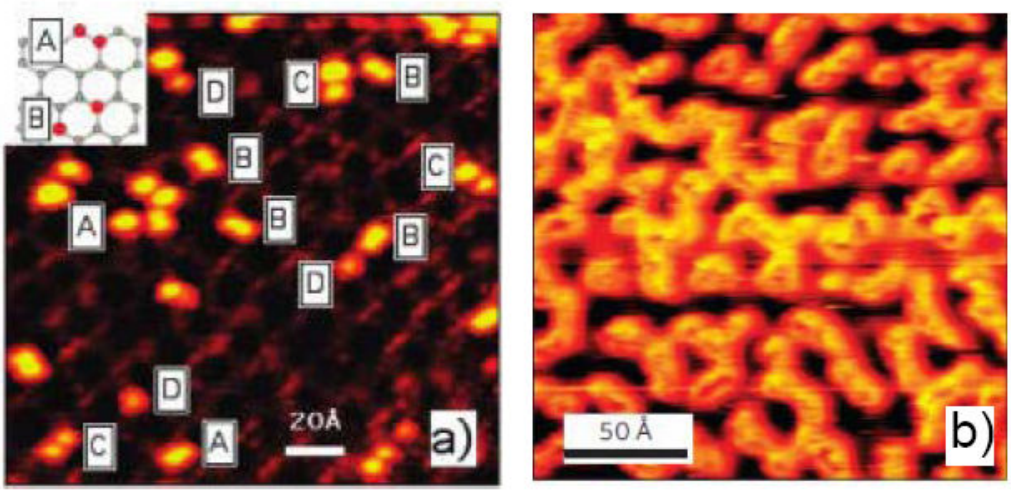

Figure 1: *a) Hydrogen dimer structures on graphene on SiC [8], b) Hydrogen clusters on graphene on Ir(111) [6].*

NANO-CARBON MATERIALS: SYNTHESIS AND CHARACTIRIZATION

Sumio Iijima

Faculty of Science and Technology, Meijo University, Tenpaku, Nagoya, Aichi, Japan
National Institute of Advanced Industrial Science and Technology / Nanotube Research Center
and, NEC Corporation
iijimas@meijo-u.ac.jp

Formation of a large size graphene sheet by a thermal CVD method using a copper substrate foil has been reported. The method requires a high temperature CVD reactor (near 1000ºC), so that it cannot be used in a conventional Si device process and therefore an alternative low temperature synthesis of graphene is needed. For this purpose we utilized a new surface-wave micro-wave CVD method which has been developed originally for the nano-diamond film growth at low temperature down to room temperature. We shall demonstrate the growth of an A4-size graphene sheet formed at 300ºC.

Another subject to be presented is concerned with structural characterization of nano-carbon materials using atom-resolution electron microscopes as well as other characterization methods. The advantage of high resolution electron microscopy (HRTEM) over other techniques is to be able to characterize local atomic structures such as lattice defects and edge structures of nano materials which cannot be studied in conventional techniques. Another emphasis of HRTEM will be on dynamic observation of a reaction process which is not available for other high resolution probe microscope techniques such as STM. A recent progress of HRTEM technology such as aberration correction and EELS, has allowed us to do elemental analysis, distinction of charge valency and more on the individual atom basis. Some latest examples of above mentioned observations on graphene edge structures and electronic states will be demonstrated.

ELECTRONIC TRANSPORT IN GRAPHENE ON HEXAGONAL BORON NITRIDE DEVICES

Pablo Jarillo-Herrero

Massachusetts Institute of Technology
77 Massachusetts Avenue, Bldg. 13-2017; Cambridge, MA 02139, USA
pjarillo@mit.edu

Hexagonal boron nitride (hBN) has been recently shown to be a high quality substrate for graphene devices. In this talk I will review our recent experiments on graphene on hBN devices. In particular I will describe STM measurements that show that electron-hole puddles are much reduced for graphene on hBN compared to graphene on SiO_2, and also our experiments on quantum Hall effect and Landau level crossings of Dirac fermions on high mobility trilayer graphene on hBN.

GRAPHENE SPINTRONICS

Roland Kawakami, Wei Han, Kathy McCreary, Keyu Pi

Department of Physics and Astronomy, University of California, Riverside, CA, 92521, USA
roland.kawakami@ucr.edu

Graphene is an attractive material for spintronics due to the low intrinsic spin-orbit coupling, low hyperfine coupling, and high electronic mobility. These should lead to long spin lifetimes and long spin diffusion lengths. Experimentally, the gate-tunable spin transport at room temperature has been achieved with spin diffusion lengths of ~2 microns. This makes it a very unique and promising material for spin transport. However, the spin injection efficiency has been low and the spin lifetime is still much shorter than expected theoretically. Overcoming these challenges will make graphene a very strong material for spintronics.

In this talk, I will present three of our recent results in graphene spintronics.

(1) **Tunneling spin injection into graphene [1].** We utilized TiO2-assisted deposition of MgO tunnel barriers in order to reduce pinholes, which easily form for thin films on graphene. The use of tunnel barriers enhances the spin injection efficiency by alleviating the conductivity mismatch between the ferromagnetic metal (Co) and the single layer graphene (SLG). The non-local spin signal is found to be as high as 130 ohms at room temperature, with a spin injection efficiency of 30%. This is the highest spin injection efficiency observed in graphene spin valves.

(2) **Long spin lifetimes in graphene [2].** In addition to enhancing the spin injection efficiency, we find that the measured spin lifetime is also enhanced by the tunnel barriers. This indicates that the reported values of spin lifetime are shorter than the actual spin lifetime in graphene due to the invasive nature of the ferromagnetic contacts. Using the tunneling contact to suppress the contact-induced spin relaxation, we investigate the gate and temperature dependence of SLG and bilayer graphene (BLG) spin valves. We find spin lifetimes as high at 771 ps at 300 K in SLG, 1.0 ns at 4 K in SLG, and 6.2 ns at 20 K in BLG (see figure). These are the longest spin lifetimes observed in SLG, and the 6.2 ns is longest spin lifetime observed in a graphene spin valve so far.

(3) **Modification of spin transport properties by surface doping [3].** Because graphene is extremely surface sensitive, there are opportunities to manipulate the spin transport properties by modifying the surface with various dopants. In the initial study, we investigated the effect of gold doping on spin transport and spin lifetime. We find that the spin transport properties such as nonlocal signal and spin lifetime can be enhanced, despite the presence of additional charged-impurity scattering. Mainly, the presence of the gold impurities does not produce a degradation of spin transport, despite greatly reducing the electronic mobility.

These advances are important for the development of spin-based computing with integrated logic and memory.

References:

[1] Wei Han, K. Pi, K. M. McCreary, Yan Li, Jared J. I. Wong, A. G. Swartz, and R. K. Kawakami, Physical Review Letters, 105 (2010) 167202.
[2] Wei Han and R. K. Kawakami, arXiv:1012.3435 (2010).
[3] K. Pi, Wei Han, K. M. McCreary, A. G. Swartz, Yan Li, and R. K. Kawakami, Physical Review Letters, 104 (2010) 187201.

Figures:

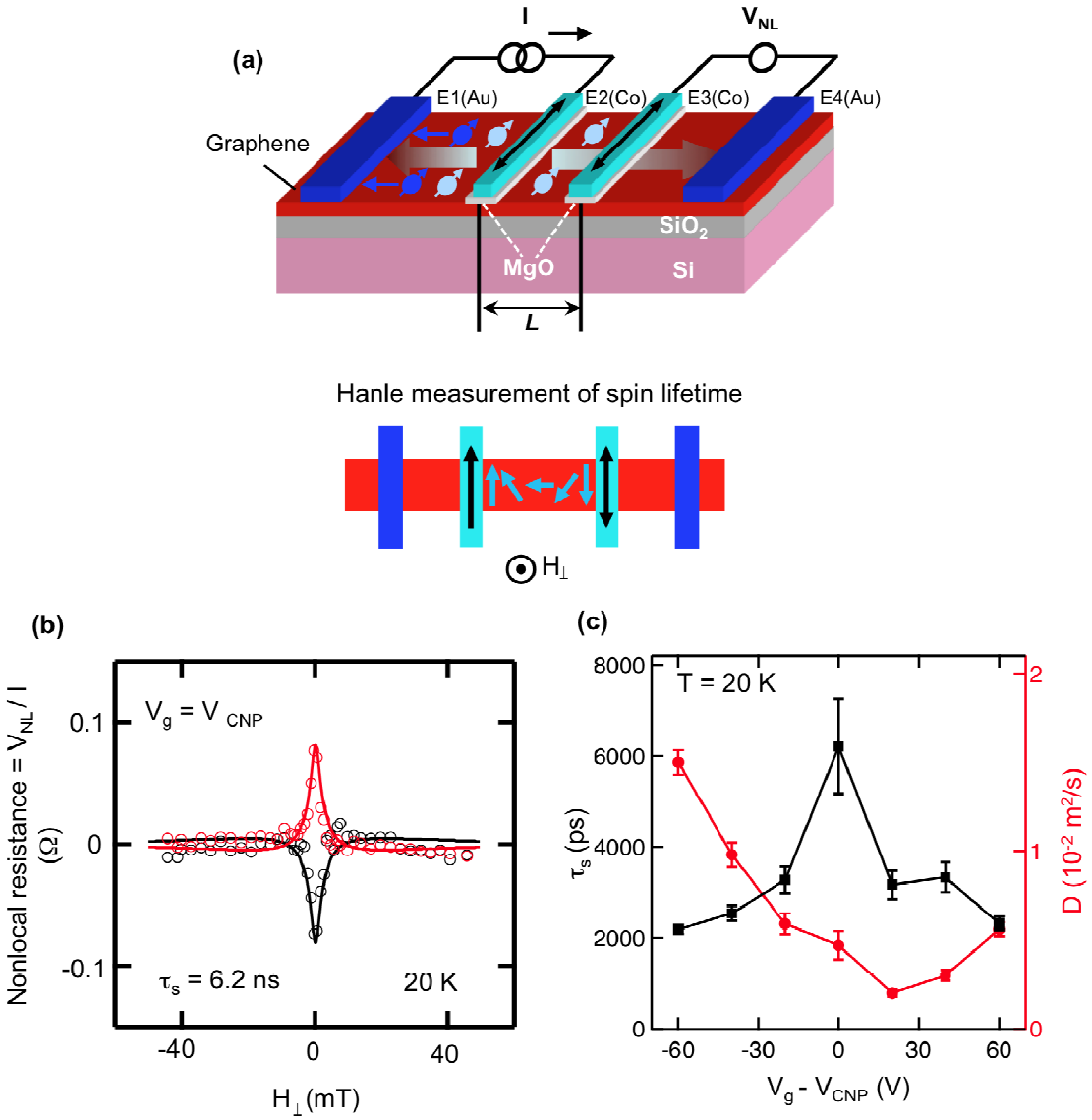

Figure 1: *Long spin lifetimes in graphene. (a) Schematic drawing of a graphene spin valve in the nonlocal measurement geometry. A current source (I) is utilized to inject spin-polarized carriers into the graphene at electrode E2. The spins subsequently diffuse to electrode E3 where they are detected as a voltage V_{NL} measured across electrodes E3 and E4. The spin injection and transport is measured as the nonlocal resistance ($R_{NL} = V_{NL}/I$). Hanle spin precession measurements are performed to determine the spin lifetime. An out-of-plane magnetic field is applied to induce spin precession. (b) Hanle measurement of a bilayer graphene spin valve with L = 3.05 microns, gate voltage (V_g) tuned to the charge neutrality point (CNP), and T = 20 K. The red (black) data is for parallel (antiparallel) alignment of the the Co magnetizations. The narrow Hanle peak corresponds to a spin lifetime of 6.2 ns. (c) Gate dependence of spin lifetime (black) and diffusion coefficient (red) in bilayer graphene at 20 K. Their opposite behaviors indicate the relevance of Dyakonov-Perel spin scattering.*

MANIFEST OF ELECTRON INTERACTIONS IN QUANTUM HALL EFFECT IN GRAPHENE

Philip Kim

Columbia University, USA

The quantum Hall ferromagnetism (QHFM) and fractional quantum Hall effect (FQHE) in 2-dimensional electron gas with multiple internal degrees of freedom provides a model system to study the interplay between spontaneous symmetry breaking and emergent topological order. In graphene, the structure of the honeycomb lattice endows the electron wavefunctions with an additional quantum number, termed valley isospin, which, combined with the usual electron spin, yields four-fold degenerate Landau levels (LLs). This additional symmetry modifies the QHFM and FQHE with intriguing interplay between two different spin flavours. As a consequence, it is conjectured to produce new incompressible ground states in graphene, reflecting strong electron interactions. In this presentation we report multiterminal measurements of the FQHE in high mobility graphene devices fabricated on hexagonal boron nitride substrates. The measured energy gaps of observed FQHE are large, particularly in the second Landau level where they measure up to times larger than those reported in the cleanest conventional systems. In the lowest Landau level, the hierarchy of FQH states reflects the additional valley degeneracy. We will also discuss the implication of QHFM with spin and valley spin degree of freedoms.

UNDERSTANDING THE POTENTIAL OF GRAPHENE WITHIN COMPOSITES: INTERFACIAL STRESS TRANSFER IN IDEAL GRAPHENE COMPOSITES

I.A. Kinloch[1], L. Gong[1], A. Raju[1], I. Riaz[2], R. Jalil[2], K.S. Novoselov[2], R.J. Young[1]

[1]School of Materials, [2]School of Physics and Astronomy, University of Manchester, Manchester, U.K
ian.kinloch@manchester.ac.uk

Graphene is one of the stiffest and strongest known materials with a Young's modulus of the order of 1 TPa and a fracture stress ~ 130 GPa. These properties make graphene an ideal candidate for use as a reinforcement in high-performance composites. However, being one-atom thick crystalline material, graphene poses several rather fundamental questions: (1) Can decades of research on carbon based composites be applied to such ultimately thin crystalline material? (2) Would traditionally used continuous mechanics still be valid at atomic level? (3) How does the macroscopic matrix interact with microscopic graphene crystals (in terms of stress transfer, for instance) and what kind of theoretical description would be appropriate? (4) How does stress transfer between the layers in bilayer and thicker graphene?

We have prepared model composites consisting of single graphene flakes (monolayer and thicker) sandwiched between thin polymer films and employed Raman spectroscopy to monitor stress transfer from the polymer matrix to the graphene during deformation of the composite [1]. Typically, a PMMA beam was coated with 300 nm of epoxy, onto which mechanically exfoliated graphene was placed, finally a 50 nm PMMA coating was then spun onto the graphene. The coated beam was tested in 4-point bending and the Raman spectra were collected to confirm the morphology of the flake being studied and map the strain within it.

The rate of peak shift of the G' peak with applied strain has been shown for carbon reinforcements to be proportional to the effective modulus of the filler in the composite [2]. (This effective modulus takes into account the efficiency of the polymer-filler interface). A shift of ~ 35 cm^{-1}/% was obtained for the monolayer graphene upon initial loading, corresponding to an modulus of ~ 0.6 TPa. The polymergraphene interface was found to fail at high strains but would heal upon relaxation of the sample. The peak shift rate upon unloading, however, was 60 cm^{-1}/%. This shift rate is the highest we have ever observed in any composite system and corresponds to an effective modulus of ~ 1 TPa. This result shows that the full modulus of graphene can be achieved within a polymer matrix.

Mapping the G' peak shift across the flake showed that the strain in a flake was virtually zero at the ends of the flake and built up to the applied, global strain value in the middle. This behaviour was successfully modeled using the continuum shear-lag theory, which is the established model for macroscale fillers. In particular, the diamond shape of the flake that was studied allowed an accurate fit of the model since it meant that the strain data over a range of aspect ratios could be obtained. The maximum shear force at the polymer-graphene interface was calculated as 3 MPa, which is an order magnitude less than that typically achieved in conventional carbon fibre-epoxy composites. Such a low shear force maybe expected, given the weak nature of the van der Waal forces at the interface. One result of these poor interfacial properties is that the critical length of the graphene required to obtain efficient reinforcement was found to be 30 microns. This result implies that in order for graphene to be used in structural composites, the graphene flakes either need to be large (> 30 microns long) or chemically functionalised to improve the interfacial strength with the matrix.

References:

[1] L. Gong, I. A. Kinloch, R. J. Young, I. Riaz, K. S. Novoselov, Advanced Materials, 24 (2010), 2694- 2697.
[2] C. A. Cooper, R. J. Young, M. Halsall, Composites Part A- Applied Science and Manufacturing, 32 (2010), 401-411

Figures:

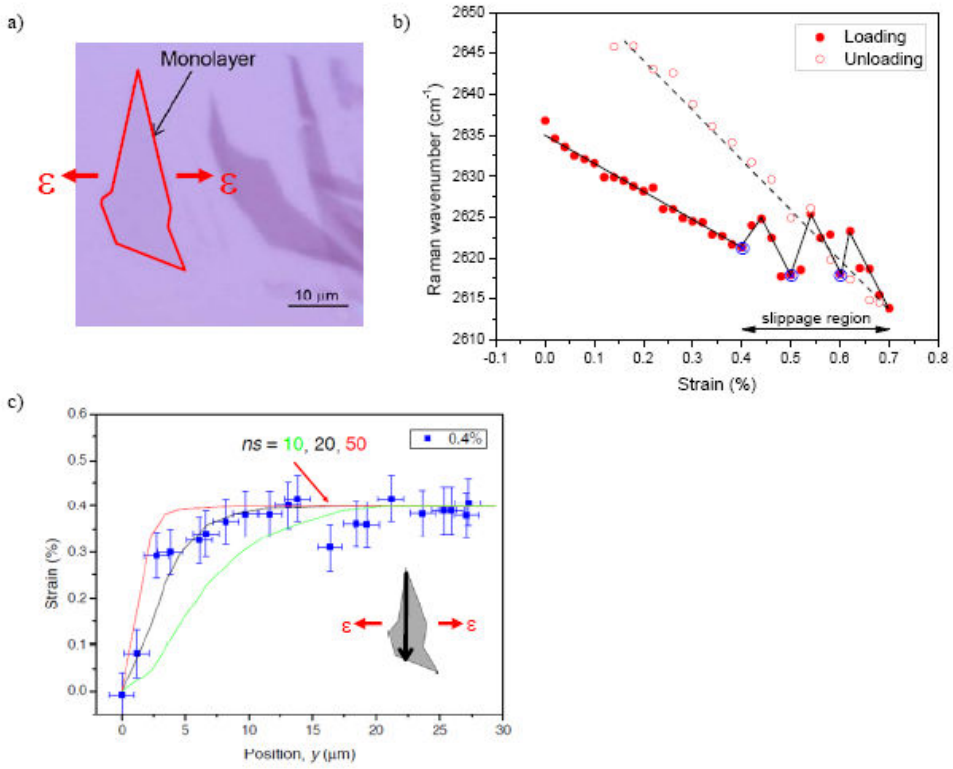

Figure 1: *1a) An optical micrograph showing the flake studied for b) and c), with its outline and the direction the deformation was applied highlighted. b) The position of the G' band at the centre of the flake as function of global strain. The relaxation in the slippage region occurred during mapping of the strain in the flakes. c) The strain distribution down the centre of the flake, scanned perpendicular to the direction of the applied deformation. The curves show the fits of the shear lag model for different values of the factor of stress efficiency transfer, n, and aspect ratio, s.*

LOCAL ON-OFF CONTROL OF A GRAPHENE P-N PHOTODETECTOR

F.H.L. Koppens[1,4], M.C. Lemme[1], A.L. Falk[1], M.S. Rudner[1], H. Park[1,2], L.S. Levitov[3], C.M. Marcus[1]

[1]Department of Physics, Harvard University, Cambridge, MA 02138, USA
[2]Department of Chemistry and Chemical Biology, Harvard University, Cambridge, MA 02138, USA
[3]Department of Physics, Massachusetts Institute of Technology, Cambridge, MA 02139, USA
[4]ICFO, The institute of Photonic Sciences, Barcelona, Spain
frank.koppens@icfo.es

Graphene is a promising photonic material whose gapless band structure allows electron-hole pairs to be generated over a broad range of wavelengths, from UV, visible, and telecommunication bands, to IR and THz frequencies [1]. Previous studies of photocurrents in graphene have demonstrated photoresponse near metallic contacts [2] or at the interface between single-layer and bilayer regions. Photocurrents generated near metal contacts were attributed to electric fields in the graphene that arise from band bending near the contacts and could be modulated by sweeping a global back-gate voltage with the potential of the contacts fixed.

Here, we will discuss the photoresponse of graphene devices with top gates, separated from otherwise homogeneous graphene by an insulator. When the top gate inverts the carrier type under the gate, and a p-n junction is formed at the gate edges, a highly localized photocurrent is observed using a focused scanning laser [3]. Interestingly, a density difference induced by the top gate that does not create a p-n junction does not create local photosensitivity. In this way, by switching from the bipolar to ambipolar regime, our devices allow for on-off control of photodetection (see Figure).

Comparing experimental results to theory suggests that the photocurrent generated at the p-n interface results from a combination of direct photogeneration of electron-hole pairs in a potential gradient, and a photothermoelectric effect in which electric fields result from optically induced temperature gradients. We envision that this type of local on-off control of photodetection allows for the implementation of broadband bolometers with submicron pixelation.

References:

[1] F Bonaccorso, Z Sun, T Hasan, A. C Ferrari, Graphene photonics and optoelectronics. Nature Photonics (2010) vol. 4 (9) pp. 611-622
[2] Lee, E. J. H., Balasubramanian, K., Weitz, R. T., Burghard, M. & Kern, K. Contact and edge effects in graphene devices. Nature Nano. 3, 486 (2008)
[3] M. C Lemme, F. H. L Koppens, A. L Falk, M. S Rudner, H Park, L. S Levitov, C. M Marcus Local On- Off Control of a Graphene p-n Photodetector. arXiv:1012.4745v1 (2010)

Figures:

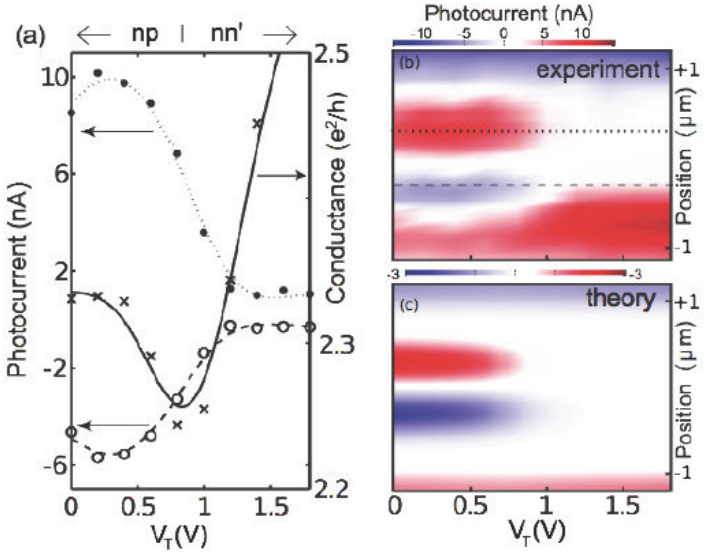

Figure 1: *a) Photocurrent (left axis, circle markers) as a function of top gate voltage with the laser positioned on either side of the top gate. Photocurrents turn on at the charge neutrality point under the top gate, as the device is switched from n-n'-n to n-p-n configuration. Source-drain conductance (right axis, cross markers) of the photodetector measured in FET configuration as a function of top gate voltage with charge neutrality point at V_T = 0.9 V (drain voltage V_D = 0.6 mV). Due to hysteresis when sweeping the top gate voltage, this curve is shifted compared to the data in Fig 1c. b) Photocurrent as a function of top gate voltage taken across the center of the photodetector in Fig 1. The laser wavelength was λ = 600 nm and the power was P = 40 μW. c) Theoretical model of the photocurrent (Eq. 1), plotted as a function of top gate voltage and position along the center of the photodetector. P_0 = 40 μW and we assume 4.6% absorption of the laser light because it passes through the graphene sheet twice due to mirroring at the SiO_2/Si interface.*

TUNABLE MANY BODY INTERACTIONS IN GRAPHENE

Alessandra Lanzara

University California, Berkeley
Materials Sciences Division, Lawrence Berkeley National Laboratory, USA

The discovery of graphene in 2004 has opened a new exciting area of research in condensed matter physics. Not only graphene is the first real two dimensional material ever observed in nature, but it is also characterized by an unusual electronic structure with respect to most condensed matter systems. Indeed, the low energy excitations in graphene behave as Dirac fermions, chiral quasiparticles with zero effective mass, and obey the relativistic Dirac equation, where the speed of light is replaced by the Fermi velocity. This is in striking contrast with most of materials known today, where the low energy excitations obey the non-relativistic Shcroedinger equation and have finite effective mass.

This unusual electronic structure leads to a variety of novel properties and huge potential for applications, the most striking one being the failure of the standard Landau-Fermi liquid picture for quasiparticles.

In this talk I will present an overview of the electronic structure of this amazing two dimensional material and will discuss how this linear dispersion can be easily modified by quantum size effects, substrate interaction, doping and disorder.

Moreover, I'll discuss how fundamental properties such as electron-phonon and electron-electron interactions are modified with respect to a standard metal and do not obey the Fermi liquid picture for quasiparticles.

The implications of our study on the properties of Dirac materials and their potential role for applications are also discussed.

DOUBLE RESONANT RAMAN IN GRAPHENE: ALL YOU WANTED TO KNOW ABOUT

M. Lazzeri[1], P. Venezuela[1,2], F. Mauri[1]

[1]IMPMC, Paris 7, CNRS, Paris, France
[2]Instituto de Fisica, Universidade Federal Fluminense, 24210-346, Niteroi RJ, Brazil
michele.lazzeri@impmc.jussieu.fr

Raman specrtroscopy is the most widely used experimental characterization technique to study graphene samples. Raman lines such as the defect-induced D and D', their overtones and the D'+D'', are usually interpreted within the double resonance mechanism. These lines are very well studied since they can be used as an experimental probe of the presence of defects but, also, to determine the presence of a monolayer in few-layers graphene samples.

Several excellent theoretical works already appeared on this topic providing an overall good understanding of the situation. However, the many different approximations used by different authors (e.g. constant electron-phonon matrix elements, resonant phonons are assumed to be on some high symmetry line, in some cases the electronic dispersion is conic, the electronic life-time is a parameter, etc.) and the several debates still going on leave with the unpleasant sensation that something is missing. Besides, some fundamental questions are basically untouched: Which kind of defects are probed by measuring different lines? Does Raman spectroscopy probe the defects which mostly influence electronic transport?

We determined [1] the DR Raman spectra of graphene by using the most precise available electronic bands, phonon dispersions, and electron-phonon coupling matrix elements (obtained by combining ab-initio density functional theory and many-body GW methods). Three different model defects are considered. The method results in a consistent framework to determine the position, the shape, the width and the intensity of the Raman lines as a function of the laser energy and of the defect concentration. Moreover it allows to treat at the same level defect-induced lines and two-phonon lines. The overall agreement with available experimental data is very good.

References:

[1] P. Venezuela, M. Lazzeri, and F. Mauri, to be published.

MAKING NANO-GRAPHENE

Kian Ping Loh

Department of Chemistry, National University of Singapore, 3 Science Drive 3, Singapore 117543
chmlohkp@nus.edu.sg

In this talk, I will discuss new chemical strategies to synthesize graphene, from large area sheets to nanographene.

Majority of the solution-phase methods produce irregularly-sized and shaped graphene sheets due to the intrinsic randomness in the defect-mediated exfoliation or cutting process of the precursor graphitic flakes. To produce highly regular graphene nanostructures, a fabrication process that is driven by thermodynamics, as in crystal growth, should be more suitable than defect-mediated fragmentation processes. To this end, we will show how we apply templated-directed synthesis to fabricate regular-sized graphene quantum dots. The dynamics of carbon cluster diffusion and aggregation to form nanographene islands is recorded by dynamic Scanning Tunneling Microscopy. The charge transfer interactions between graphene and fullerene, as well as the Van der waals epitaxy of Grapnene on self-assembled C60 will be discussed.

Graphene form functional hybrids with organic molecules, quantum dots and polymers and these can exhibit non-linear optical limiting properties, saturable absorption properties, outstanding photovoltaic and biosensing properties. Some examples of these applications studied in our laboratory will be given in this talk.

Acknowledgement:

This project is funded by the National Research Foundation Competitive Research Funding - Graphene and Related Materials R-143-000-360-281.

References:

[1] Kian Ping Loh, Qiaoliang Bao, Goki Eda, Manish Chhowalla; Graphene oxide as a chemically Tunable Platform for Optical Applications, Nature Chemistry, ASAP (Dec 2010)
[2] Tang LAL, Wang JZ, Loh KP*; Graphene-Based SELDI Probe with Ultrahigh Extraction and Sensitivity for DNA Oligomer, Journal of the American Chemical Society,: 132, 32, 10976-10977 (2010)
[3] J., Yang, J.-X., Xiao, S., Bao, Q., Jahan, M., Polavarapu, L., Wei, J., Xu, Q.-H. and Loh, K.P; A Graphene Oxide–Organic Dye Ionic Complex with DNA-Sensing and Optical-Limiting Properties Balapanuru, . Angewandte Chemie International Edition, 49 (37), 2010, 6549–6553.
[4] Wang SA, Tang LAL, Bao QL, Kian Ping LOH*; Room-Temperature Synthesis of Soluble Carbon Nanotubes by the Sonication of Graphene Oxide Nanosheets, Journal Of The American Chemical Society, 131,46, 16832 (2009)
[5] bAng PK, Chen W, Wee ATS, Kian Ping LOH* et al; Solution-Gated Epitaxial Graphene as pH Sensor, Journal Of The American Chemical Society, 130,44, 14392 (2008)
[6] Zhou Y, Bao QL, Varghese B, Kian Ping LOH* et. al.; Microstructuring of Graphene Oxide Nanosheets Using Direct Laser Writing Advanced Materials, 22, 1 (2010)
[7] Wang SA, Ang PK, Wang ZQ, Kian Ping LOH*; High Mobility, Printable, and Solution-Processed Graphene Electronics; Nano Letters, 10, 1, 92-98 (2010)
[8] Lu J, Kian Ping LOH*, Huang Han, Chen Wei, Andrew Wee TS; Plasmon dispersion on epitaxial graphene studied using high-resolution electron energy-loss spectroscopy Physical Review B 80, 11 113410 (2009)
[9] Bao QL, Zhang H, Wang Y, Kian Ping LOH*; Atomicic-Layer Graphene as a Saturable Absorber for Ultrafast Pulsed Lasers; Advanced Functional Materials, 19 ,19 Pages: 3077-3083 (2009)
[10] Wang Y, Chen XH, Zhong YL, et al.; Large area, continuous, few-layered graphene as anodes in organic photovoltaic devices; Applied Physics Letters, 95, 6, 063302 (2009)

PROBING QUANTUM INTERFERENCE EFFECTS IN EPITAXIAL GRAPHENE BY STM AND MAGNETOTRANSPORT STUDIES

A. Mahmood [1], C. Naud[1], C. Bouvier, F. Hiebel, J.-Y. Veuillen[1], P. Mallet[1], D. Chaussende[2], T. Ouisse[2], L.P. Lévy[1]

[1]Institut Néel, CNRS-UJF, BP 166, 38042, Grenoble Cedex 9, France
[2]Laboratoire des Matériaux et du Génie Physique, CNRS UMR5628 - Grenoble INP, Minatec, 3 parvis Louis Néel BP257 38016 Grenoble, France
ather.mahmood@grenoble.cnrs.fr

A comprehensive understanding of the relationship between growth conditions and the resulting atomic and electronic structure is expected by characterizing the morphology of grown grapheme layers which also allows comparing the mechanisms of electron diffusion in graphene and hence controlling the charge transport through it. The graphitization can be achieved under ultra-high vacuum (UHV) conditions or in controlled atmosphere, starting from either the 6H-SiC(0001) (Si face) or 6H-SiC(000-1) (C face) surfaces. The resulting graphene layers have different disorder and morphologies depending on the growth conditions.

We present the scanning probe characterization of a gently graphitized 6H–SiC (0001) [1] surface prepared under ultra-high vacuum conditions and compare it with low temperature magneto-transport studies. The general surface morphology and atomically resolved Local Density of States (LDOS) is mapped by Scanning Tunneling Microscopy (STM). The differentiation between mono- and bi-layer graphene, presence of defects and interlayer coupling is determined by STM. LDOS mapping demonstrates the observation of quantum interference effects when quasiparticles are scattered off graphene edges, where the later represents line defects. The quantum transport properties are quite sensitive to the nature of disorder in graphene, due mainly to the presence of two additional symmetries: the symmetry between A and B sites in the unit cell (isospin) and the symmetry between the different valleys K-K' (pseudospin). The nature of disorder (local defects or folds in grapheme sheets for example), is responsible for locally breaking either of these symmetries, opening intra- and intervalley scattering processes [2].

Depending on the intrinsic disorder observed in the sample's morphology and on its mobility, the magneto-resistance shows either the conventional weak localization when intervalley scattering is strong or the weak anti localization (WAL), in agreement with the recent WAL theory for graphene [3]. Typically, the feature at small values of magnetic field, show a negative magneto resistance characteristic of weak localization, whereas at larger field a positive magneto resistance typical of antilocalization is observed. The weak localization at small fields depends only upon the phase coherence time, whereas the high field behaviour is dominated by a combination of the intervalley and intravalley scattering time. Each of these scattering times can be extracted from the magneto resistance curves and correlated to the surface morphologies. The consistency of this analysis has been checked using a "universal" scaling for the magneto-transport which will be presented [4].

References:

[1] P. Mallet, F. Varchon, C. Naud, L. Magaud, C. Berger, J.-Y. Veuillen, Phys. Rev. B, 2007, 76, 041403(R)
[2] X. Wu, X. Li, Z. Song, C. Berger, and W. A. de Heer, Phys. Rev. Lett. 2007, 98, 136801 2007.
[3] E. McCann, K. Kechedzhi, V. I. Fal'ko, H. Suzuura, T. Ando, and B. L. Altshuler, Phys. Rev. Lett., 2006, 97, 146805; V. I. Falko, K. Kechedzhi, E. McCann, and B. L. Altshuler H. Suzuura and T. Ando, Solid State Comm, 2007, 143, 33.; K. Kechedzhi, E. McCann, V. I. Falko, H. Suzuura, T. Ando, and B. L. Altshuler, eur. Phys. J. Spec.; Topics, 2008, 148, 39
[4] C. Naud, A. Mahmood, C. Bouvier, F. Hiebel, P. Mallet, J-Y. Veuillen, D. Chaussende, T. Ouisse,
[5] L. Levy, submitted to Phys. Rev. B

Figures:

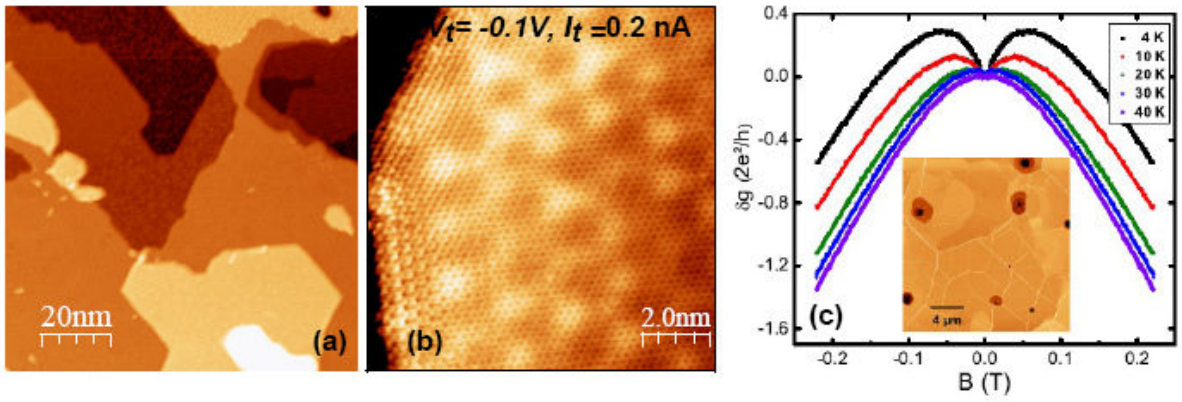

Figure 1: *(a) STM topographic image of graphene on Si face SiC showing terraces of buffer zone, monolayer and bilayer graphene. (b) Low bias STM image of zig-zag and armchair edges present on a monolayer graphene on SiC. (c) Magnetoresistance curves for mulitlayered graphene samples grown under Ar atmosphere (shown in inset).*

DESIGNING ALL-GRAPHENE NANO-JUNCTIONS BY EDGE FUNCTIONALIZATION: OPTICS AND ELECTRONICS

Elisa Molinari[1,2], Caterina Cocchi[1,2], Deborah Prezzi[1], Alice Ruini[1,2] and Marilia J. Caldas[3]

[1]Centro S3 - CNR Istituto Nanoscienze, Via Campi 213/A, 41125 Modena, Italy
[2]Dipartimento di Fisica, Universita' di Modena e Reggio Emilia, Via Campi 213/A, 41125 Modena, Italy
[3]Instituto de Fisica, Universidade de São Paulo, 05508-900 São Paulo, SP, Brazil
elisa.molinari@unimore.it

The recent advances in production techniques of graphene nanostructures call for strategies towards all-graphene nanodevices. We study the effect of covalent edge functionalization on the opto-electronic properties of realistic graphene nano-flakes and junctions.

By means of well tested semi-empirical methods, we compute both mean-field ground state electronic properties and configuration-interaction optical excitations. Our study shows that functionalization can be designed to tune electron affinities and ionization potentials of graphene nanoflakes [1]. This effect can be exploited to realize both *type-I* (straddling) and *type-II* (staggered) all-graphene nano-junctions. At variance to *type-I* [2], we find that *type-II* junctions can display indirect excitations with electrons and holes localized on different sides. The optical properties are characterized in terms of size and functionalization, and the conditions to obtain charge transfer excitons are discussed [3].

References:

[1] C. Cocchi et al. J. Phys. Chem C, in press (2011).
[2] D. Prezzi et al. Phys. Rev. B 77 (2008) 041404(R) and D. Prezzi et al. to be published.
[3] C. Cocchi et al. to be published.

Figures:

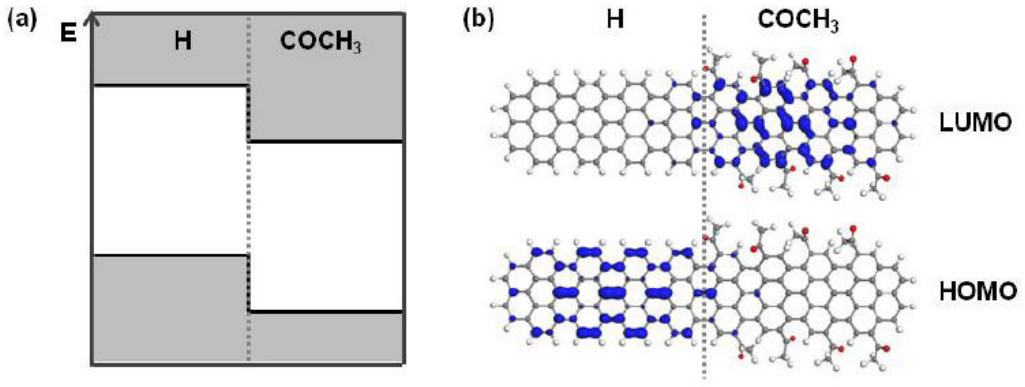

Figure 1: *(a) Scheme for type-II graphene nano-junction: edge covalent functionalization with electron-withdrawing $COCH_3$ groups down shifts the gap region with respect to the hydrogenated side (H); (b) Localized frontier orbitals of H-$COCH_3$ nano-junction.*

THE POLYMER CHEMISTRY OF CARBON MATERIALS AND GRAPHENES

Klaus Müllen

Max-Planck-Institute for Polymer Research, Mainz, 55128, Germany
muellen@mpip-mainz.mpg.de

Research into energy technologies and electronic devices is strongly governed by the available materials. We introduce a synthetic route to graphenes which is based upon the cyclodehydrogenation ("graphitization") of well-defined dendritic (3D) polyphenylene precursors. This approach is superior to physical methods of graphene formation such as chemical vapour deposition or exfoliation in terms of its (i) size and shape control, (ii) structural perfection, and (iii) processability (solution, melt, and even gas phase). The most convincing case is the synthesis of graphene nanoribbons under surface immobilization and in-situ control by scanning tunnelling microscopy.
Columnar superstructures assembled from these nanographene discs serve as charge transport channels in electronic devices. Field-effect transistors (FETs), solar cells, and sensors are described as examples.
Upon pyrolysis in confining geometries or "carbomesophases", the above carbon-rich 2D- and 3D-macromolecules transform into unprecedented carbon materials and their carbon-metal nanocomposites. Exciting applications are shown for energy technologies such as battery cells and fuel cells. In the latter case, nitrogen-containing graphenes serve as catalysts for oxygen reduction whose efficiency is superior to that of platinum.

DEFECTS IN GRAPHENE: A RAMAN SPECTROSCOPIC INVESTIGATION

Zhenhua Ni[1], Zexiang Shen[2], Kostya Novoselov[3] and Andre Geim[3]

[1]Department of Physics, Southeast University, Nanjing, China 211189
[2]Division of Physics and Applied Physics, School of Physical and Mathematical Sciences, Nanyang Technological University, 21 Nanyang Link, Singapore 637371
[3]Centre for Mesoscience and Nanotechnology, University of Manchester, Manchester M13 9PL, U.K
zhni@seu.edu.cn

Graphene, the one monolayer thick flat graphite, has been attracting much interest since it was firstly reported in 2004. Graphene has many unique properties which make it an attractive material for fundamental study as well as for potential applications. Raman spectroscopy has been extensively used to study graphene, i.e. identify graphene layer numbers; probe electronic band structure; determine type of edges (zigzag or armchair); measure the concentration of electron and hole dopants. Here, we present our results on the Raman spectroscopic investigation of defects in graphene.

The Raman D peak (~1345 cm^{-1}) is commonly used to estimate the amount of defects in graphitic materials. However, no such peak has been reported for pristine cleaved graphene, this seems suggest that pristine cleaved graphene is a perfect crystal without defects (or defects are undetectable). Here, we point out that, although small and usually unnoticed under the noise level, the D peak is generally present in cleaved graphene and, typically, reaches ~1.5% in amplitude with respect to the G peak.[1] This small D peak could be due to a certain concentration of sp^3 adsorbates and vacancies in grapheme (in other words, defects), and such resonant scatters can effectively limit the carrier mobility in graphene. By comparing the amplitude of D peak and carrier mobilities obtained in transport measurement; we show that the observed small D peak is sufficient to account for the limited mobilities (~2 m^2/Vs) currently achievable in graphene on a substrate.

We have also monitored graphene sheets with defects that are introduced during insulator layer (such as SiO_2, HfO_2) deposition using different methods (Sputtering, PLD, E-beam evaporation), and our results show that defects were introduced in graphene during deposition and the amounts of defects increase as the graphene thickness decreases. After annealing, the defects in graphene can be greatly reduced.[2] In addition, we also studied the defects in epitaxial graphene grown on SiC substrate [3] and graphene treated by plasma (H_2 and Ar) and electron beam.

References:

[1] Ni ZH, Ponomarenko LA, Nair RR, Yang R, Anissimova S, Grigorieva IV, Schedin F, Shen ZX, Hill EH, Novoselov KS, Geim AK Nano Letters 10, 3868-3872 (2010)
[2] Ni ZH, Wang HM, Ma Y, Kasim J, Wu YH, Shen ZX Tunable stress and controlled thickness modification in graphene by annealing ACS Nano 2, 1033 (2008)
[3] Ni ZH, Chen W, Fan XF, Kuo JL, Yu T, Wee ATS, Shen ZX Raman spectroscopy of epitaxial graphene on a SiC substrate Physical Review B 77, 115416 (2008)

Figures:

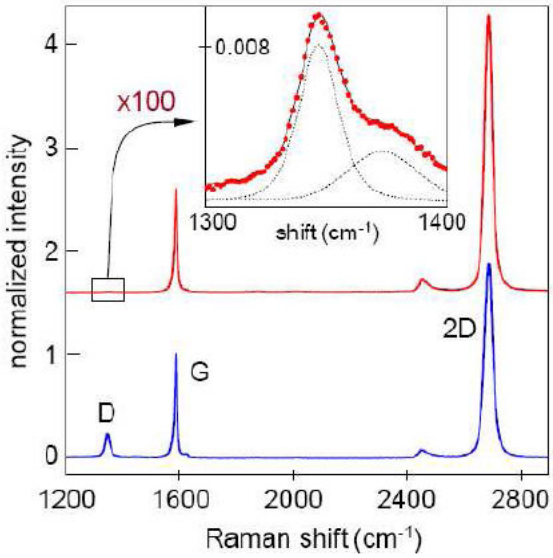

Figure 1: *Raman spectra for pristine and defected graphene (red and blues curves, respectively). In the latter case, the defects were induced by exposure to atomic H. The curves are normalized with respect to the G peak amplitude and shifted for clarity. The inset zooms into the D band region. In our experience, such small D peaks are universally present in Raman spectra of cleaved graphene.*

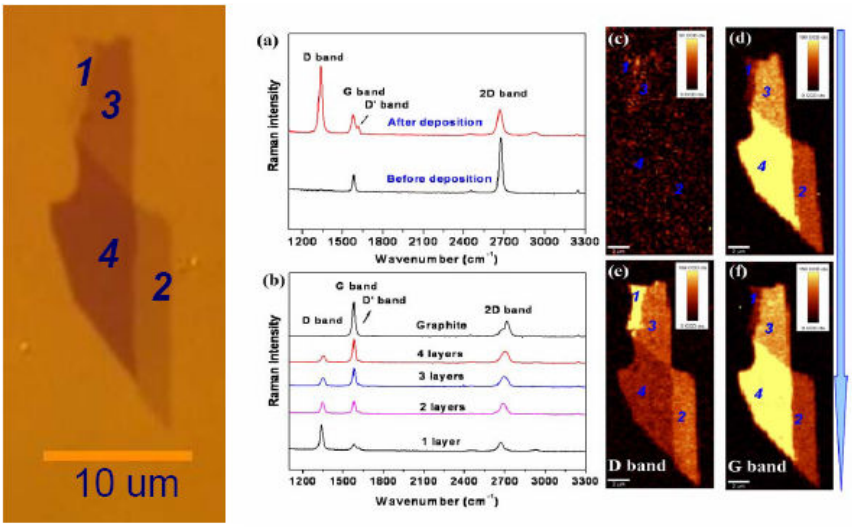

Figure 2: *(a) Raman spectra of single layer graphene before and after the 5 nm SiO_2 deposition. (b) Raman spectra of graphene with different thicknesses as well as that of bulk graphite after 5 nm SiO_2 deposition. Raman images of graphene sheets before SiO_2 deposition generated from the intensity of the D band (c) and G band (d). Raman images of graphene sheets after 5 nm SiO_2 deposition using the intensity of D band (e), and G band (f). The thinner graphene sheets have stronger D band, hence they contain more defects.*

WEAK LOCALIZATION VS WEAK ANTILOCALIZATION IN GRAPHENE

Frank Ortmann, Alessandro Cresti, Gilles Montambaux, Stephan Roche

INAC/SPrAM, CEA Grenoble, 17 Rue des Martyrs, 38054 Grenoble, France
IMEP-LAHC, Minatec, 3 Parvis Louis Neel, 38016 Grenoble, France
Laboratoire de Physique des Solides, UMR 8502 du CNRS, Univ Paris-Sud, 91405 Orsay, France
CIN2 (ICN-CSIC) Barcelona, Campus UAB, 08193 Bellaterra, Spain
ICREA, 08010 Barcelona, Spain
ortmann.f@googlemail.com

The understanding of quantum-transport phenomena in graphene-based materials is the current subject of great excitation. Indeed, low energy excitations can be formally described as massless Dirac Fermions exhibiting a linear dispersion relation together with an additional degree of freedom, namely pseudospin, which stems from the underlying sublattice degeneracy. In the presence of disorder, one of the predicted signatures of pseudospin is the change in sign of the quantum correction to the semiclassical Drude conductivity (1). This phenomenon, referred to as weak antilocalization (WAL), indeed results from complex quantum-interferences effects of charge carriers in a disordered potential landscape, and in grapheme these characteristics are markedly different from ordinary metals.

The effect of WAL has been recently observed experimentally with weak-field magneto-transport measurements in samples of high quality because the quantum-interference effects are preserved when the phase-relaxation length of the electrons is large enough. (2)

In this talk we present a numerical weak-field magneto-transport study of huge graphene samples and the influence of a realistic disorder potential describing charges trapped in the gate oxide causing long-range scattering potentials (3). Our simulations give clearly different magneto-conductance responses in different regimes which are fingerprint of either weak localization or WAL. Depending on the strength of the perturbing potential, the magneto-conductance can be tuned from positive to negative. The energy of the charge carriers as determined by the gate potential provides a second handle to modify these characteristics.

Our results therefore shed new light on experiments and unveil the possible origin of multiple crossovers from positive to negative magneto-conductance.

References:

[1] E. McCann, K. Kechedzhi, V. I. Fal'ko, H. Suzuura, T. Ando, B. L. Altshuler; Phys. Rev. Lett. 97 (2006), 146805
[2] F. V. Tikhonenko, A. A. Kozikov, A. K. Savchenko Phys. Rev. Lett. 103 (2009), 226801
[3] F. Ortmann, A. Cresti, G. Montambaux, S. Roche (submitted)

Figures:

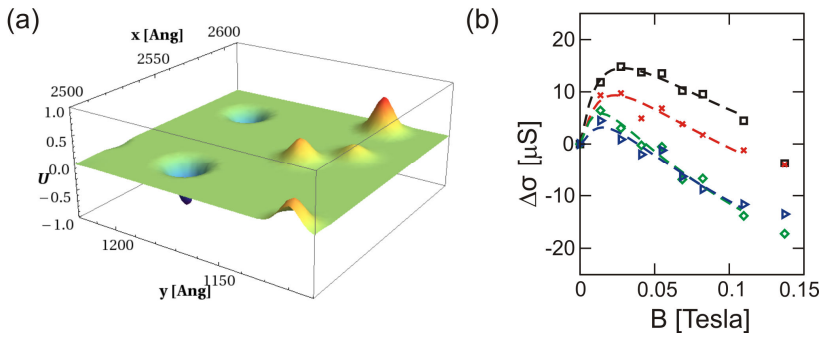

Figure 1: *(a) Typical long-range disorder potential. (b) Magneto-transport response.*

THERMODYNAMICALY STABLE GRAPHENE SOLUTIONS

Alain Pénicaud

Université de Bordeaux, Centre de Recherche Paul-Pascal, CNRS, 115 av. Schweitzer, 33600 Pessac, France
penicaud@crpp-bordeaux.cnrs.fr

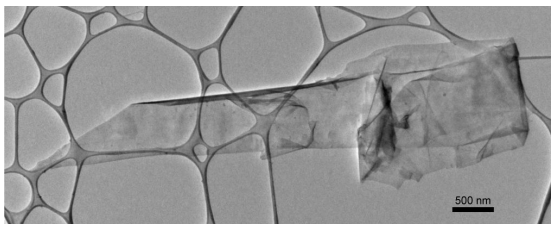

Graphite is insoluble in all media but may be dispersed with surfactants and/or sonication to obtain metastables suspensions. However, some graphite intercalation compounds (GICs) have been shown to be spontaneously soluble in polar organic solvents without the need for any kind of additional energy, such as sonication or high shear mixing.[1-3] Flakes of several μm^2 can be deposited from these solutions.

References:

[1] Solutions of graphene, C. Vallés and A. Pénicaud, patent, WO 2009/087287; FR 07/05803 august 9, 2007.
[2] Solutions of Negatively Charged Graphene Sheets and Ribbons, C. Vallés et al., J. Am. Chem. Soc., 2008, 130, 15802–15804.
[3] Graphene solutions, A. Catheline, C. Vallés, C. Drummond, L. Ortolani, V. Morandi, M. Marcaccio, M. Iurlo, F. Paolucci, A. Pénicaud, submitted.

TRANSPORT SCATTERING TIME PROBED THROUGH RF ADMITTANCE OF A GRAPHENE CAPACITOR

B. Plaçais, E. Pallecchi, A.C. Betz, J. Chaste, G. Feve, B. Huard, T. Kontos, J.-M. Berroir

Laboratoire Pierre Aigrain, Ecole Normale Superieure, 24, rue Lhomond, 75005 Paris, France
placais@lpa.ens.fr

We have investigated electron dynamics in top gated graphene by measuring the gate admittance of a diffusive graphene capacitor in a broad frequency range as a function of carrier density. The density of states, conductivity and diffusion constant are deduced from the low frequency gate capacitance, its charging time and their ratio. The admittance evolves from an RC-like to a skin-effect response at GHz frequency with a crossover given by the Thouless energy. The scattering time is found to be independent of energy in the 0- 200 meV investigated range at room temperature.
This is consistent with a random mass model for Dirac Fermions.

References:

[1] E. Pallecchi et al, arXiv:/1005.3388v1 (2010).

IDENTIFYING REACTIVE SITES ON GRAPHENE SHEETS AGAINST 1,3-DIPOLAR CYCLOADDITION AND AMIDATION REACTIONS

M. Quintana[1], A. Montellano[1], X. Ke[2], G. Van Tendeloo[2], C. Bittencourt[2], and **M. Prato[1]***

[1]Center of Excellence for Nanostructured Materials (CENMAT), INSTM UdR di Trieste, Dipartimento di Scienze Chimiche e Farmaceutiche, University of Trieste, Trieste, Italy
[2]Electron Microscopy for Material Science (EMAT), Physics Department, University of Antwerp, Antwerp, Belgium,

The production of graphene by micromechanical cleavage [1] has triggered an enormous experimental activity. Since then, many studies have demonstrated that graphene monolayers possess novel structural, [2] electrical [3] and mechanical [4] properties. However many important issues need to be addressed before this material can be used in an ideal way. Much workhas been produced that proposes chemical functionalization as a tool for tuning graphene chemical and physical properties. For example, chemical functionalization can render graphene dispersable in different solvents. [5] To exploit the high mobility of graphene, the band gap engineering and controllable doping of semimetal graphene can be achieved by chemical functionalization. [6] Moreover, the non-uniformity of graphene edges and the potential for dangling bonds are thought to have significant influence on their chemical properties and reactivity. [7] Chemical modification of various forms of graphene, including reduced graphene oxide, [8] liquid-phase exfoliated graphite, [9] pristine graphene and its multilayers has been obtained. [5] For instance, the aryl diazonium-based reaction has been extensively studied as a specific radical reaction on graphene layers. [10] In graphene, the edges exhibit a higher reactivity than the interior during this specific reaction. Instead, we have recently reported the functionalization of graphene layers by condensation of a protected α-amino acid and paraformaldehyde, [11] demonstrating that even if the reactivity of graphene differs from that of fullerenes and carbon nanotubes, the 1,3-dipolar cycloaddition can be efficiently performed and yields a highly functionalized material taking place not just at the edges but also at the C=C bonds in the center of graphene sheets. However, further work needs to be performed for understanding the chemical structure of the functionalized graphene and their reaction mechanisms.

In this work we present a detailed study on the reactivity of graphene sheets stabilized in DMF using two different reactions: the 1,3-dipolar cycloaddition reaction and the amide-bond condensation reaction achieved between the free carboxylic groups already present in the exfoliated graphene and the amino functionalities of the attached moieties. Thus, we have functionalized graphene with a first generation polyamidoamine (PAMAM) dendron possessing an anchoring amine point and two terminal Boc-protected amines. Indeed, dendrimers and dendrons containing polar groups in their structures have been widely conjugated to carbon nanostructures in order to increase the solubility, modifying in this way their inherent apolar character to obtain more tunable structures. [12] Even more, the presence of free terminal amino groups can serve as ligands in the stabilization of gold nanostructures. [13] As first step to identify the reactive sites on graphene layers the free amino groups were quantified by the Kaiser test. These amino groups selectively bind to gold nanoparticles, which can then be employed as contrast markers. The interaction between Au nanoparticles and functionalized graphene was followed by UV-Vis spectroscopy, while the morphological changes were characterized by transmission electron microscopy (TEM). The presence of the organic groups and their interaction with Au nanoparticles were verified by X-ray photoelectron spectroscopy. Au nanoparticles distributed uniformly all over the graphene surface were found for functionalized graphene via 1,3-dipolar cycloaddition. Instead, in functionalized graphene by amidation reaction Au nanoparticles were observed mainly at the edges of graphene sheets. All these results confirm that graphene produced by mild sonication of graphite in DMF are relatively free of defects and can be efficiently functionalized by well establish organic reactions.

References:

[1] Novoselov, K. S.; Geim, A. K.; Morozov, S. V.; Jiang, D.; Zhang, Y.; Grigorieva, S. V.; Firsov, A. A.; Science (2004) 306, 666-669.
[2] Meyer, J. C.; Geim, A. K.; Katsnelson, M. I.; Novoselov, K. S.; Booth, T. J.; Roth, S.; Nature (2007) 446, 60-63
[3] a) Castro, N.; Guinea, F.; Peres, N. M. R.; Novoselov, K. S.; Geim, A. K.; Rev. Mod. Phys. (2009) 81, 109-162; b) Berger, C.; Song, Z.; Li, T. X.; Ogbazghi, A. Y.; Feng, R.; Dai, Z.; Marchenkov, A. N.; Conrad, E. H.; First, P. N.; de Heer, W. A.; J. Phys. Chem. B (2004) 108, 19912-19916.
[4] Frank, I. W.; Tanenbaum, D. M.; van der Zande, A. M.; McEuen, P. L.; J. Vac. Sci. Technol. (2007) 25, 2558-2561
[5] Park, S.; Ruoff, R. S.; Nat. Nanotech. (2009) 217-224.
[6] Sharma, R.; Baik, H. J.; Perera, C. J.; Strano, M. S.; Nano Lett. (2010) 10, 398-405
[7] Ritter, K. A.; Lyding, J. W.; Nat. Mater. (2009) 8, 235-242.
[8] Lomeda, J. R. Doyle, C. D. Kosynkin, D. V. Hwang, W. F. Tour, J. M. J. Am. Chem. Soc. (2008) 130, 16201-16206
[9] Hernandez, Y. Nicolosi, V. Lotya,M. Blighe, F. M. Sun,Z. De, S. McGovern,I. T. Holland, B. Byrne, M. GunKo, Y. K. Boland, J. J. Niraj, P. Duesberg, G. Krishnamurthy, S. Goodhue, R. Hutchison, J. Scardaci, V. Ferrari, A. C. Coleman, J. N. Nature Nanotechnology (2008) 3 563-568
[10] Sharma, R.; Huun, B.; Perera. C. J.; Strano, M. S.; Nano Lett. (2010) 10, 398-405.
[11] Quintana, M.; Spyrou, K.; Grzelczak, M.; Browne, W. R.; Rudolf, P.; Prato, M.; ACS Nano (2010) 4, 3527-3533.
[12] Herrero, M. A.; Toma, F. M.; Al-Jamal, K. T.; Kostarelos, K.; Bianco, A.; Da Ros, T.; Bano, F.; Casalis, L.; Scoles, G.; Prato, M.; J. Am. Chem. Soc. (2010) 132, 1731.
[13] Templeton, A. C.; Chen, S.; Gross, S. M.; Murray, R. W.; Langmuir (1999) 15, 66-76.

[14] This work was supported by the Italian Ministry of Education MIUR (cofin Prot. 20085M27SS and Firb RBIN04HC3S).

Figures:

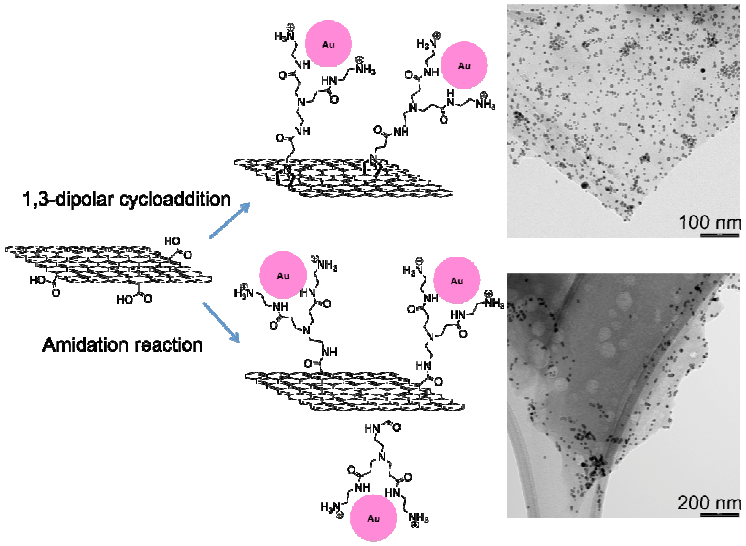

Figure 1: *Schematic representation of functionalized graphene (left). TEM images of reactive sites on graphene marked by Au nanoparticles.*

NON-COVALENT FUNCTIONALISATION OF GRAPHENE USING SELF-ASSEMBLED MONOLAYERS

A.J. Quinn[a], B. Long[a], B. N. Szafranek[b], G. Visimberga[a], M. Manning[a], D. Thompson[a], J.C. Greer[a], I.M. Povey[a], J. MacHale[a], D. Neumaier[b], H. Kurz[b]

[a]Tyndall National Institute, Univeristy College Cork, Lee Maltings, Dyke Parade, Cork, Ireland
[b]Advanced Microelectronic Center Aachen (AMICA), AMO GmbH, Otto-Blumenthal-Str. 25, 52074 Aachen, Germany
aidan.quinn@tyndall.ie

Graphene, monolayer sheets of sp^2-bonded carbon atoms arranged in a honeycomb-like structure, continues to attract intense research interest due to its unique electronic properties and potential applications. As a "surface-only" nanomaterial, the properties of monolayer or few-layer grapheme structures are extremely sensitive to adsorbed ambient contaminants, with a correspondingly severe impact on the electrical characteristics and stability of graphene-based devices. Development of strategies for functionalisation of graphene without adversely affecting its electronic properties are of key importance. Here we report on a simple, versatile functionalisation method based on solution-phase formation of alkane-amine self-assembled monolayers (SAMs) on graphene; see Figure 1a for a schematic.

Ab initio calculations (2nd order Møller–Plesset perturbation theory), applied to a cluster model (methylamine on pyrene) yield a binding energy, E_b = -220 meV for the anchor amine group, when the amine is located above a C-C bond (an "over-bond" site). Similar values were found for calculations with the amine group located over a carbon atom ("over-atom" site, E_b = -223 meV) and for the amine located over the centre of one of the phenyl rings ("over-ring" site, E_b = -215 meV), indicating that there is no strong preferential bonding site to the graphene plane. The results are consistent with a noncovalent amine-graphene interaction (~220 meV binding energy), which is strong enough to enable formation of a stable aminodecane monolayer at room temperature (T = 300 K, E_b ~ 8 kT), but also sufficiently labile to allow the necessary mobility of the molecules required for formation of a closepacked monolayer. Atomistic molecular dynamics simulations for 784 1-aminodecane molecules on a 13 nm x 15 nm graphene substrate (not shown) predict formation of a mobile but stable alkane-amine SAM, with nearest-neighbour distances for the amine anchor groups ~ 0.33 nm.

Measured Raman spectroscopy data for graphene monolayers deposited on thermally oxidised silicon substrates and then functionalized with 1,10-diaminodecane (red data in Fig. 1b) are also consistent with a non-covalent, charge-transfer interaction between the alkane-amine molecules and graphene. The presence of a sharp two-phonon *2D* peak (full-width at half-maximum intensity, FWHM ~ 24.5 cm^{-1}), a characteristic of monolayer graphene, and the absence of a defect (*D*) peak close to 1350 cm^{-1} following functionalization (Fig. 1b, inset) confirms that the layer of 1,10-diaminodecane molecules does not perturb the sp^2-hybridisation of the graphene monolayer and does not introduce additional structural defects. Further, the spectrum for the functionalised monolayer shows several significant differences when compared with data measured for an as-deposited graphene monolayer (Fig. 1b, gray data). Both the shift in the G peak position towards higher energy and the reduction in intensity of the *2D* peak following functionalisation of the exposed graphene surface with 1,10-diaminodecane are consistent with doping, likely via charge transfer from the amine anchor groups to the graphene.

Figure 1c shows two-probe resistance (R_{2P}) vs gate voltage (V_g) data measured in vacuum for a monolayer graphene field-effect device following fabrication. The data show the expected behaviour for unpassivated graphene devices exposed to ambient conditions – hysteretic ambipolar conduction, with minimum conductivity (Dirac Point, $V_{g,DP}$) at positive gate voltage. This positive value of $V_{g,DP}$ indicates unintentional hole doping, likely from contaminants at the graphene surface and the graphene-substrate interface, e.g., adsorbed water and organic residue from the fabrication process. Figure 1d shows the R_{2P}-V_g data for the same device, acquired following ex situ annealing to 250 ºC under nitrogen for 1 hour, functionalisation in solution with 1-aminodecane and transfer under ambient conditions (~ 1 hour) to the vacuum measurement chamber. Several significant changes are evident, including a shift in the Dirac Point to negative gate voltage and a sharper resistance peak (higher carrier mobility) around the Dirac Point for each sweep. These negative values for $V_{g,DP}$ in the functionalised device indicate adsorbate-induced electron doping, presumably from the amine anchor groups in the 1-aminodecane molecular layer. Kim et al. have proposed a simple device model to interpret two-probe R_{2P}-V_g data[25]. Using three fit parameters — the contact resistance (R_c), the impurity carrier density (n_0) and the fieldeffect mobility (μ_{FE}) — the two-probe device resistance can be expressed as

$$R_{2P}(V_g) = R_C(V_g) + \frac{L}{We\mu_{FE}\sqrt{n_0^2 + [n(V_g, V_{g,DP})]^2}} \quad (1)$$

where L (≈ 6μm) and W (≈ 10μm) are the device length and width, respectively, e is the electronic charge and *n* is the gate-induced carrier density, $n \propto |V_g - V_{g,DP}|$ if quantum capacitance effects are excluded. The inset to Fig. 1d shows fits to Equation 1 for the data in the main panel, yielding estimates for both the mobility, $\mu_{FE} \approx$ 2350–2500cm^{2}V^{-1}s^{-1}, and the impurity carrier density, $n_0 \approx 0.8 \times 10^{12}$ cm^{-2}, assuming a constant contact resistance R_c = 200Ω for both sweeps. In general, devices functionalized with 1-aminodecane following annealing show higher carrier mobilities and also improved stability upon re-exposure to ambient conditions compared with annealed "bare" devices, suggesting that the 1-aminodecane layer can act as a barrier to hinder the readsorption of contaminants, e.g., water.

A key challenge in the development of graphene-based nanoelectronics is the deposition of inorganic dielectrics onto graphene for top-gated devices. "Seeding" processes for atomic layer deposition (ALD) of inorganic dielectrics onto graphene have been reported, including ozone pre-treatment, and also deposition of thin (~10 nm) polymer layers containing appropriate binding groups. Use of selfassembled monolayers represents an attractive complementary process. The smaller thickness of the alkane-amine SAM, compared to polymer layers, would increase the effective total dielectric capacitance, and the defect density in SAM-modified graphene should be lower than for ozone-treated graphene. Figure 1e shows a scanning electron microscopy image of an ultra-thin film of aluminium oxide (5 nm nominal thickness), which was deposited onto highly-oriented pyrolytic graphite that had been functionalised with 1,10-diaminodecane. Uniform coverage of the substrate (including some small defects and a step edge) is evident. Figure 1f shows the edge of the aluminium oxide film following removal of part of the film using adhesive tape. The remaining aluminium oxide shows good adhesion to the substrate. The film is quasi-continuous film arising from coalescence of two-dimensional islands, as expected for the chosen film thickness.

In conclusion, self-assembled monolayers of alkane-amines represent a versatile new route for noncovalent functionalisation of graphene without adversely affecting its unique properties. Advantages for nanoelectronic applications include adsorbate doping, surface passivation and seeded ALD. Selection of suitable terminal groups for binding of target species onto graphene opens up possibilities for selective and sensitive graphene-based electromechanical or electrochemical (bio)sensors.

This work was supported by the European Commission under the FP7 ICT project "GRAND" (215572).

Figures:

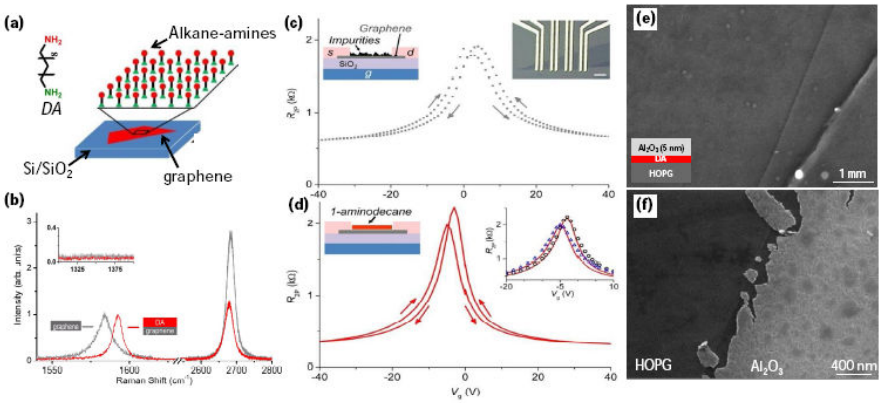

Figure 1: *(a) Left: Structure of 1,10-diaminodecane (DA). Right: Schematic of a graphene layer functionalised with a monolayer of alkane amines. (b) Raman spectra (514.5 nm excitation) for a graphene monolayer deposited onto an unmodified Si/SiO$_2$ substrate (gray) and also for a graphene monolayer (red) following following functionalisation in solution with 1,10-diaminodecane (DA). Inset: No defect (D) peak ~ 1350 cm^{-1} is observed following functionalisation. (c) Two-probe resistance vs. gate-voltage (R_{2P}–V_g) characteristics measured in vacuum for a back-gated, monolayer graphene device following fabrication.(d) R_{2P}–V_g characteristics for the same device measured following ex situ thermal annealing under nitrogen (200 C) and functionalisation in solution with 1-aminodecane. Fits to the R_{2P}–V_g data for the functionalised device (d, inset) yield estimates for the device mobility, $\mu_{FE} \approx$ 2350–2500 cm^{2}V^{-1}s^{-1}. (e) SEM image of a conformal 5 nm thick Al$_2$O$_3$ film deposited using atomic layer deposition onto a graphite substrate, which had been functionalised with 1,10-diaminodecane. (f) SEM image of the edge of the Al$_2$O$_3$ film and the underlying graphite (HOPG) substrate following removal of part of the Al$_2$O$_3$ film using adhesive tape.*

HIGH EFFICIENCY ENERGY STORAGE OF GRAPHENE-BASED COMPOSITES

Wencai Ren, Zhongshuai Wu, Dawei Wang, Guangmin Zhou, Na Li, Jinping Zhao, Songfeng Pei, Feng Li, and Hui-Ming Cheng

Shenyang National Laboratory for Materials Science, Institute of Metal Research, Chinese Academy of Sciences, Shenyang 110016, P.R. China
wcren@imr.ac.cn

Energy storage is vital to meet the challenge of global warming and finite fossil-fuel supplies in modern society [1]. Graphene, a unique two-dimensional carbon material, is predicted to be an excellent electrode material candidate for energy conversion/storage in supercapacitors and lithium ion batteries (LIBs) because of its high specific surface area, good chemical stability, excellent electrical and thermal conductivity as well as remarkably high mechanical strength and Young's modulus [2-4].

Controllable synthesis of graphene sheets (GSs) in a large scale is the prerequisite and essentially important for the energy storage applications of graphene. We proposed a simple and effective strategy to tune the number of graphene layers by selecting suitable starting graphite using a chemical exfoliation method [5], developed a mild oxidation and exfoliation method to prepare large-area graphene oxide with a size up to 200 micrometers and realized the size-controlled synthesis of graphene oxide by simply tuning the content of C-O in graphite oxide [6], proposed a hydrogen arc discharge exfoliation method for the synthesis of GSs with excellent electrical conductivity from graphite oxide [7], and developed a rapid and nondestructive low-temperature reduction method to effectively improve the electrical conductivity of graphene oxide by using HI acid [8].

In order to fully utilize the advantages of GSs for energy storage, we proposed the use of GSs/metal oxide (or conducting polymer) as electrode materials for high performance supercapacitors and LIBs. Based on this idea, we designed and synthesized a series of graphene/metal oxide nanoparticles composites by combining sol-gel and low-temperature annealing processes, including GSs/hydrous RuO_2 composites for high energy supercapacitors [9], GSs/Co_3O_4 and GSs/Fe_3O_4 composites for high energy LIBs [10, 11], and GSs/TiO_2 and GSs/$Li_4Ti_5O_{12}$ composites for high power LIBs [12]. In order to achieve high energy and power densities, we also developed a high-voltage asymmetric electrochemical capacitor based on graphene as negative electrode and a GSs/MnO_2 nanowire composite as positive electrode in a neutral aqueous Na_2SO_4 solution as electrolyte [13]. Moreover, by incorporating with polyaniline, we fabricated GSs/polyaniline composite paper via *in situ* anodic electropolymerization for high performance flexible supercapacitor electrodes [14].

All the above composites show a greatly improved capacity, cycling stability and rate capability compared to solo graphene and metal oxide, demonstrating the positive synergistic effect of GSs and metal oxide on the improvements of electrochemical performance. We believe that the performance of GSs-based composite electrodes can be further improved by optimizing the composition and structure of GSs and particles, and the architecture and synthesis process of composites, to meet the future requirements for high energy and high power energy storage systems.

References:

[1] C. Liu, F. Li, L.P. Ma, H.M. Cheng, Adv Mater 8 (2010) E28.
[2] K.S. Novoselov, A.K. Geim, S.V. Morozov, D. Jiang, Y. Zhang, S.V. Dubonos, I.V. Grigorieva, A.A. Firsov, Science, 306 (2004) 666.
[3] A.K. Geim, K.S. Novoselov, Nature Mater. 3 (2007) 183.
[4] A.K. Geim, Science 5934 (2009) 1530.
[5] Z.S. Wu, W.C. Ren, L.B. Gao, B.L. Liu, C.B. Jiang, H.M. Cheng, Carbon 2 (2009) 493.
[6] J.P. Zhao, S.F. Pei, W.C. Ren, L.B. Gao, H.M. Cheng, ACS Nano 9 (2010) 5245.
[7] Z.S. Wu, W.C. Ren, L.B. Gao, J.P. Zhao, Z.P. Chen, B.L. Liu, D.M. Tang, B. Yu, C.B. Jiang, and H.M. Cheng, ACS Nano 2 (2009) 411.
[8] S.F. Pei, J.P. Zhao, J.H. Du, W.C. Ren, H.M. Cheng, Carbon 15 (2010) 4466.
[9] Z.S. Wu, D.W. Wang, W.C. Ren, J.P. Zhao, G.M. Zhou, F. Li, H.M. Cheng, Adv. Funct. Mater. 20 (2010) 3595.
[10] Z.S. Wu, W.C. Ren, L. Wen, L.B. Gao, J. P. Zhao, Z. P. Chen, G.M. Zhou, F. Li, H.M. Cheng, ACS Nano 6 (2010) 3187.
[11] G.M. Zhou, D.W. Wang, F. Li, L.L. Zhang, N. Li, Z.S. Wu, L. Wen, G.Q. Lu, H.M. Cheng, Chem Mater 18 (2010) 5306.
[12] N. Li, G. Liu, G.M. Zhou, F. Li, H.M. Cheng, Adv Mater In revision.
[13] Z.S. Wu, W.C. Ren, D.W. Wang, F. Li, B.L. Liu, H.M. Cheng, ACS Nano 10 (2010) 5835.
[14] D.W. Wang, F. Li, J.P. Zhao, W.C. Ren, Z.G. Chen, J. Tan, Z.S. Wu, I. Gentle, G.Q. Lu, H.M. Cheng, ACS Nano 7 (2009) 1745.

Figures:

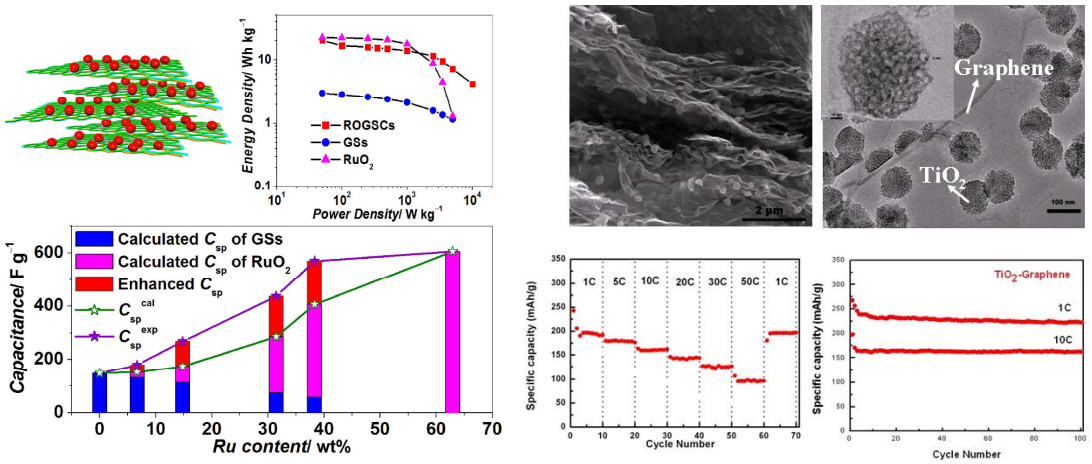

Figure 1: *GSs/hydrous RuO_2 composites for high energy supercapacitors (left panel) [9] and GSs/TiO_2 composites for high power LIBs (right panel) [12].*

DEVELOPMENT OF GRAPHENE FOR HIGH FREQUENCY ELECTRONICS

J. A. Robinson, D. Snyder, Mark Fanton, M. J. Hollander, M. Labella, Z. Hughes, K. Trumbull, R. Cavalero, B. Weiland, E. Hwang, and S. Datta

The Pennsylvania State University, University Park, PA, U.S.A
jrobinson@psu.edu

Graphene's high carrier mobility [1], large saturation current [2], low noise, and superior scalability make it of interest as a channel material for RF-FET applications. The practicality and success of such a technology depends on the ability to, first, regularly and controllably synthesize graphene, second, integrate it with metals and dielectrics in a reproducible manner, and, finally, to develop device designs that take advantage of (or overcome) graphene's unique properties while minimizing performance-limiting parasitics. In this talk, we will provide insight into ultra-large area growth, integration of graphene with ultra-thin dielectrics (EOT ~ 1nm), and how growth and device processing effect the transport properties of epitaxial graphene.

Graphene synthesis is accomplished on SiC (Figure 1) and Sapphire up to 100mm wafers, with excellent uniformity (Figure 2). Graphitization of SiC(0001) is achieved by low-pressure sublimation of Si from the Si-face of semi-insulating 6H-SiC (II-VI, Inc.) at 1600°C and mediated by an Ar atmosphere [3]. Graphene films grown under these conditions are primarily one- to two-layers thick according to Raman spectroscopy and transmission electron microscopy, [4] with a D/G peak ratio of 0.07 ± 0.03. Direct growth of graphene on sapphire is accomplished via the decomposition of methane at 1425 – 1600ºC, where film nucleation and quality are found to be a strong function of methane concentration, growth time, and growth temperature [5]. Raman spectroscopy confirms, for the first time, the formation of monolayer and bilayer graphene on sapphire, with improved structural quality as deposition temperature increases.

In addition to synthesis of large area, high quality graphene, the successful implementation of a graphene-based electronic technology must address low resistance metal/graphene contacts, and the integration of graphene with high-k dielectrics. We have developed a robust method for forming high quality ohmic contacts to graphene, which improves the contact resistance by nearly 6000x compared to untreated metal/graphene interfaces [6]. Optimal specific contact resistance for treated Ti/Au contacts is found to average $5x10^{-8}$ Ohm-cm^2, demonstrating a significant improvement in ultimate resistance compared to current technology. It is found that most metallizations result in similar contact resistances in this work (Figure 3), regardless of the work function difference between graphene and the metal over layer, which is explained by the chemical and structural modification of graphene during device processing.

Finally, we discuss the successful integration of ultra-thin high-k dielectrics and their impact on graphene transport. All oxides deposited via atomic layer deposition require some type of seeding method. Additionally, heterostructures (seed ≠ overlayer) have deleterious effects on Hall mobility while homostructures can lead to an increase in Hall mobility (Figure 4). Doping appears to be material dependent and varies with film thickness. Importantly, 5nm thick EBPVD HfO_2 gate dielectrics with an EOT of ~1nm are successfully demonstrated and show improved Hall mobility, on-off ratio, and transconductance relative to Al_2O_3 gates and heterostructure gates comprised of various dielectrics (Figure 5).

References:

[1] Novoselov, K.S.; Geim, A.K.; Morozov, S.V.; Jiang, D.; Zhang, Y.; Dubonos, S.V.; Grigorieva, I.V.; Firsov, A.A.; Science 2004 306, 666-669
[2] Moon, J.S.; Curtis, D.; Bui, S.; Hu, M.; Gaskill, D.K.; Tedesco, J.L.; Asbeck, P.; Jernigan, G.G.; VanMil, B.L.; Myers-Ward, R.L.; Eddy, C.R.; Campbell, P.M.; Weng, X.; IEEE Electron Device Letters 2010, 31, 4, 260-262
[3] Robinson, J.A.; Labella, M.; Trumball, K.A.; Weng, X.J.; Cavelero, R.; Daniels, T.; Hughes, Z.; Hollander, M.J.; Fanton, M.; Snyder, D.; ACS Nano 4 (5), 2667-2672

[4] Robinson, J.A.; Wetherington, M.; Tedesco, J.L.: Campbell, P.M.; Weng, X.; Stitt, J.; Fanton, M.; Frantz, E.; Snyder, D.; VanMil, B.L.; Jernigan, G.G.; Meyers-Ward, R.L.; Eddy, C.R.; Gaskill, D.K.; Nano Letters 2009, 9, 2873-2876
[5] Fanton, M.; Robinson, J.; Weiland, B.; LaBella, M.; Trumbull, K.; Kasarda, R.; Howsare, C.; Stitt, J.; Snyder, D.; Nano Lett., Submitted Dec 2010
[6] Robinson, J.A.; LaBella, M; Zhu, M.; Hollander, M.; Kasarda, R.; Hughes, Z.; Trumbull, K.; Cavalero, R.; Snyder, D.; Applied Physics Letters, Submitted Dec.2010

Figures:

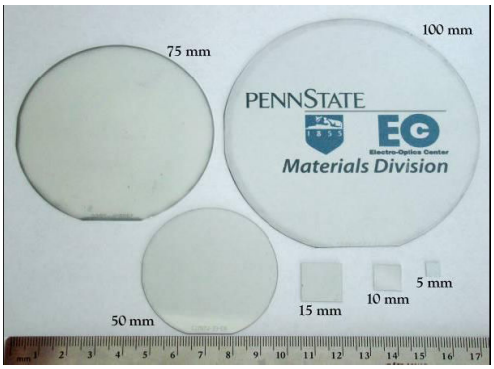

Figure 1: *Photographic image of graphene grown SiC(0001) wafers up to 100 mm*

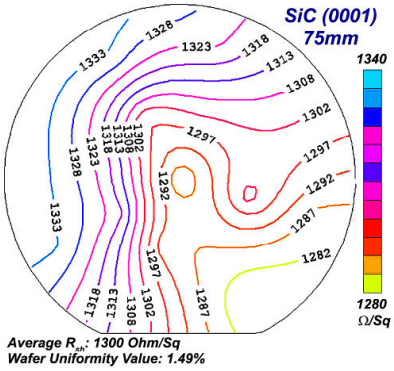

Figure 2: *Sheet resistance (Ohm/sq) map of a 75mm graphene wafer illustrating high uniformity*

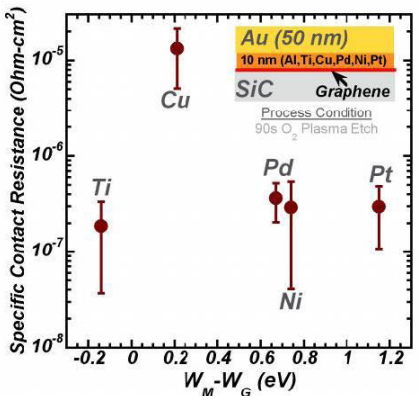

Figure 3: *Specific contact resistance of various metals versus graphene/metal work function difference.*

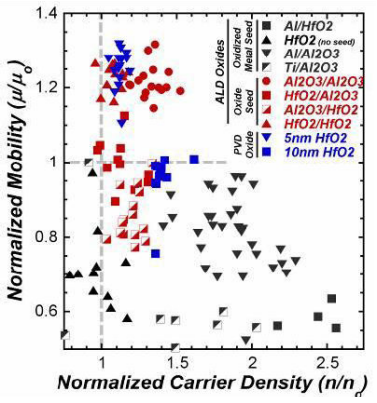

Figure 4: *Normalized Graphene carrier mobility vs. density as a function of dielectric overlayer.*

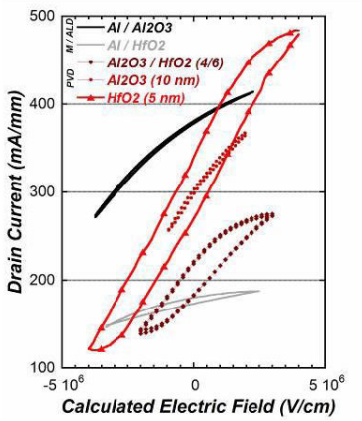

Figure 5: *Graphene transistor drain current vs. gate electric field. 5 nm HfO_2 exhibits superior transport characteristics compared to all other dielectrics.*

NON-ADIABATIC GRAPHENE QUANTUM PUMPS

Pablo San-Jose[1], Elsa Prada[2], Sigmund Kohler[2], Henning Schomerus[3]

[1]Instituto de Estructura de la Materia (CSIC), Serrano 123, 28006 Madrid, Spain
[2]Instituto de Ciencia de Materiales de Madrid (CSIC), Cantoblanco, 28049 Madrid, Spain
[3]Department of Physics, Lancaster University, Lancaster, LA1 4YB, United Kingdom
sanjose@iem.cfmac.csic.es

We present a theoretical study of the non-adiabatic operation of graphene-based quantum pumps, along with a comparison to the semiconductor-based analogues. We show that due to the open nature of graphene contacts resulting from quasiparticle chirality conservation, the current pumped through evanescent modes scales linearly with frequency, and may allow for a competitive advantage respect to the semiconductor-based alternative. Moreover, the scale-free nature of graphene pumps at the neutrality point results in a universal weak-pumping response, reminiscent of that previously identified in the adiabatic regime [1]. In contrast to the latter, however, the differential pumping response becomes maximum at the neutrality point. We provide a full analytical solution of the pumping problem in the weak pumping regime.

References:

[1] E. Prada, P. San-Jose and H. Schomerus, Phys. Rev. B 80, 245414 (2009)

Figures:

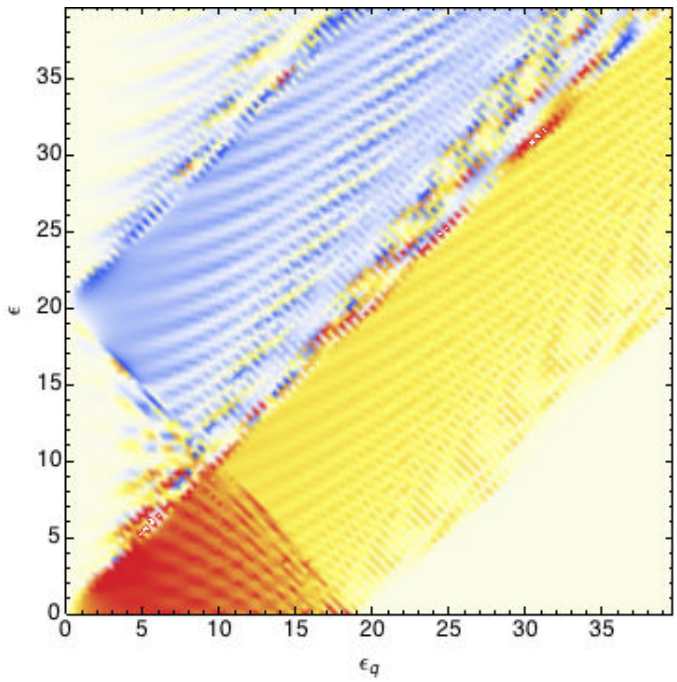

Figure 1: *Differential pumping response $dI/d\epsilon$ as a function of Fermi energy ε and transverse momentum $\varepsilon_q = \hbar v_F q$ in a single parameter graphene quantum pump. The red region, extending up to the pumping frequency $\varepsilon_q=\omega$ at the neutrality point $\varepsilon=0$, represents efficient pumping of evanescent modes.*

MAGNETISM OF COVALENTLY FUNCTIONALIZED GRAPHENE

Elton J. G. Santos, Andrés Ayuela, **Daniel Sánchez-Portal**

Donostia International Physics Center, Paseo Manuel de Lardizabal 4, 20018 San Sebastián, Spain
Centro de Física de Materiales (CFM-MPC), CSIC-UPV/EHU, Paseo Manuel de Lardizabal 5, 20018 San Sebastián, Spain
sqbsapod@ehu.es

We have recently applied *ab initio* density functional calculations to explore the magnetism induced by several types of defects in graphene and graphenic nanostructure, including doping with transition metals [1,2,3] and vacancies [4]. In the present contribution we concentrate on the effect of covalent functionalization on the electronic structure and magnetism of graphene [5] and single-walled carbon nanotubes [6]. We have performed calculations of the functionalization of graphene layer alkanes, polymers, diazonium salts, aryl and alkyl radicals, nucleobases, amide and amine groups, sugar and some organic acids. We find that, independently of the particular adsorbate, whenever a molecule is linked to the carbon layer through single C-C covalent bond, a spin moment of 1.0 μ_B is induced. This is similar to the effect of H adsorption, which saturates the p_Z orbital in the layer, and can be related to the spin moment observed for a single carbon vacancy in a simple π-tight-binding description of the graphene layer. Consistently with this analogy, the calculated spin moment is almost entirely localized in the carbon layer, with an almost negligible contribution from the adsorbate (see Figure 1 below). When the electronegativity of the atom bonded to the layer increases, even if still linked through a single bond, the value of the observed spin moment is modified and eventually goes to zero.

The magnetic coupling between adsorbates has also been studied, using H and CH_3 for graphene [5] and only H for the nanotubes [6], and revealed a key dependence on the sublattice adsorption site (see Figure 2 below): Only molecules at the same sublattice stabilize a ferromagnetic spin order, with exchange coupling decaying quite slowly. When the molecules are adsorbed in different sublattices we always converge to non-magnetic solutions, at least for the supercell sizes used here. Using our previous analogy with a π-vacancy, we can now understand this behavior in terms of the so-called Lieb theorem for bipartite lattices [7]. In the case of the carbon nanotubes, exchange interactions are much larger and have a slower decay for metallic than for semiconducting tubes.

References:

[1] Elton J. G. Santos, A. Ayuela and D. Sánchez-Portal, New Journal of Physics, 12 (2010) 053012
[2] Elton J. G. Santos, D. Sánchez-Portal and A. Ayuela, Phys. Rev. B, 81 (2010) 125433
[3] Elton J. G. Santos et al. Phys. Rev. B, 78 (2008) 195420
[4] Elton J. G. Santos, S. Riikonen, D. Sánchez-Portal and A. Ayuela, arXiv:1012.3304v1.
[5] Elton J. G. Santos, A. Ayuela and D. Sánchez-Portal, submitted
[6] Elton J. G. Santos, D. Sánchez-Portal and A. Ayuela, submitted
[7] E. H. Lieb, Phys. Rev. Lett. 62, (1989) 1201

Figures:

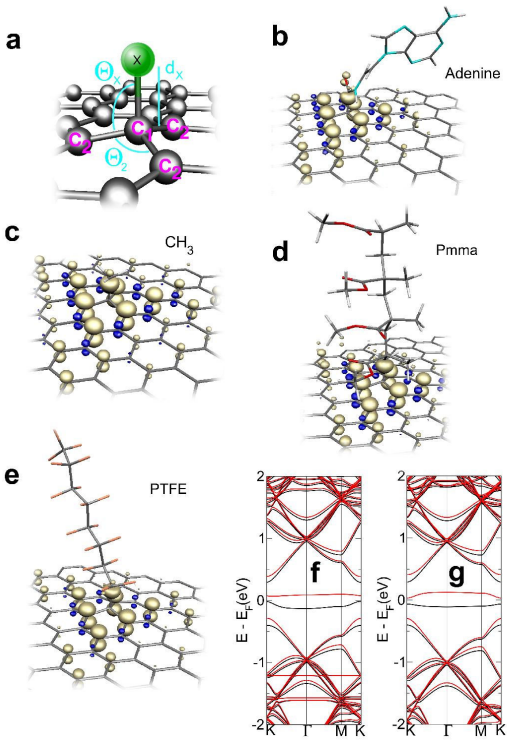

Figure 1: *(a) Scheme of the "on top" adsorption geometry, through single covalent bond to the layer, considered in this work. Panels (b)-(e) show the isosurfaces of the magnetization density induced by the adsorption of the Adenine group, CH_3, Pmma and PTFE on the carbon surface. The cutoff is at ±0.0191431 e/bohr^3. Positive and negative spin densities correspond respectively to light and dark surfaces, which alternate on graphene atoms with a slow decay length in all cases. Panels (f) and (g) show, respectively, the spin polarized band structures for a 8x8 graphene supercell with, respectively, a single Adenine radical and a CH_3 molecule chemisorbed on top of a carbon atom. The black and red lines denote the majority and minority spin bands, respectively. E_F is set to zero.*

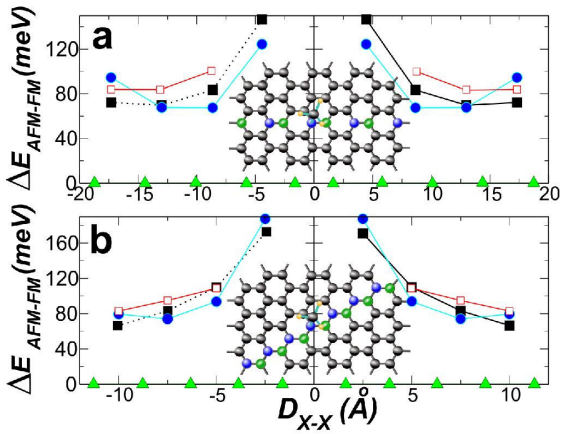

Figure 2: *Exchange coupling as a function of the position of two adsorbates, H and CH3, chemisorbed on top of a C atom in a 8x8 graphene supercell. One of the molecules is moved along (a) the armchair and (b) the zigzag directions, while the other remains at the origin. The filled and empty squares correspond, respectively, to H and CH3 at the same sublattice (e.g. AA). Triangles correspond to both adsorbates at different sublattices (e.g. AB), where it was impossible to stabilize magnetic solutions. The circles correspond to the best fit of the AA data to a Heisenberg model.*

VISUALIZATION OF CHARGE TRANSPORT THROUGH LANDAU LEVELS IN GRAPHENE

Peter Sutter,[1] George Nazin,[1] Yan Zhang,[2] Liyuan Zhang,[3] Eli Sutter[1]

[1]Center for Functional Nanomaterials, Brookhaven National Laboratory, Upton, New York 11973, USA
[2]Department of Physics, Stony Brook University, Stony Brook, New York 11794, USA
[3]Condensed Matter Physics and Materials Science Department, Brookhaven National Laboratory, Upton, New York 11973, USA
psutter@bnl.gov

Band bending and the associated spatially inhomogeneous population of Landau levels play a central role in the physics of the quantum Hall effect (QHE) by constraining the pathways for charge carrier transport and scattering. Spatially inhomogeneous charge distributions, e.g., due to adsorbate-induced surface doping, are expected to be particularly pronounced in graphene due to the proximity of the carrier gas to the surface, and can cause significant deviations from pure edge-state transport. Progress in understanding such effects in low-dimensional carrier gases in conventional semiconductors has been achieved by real-space mapping using local probes. We have recently developed spatially resolved photocurrent microscopy in the QHE regime, i.e., at variable temperature from 300 K to 4 K and at high magnetic fields, to study the correlation between the distribution of Landau levels and the macroscopic transport characteristics in graphene [1].

The conductance of typical two-terminal graphene devices (fig. 1 a) shows series of local extrema associated with individual Landau levels, with maxima predicted to occur at quantized Hall conductances of 2, 4, 6, 10, and 14 e^2/h [2]. The observed maxima are consistently higher (fig. 1 c), suggesting deviations from ideal edge transport in these devices. We find that the gate-voltage dependent photocurrent at fixed locations is oscillatory, with polarity determined by the direction of the magnetic field (fig. 1 d). Such local oscillations are due to a recurring global photocurrent distribution across the device, synchronous with the filling of consecutive Landau levels, which can be used to visualize the gate-voltage dependent distribution of Landau levels in the graphene channel.

Based on an analysis of the photocurrent generation mechanism in graphene subject to a quantizing magnetic field, we conclude that quantum Hall transport in graphene is governed by a non-uniform potential distribution across the channel (fig. 2 a). Multiple inhomogeneously filled Landau levels are populated simultaneously, with the dividing boundaries (traced in the experimental map of fig. 2 b) expected to form incompressible barriers that profoundly affect the electrostatic landscape and current pathways in the device. Besides Landau level mapping at low temperatures, we discuss the extension of photocurrent microscopy to imaging the temperature-dependent quantum Hall transport in graphene up to room temperature, and for characterizing the energy landscape across the graphene channel.

References:

[1] G. Nazin, Y. Zhang, L. Zhang, E. Sutter, and P. Sutter, Nature Physics, 6 (2010) 870.
[2] J.R. Williams, L. DiCarlo, and C.M. Marcus, Science, 317 (2007), 638.

Figures:

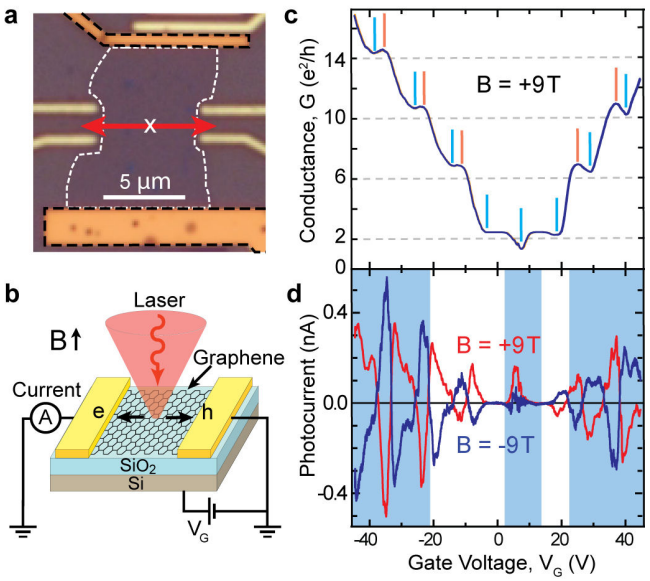

Figure 1: *Low-temperature photocurrent measurements on graphene devices. a – Optical image of a typical two-terminal device. Dashed outlines mark the channel and the two connected electrodes. b – Schematic diagram of the photocurrent measurement. c – Conventional two-terminal conductivity, G, as a function of gate voltage, V_G, measured at T = 4.2 K. Blue and red lines mark local conductivity minima and maxima. d – Photocurrent measured with laser spot at the center of the graphene channel (cross in a) for B = ±9 T.*

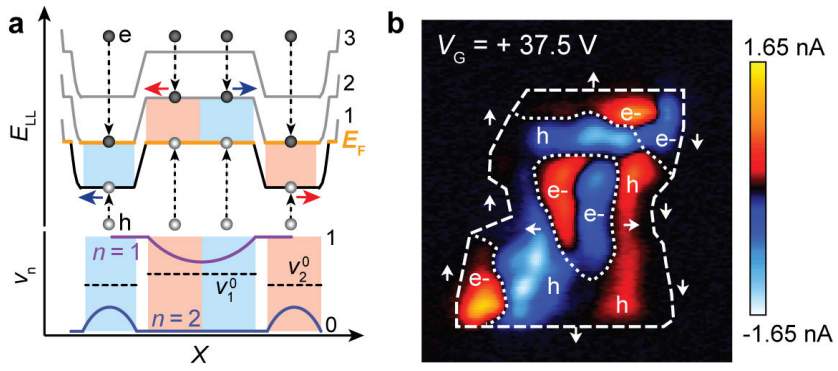

Figure 2: *Mapping photocurrent collection and the distribution of Landau levels in graphene. a – Dominant pathways of charge carrier relaxation and collection across the graphene channel (spatial dimension: X), for n-doped graphene in the case of two Landau levels (n = 1, 2) at E_F inside the channel, and local filling factors, ν_n, of these levels across the device. Colored rectangles connect the Fermi level with the Landau levels responsible for carrier transport; the color indicates the resulting photocurrent polarity. b – Experimental photocurrent map at gate voltage V_G = +37.5 V and magnetic field B = 9 T, measured on the device of fig. 1 a. The distributions of individual Landau levels at E_F, and of the incompressible boundaries between them are indicated as dotted contours.*

LARGE-SCALE ARRAYS OF SINGLE-LAYER GRAPHENE RESONATORS

Arend M. van der Zande, Robert A. Barton, Jonathan S. Alden, B. Rob Ilic, Carlos S. Ruiz-Vargas, William S. Whitney, Phi H. Q. Pham, Jiwoong Park, Jeevak M. Parpia, Harold G. Craighead, and Paul L. McEuen

Cornell University, Department of Physics, Ithaca, NY, USA
amv28@cornell.edu

Graphene's unparalleled strength, small mass per unit area, ultra-high aspect ratio, and unusual electronic properties make it an ideal candidate for nano-electro-mechanical systems (NEMS)[1,2,3,4], but the lack of control over resonance frequency and low quality factor have been major challenges to overcome.

Using graphene grown by chemical vapor deposition (CVD) on copper foils, we developed novel fabrication techniques to produce large arrays of suspended, single-layer graphene membranes on arbitrary substrates. With these fabrication methods, we produced large, high-yield arrays of both doubly-clamped graphene membranes with lengths and widths between 1 and 5 microns, and fully-clamped circular and square graphene membranes with sizes between 2 and 30 microns (See Figure).

With these membranes, we used both optical and electrical actuation and detection techniques to conduct systematic measurements of mechanical resonance as a function of size, clamping geometry, temperature, and electrostatic tensioning. We find that the CVD graphene produces tensioned, electrically-conducting, highly-tunable resonators with frequencies in the megahertz. In addition, we demonstrate that clamping the graphene membrane on all sides reduces the variation in the resonance frequency and makes the resonance frequency more predictable[5].

While doubly clamped resonators typically show quality factors of 25-150, we find that the quality factor of fully clamped membranes show a striking improvement of the membrane quality factor with increasing size[6]. At room temperature, we observe quality factors as high as 2400 ± 300 for a circular resonator 22.5 microns in diameter.

Using electrically-contacted, doubly-clamped, graphene resonators, we find the resonance frequency is tunable with both electrostatic gate voltage and temperature. In addition, the quality factors improve dramatically with cooling, reaching values up to 9000 at 10 K.

These measurements show that it is possible to produce large arrays of CVD-grown graphene resonators with reproducible properties and the same excellent electrical and mechanical properties previously reported for exfoliated graphene. In addition, we also demonstrate that the quality factor of fully clamped graphene resonators relative to their thickness are among the highest of any mechanical resonator demonstrated to date.

References:

[1] Bunch, J. S.; Van Der Zande, A. M.; Verbridge, S. S.; Frank, I. W.; Tanenbaum, D. M.; Parpia, J. M.; Craighead, H. G.; Mceuen, P. L. Science, 315, 5811 (2007) 490-493.
[2] Chen, C.; Rosenblatt, S.; Bolotin, K. I.; Kalb, W.; Kim, P.; Kymissis, I.; Stormer, H. L.; Heinz, T. F.; Hone, J. Nature Nanotech (2009) 1-7.
[3] Robinson, J. T.; Zalalutdinov, M.; Baldwin, J. W.; Snow, E. S.; Wei, Z.; Sheehan, P.; Houston, B. H. Nano Lett, 8, 10 (2008) 3441-3445.
[4] Shivaraman, S.; Barton, R. A.; Yu, X.; Alden, J.; Herman, L.; Chandrashekhar, M.; Park, J.; McEuen, P. L.; Parpia, J. M.; Craighead, H. G.; Spencer, M. G. Nano Lett, 9, 9, (2009) 3100-3105.
[5] van der Zande, A. M.; Barton, R. A.; Alden, J. S.; Ruiz-Vargas, C. S.; Whitney, W. S.; Pham, P. H. Q.; Park, J.; Parpia, J. M.; Craighead, H. G.; McEuen, P. L. Nano Letters 10, 12 (2010) 4869-4873.
[6] Barton, R. A.; Ilic B.; van der Zande, A. M.; Whitney, W. S.; McEuen, P. L.; Parpia, J. M.; Craighead, H. G. In Review

Figures:

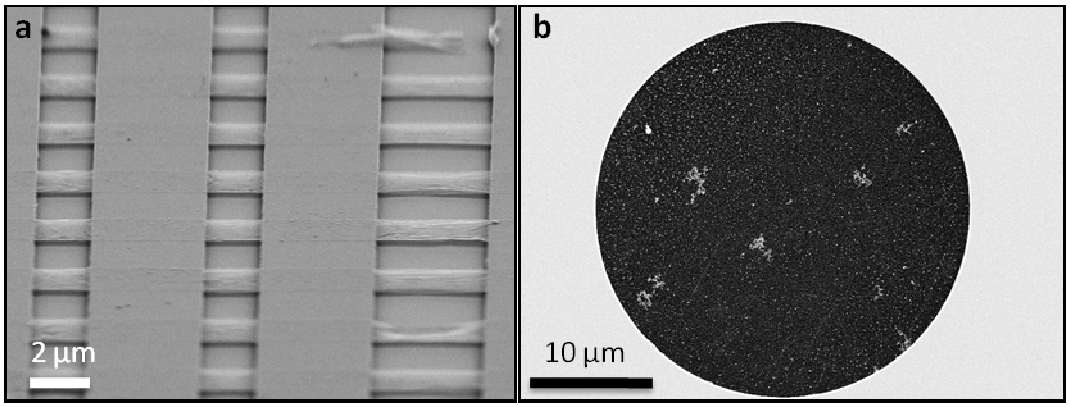

Figure 1: *a) Angled SEM of array of doubly clamped single layer graphene membranes. b) SEM of large, circularly-clamped graphene membrane. Contaminants are clearly visible on the surface.*

QUANTUM TRANSPORT PROPERTIES OF GRAPHENE NANORIBBONS AND NANOJUNCTIONS

Katsunori Wakabayashi

WPI Center for Materials Nanoarchitectonics (MANA), National Institute for Materials Science (NIMS)
Namiki 1-1, Tsukuba 305-0044, Japan
WAKABAYASHI.Katsunori@nims.go.jp

The discovery of graphene and successive fabrication of graphene devices [1,2] have triggered intensive and diverse research on carbon related systems. The honeycomb crystal structure of single layer graphene consists of two nonequivalent sublattices and results in a unique band structure for the itinerant π-electrons near the Fermi energy which behave as massless Dirac fermion. In graphene, the presence of edges can have strong implications for the spectrum of the p-electrons. In graphene nanoribbons with zigzag edges, localized states appear at the edge with energies close to the Fermi level.[3] In contrast, edge states are absent for ribbons with armchair edges. Recent experiments have succeeded to synthesize graphene nanoribbons using lithography techniques [4], chemical techniques.[5,6]

In my talk, we focus on edge and geometry effects of the electronic properties of graphene nanoribbons. The electronic states of graphene nanoribbons crucially depend on the edge orientation and boundary condition [3,7] (1) In zigzag nanoribbons, for disorder without inter-valley scattering a single perfectly conducting channel emerges associated with such a chiral mode due to edge states, i.e. the absence of the localization.[8-10] (2) In armchair nanoribbons, the single-channel transport subjected to long-ranged impurities is nearly perfectly conducting, where the backward scattering matrix elements in the lowest order vanish as a manifestation of internal phase structures of the wavefunction. [10,11] This phase structure can be related to the existence of Berry phase. [12] (3) Nano-graphene junctions are shown to have the zero-conductance anti-resonances associated with the edge states. The relation between the condition of the resonances and geometry is discussed. [13] (4) Finally, we will discuss the effect of edge chemical modification on magnetic properties of nanographene systems. [14]

References:

[1] K. S. Novoselov, A. K. Geim, S. V. Morozov, et.al., Nature, 438 (2005) 197
[2] Y. Zhang, Y.-W.Tan, H.L.Stormer, and P.Kim, Nautre, 438 (2005) 201
[3] M. Fujita, K. Wakabayashi, et.al, J. Phys. Soc. Jpn. 65 (1996) 1920.
[4] M. Y. Han, B. Oezyilmaz, Y. Zhang, and P. Kim, Phys. Rev. Lett. 98 (2007) 206805.
[5] X. Li, X. Wang, L. Zhang, S. Lee, H. Dai, Science 31, (2008) 122.
[6] J. Cai, P. Ruffieux, R. Jaafar, M. Bieri, et.al., Nature 466, (2010) 470
[7] K. Wakabayashi, K. Sasaki, T. Nakanishi, T. Enoki, Sci. Technol. Adv. Mat. 11 (2010) 054504.
[8] K. Wakabayashi, et.al., Phys. Rev. Lett. 99 (2007) 036601
[9] K. Wakabayashi, et.al., CARBON 47 (2009) 124
[10] K. Wakabayashi, New J. Phys. 11 (2009) 095016.
[11] M. Yamamoto, Y. Takane, and K. Wakabayashi, Phys. Rev. B79 (2009) 125421.
[12] K. Sasaki, K. Wakabayashi, T. Enoki, New J. Phys. 12 (2010) 083023.
[13] M. Yamamoto and K. Wakabayashi, Appl. Phys. Lett. 95 (2009) 082109.
[14] K. Wakabayashi, S. Okada et.al., J. Phys. Soc. Jpn. 79 (2010) 034706.

BOTTOM-GATED EPITAXIAL GRAPHENE ON SIC (0001)

Heiko B. Weber, Daniel Waldmann, Johannes Jobst, Florian Speck, Thomas Seyller, Michael Krieger

Lehrstuhl für Angewandte Physik, Universität Erlangen-Nürnberg,
Staudtstraße 7, 91058 Erlangen, Germany
heiko.weber@physik.uni-erlangen.de

We carry out experiments employing epitaxial graphene, fabricated by thermal decomposition on 6H SiC (0001) surfaces [1,2]. A major advantage of this material is the reproducible fabrication of large area and high-quality graphene on an insulating surface. This allows, for example for building graphene Hall bars on atomically flat substrate terraces. However, a disadvantage was so far the absence of a back gate, because the graphene is grown out of the substrate material and an intermediate insulating oxide layer is not possible.

Here we present the controlled fabrication of a bottom gate in the SiC with standard semiconductor technology [3]. A conductive layer at d = 700nm below the surface acts as gate electrode. It is created via implantation of nitrogen ions prior to the graphene growth. It is contacted to the surface with a box-like implantation of a high dose (16 different energies between 30keV and 2MeV). Hence, we define insulating layers and conducting layers by controlling the dopands. The setup is shown in Fig. 1.

A conversion of the graphene layer to quasi-freestanding epitaxial graphene turned out to be mandatory for a working device. This material is hole-filled in contrast to the electron filled standard epitaxial graphene and in magnetotransport measurements it shows the pseudo-relativistic behavior unique for graphene.

A gate voltage applied to the implanted layer enables a variation of the charge carrier density over a wide range. We, find two different regimes of gating mechanisms with strongly different gating efficiency. First for low implanted doses or low temperatures the SiC between gate electrode and surface is insulating and the device behaves like an implanted plate capacitor (IPC). Second we find a Schottky capacitor (SC) regime for high implantation doses or high temperatures. Here the SiC gains a finite conductivity and the capacitance is mainly governed by the Schottky contact between SiC and graphene. The capacitance is higher by a factor of four compared to the IPC regime and is no longer independent from the gate voltage. With this extended Schottky model we can simulate the temperature dependence of the capacitance in Fig. 2. Illumination with ultra violet light extends the SC regime to lower temperatures by generating free carriers in the SiC.

References:

[1] Emtsev et val. Nature materials 8, 203 (2009).
[2] Jobst et al. Phys. Rev. B. 81, 195434 (2010)
[3] Submitted to Nature materials

Figures:

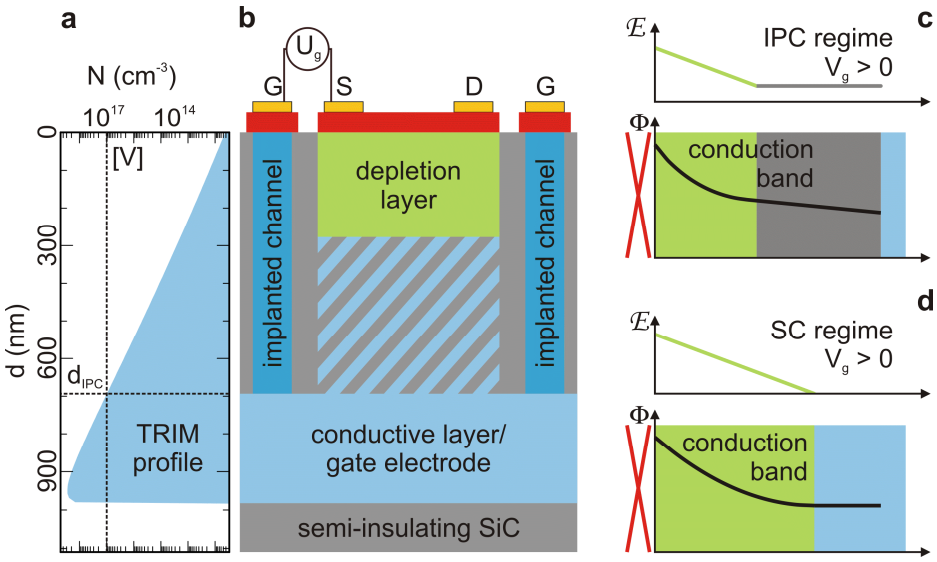

Figure 1: *a) TRIM simulation of the implantation profile. The SiC is conducting where the implanted dose exceeds the vanadium compensation [V] (dotted line) and insulating elsewhere. b) Setup of the bottom gate with source (S), drain (D) and gate (G) electrodes on graphene; conductive gate layer and implanted connections. In the IPC regime the shaded area is insulating, in the SC regime conducting c) Electric field and band diagram for the region between graphene and implanted electrode in the IPC regime, which is self-consistently calculated in our extended Schottky model. A constant external electric field is superimposed onto the built-in field of the depletion layer. d) Electric field and band diagram for the SC regime. The conductive layer extends up to the depletion layer. Hence, the whole applied voltage drops across the depletion layer.*

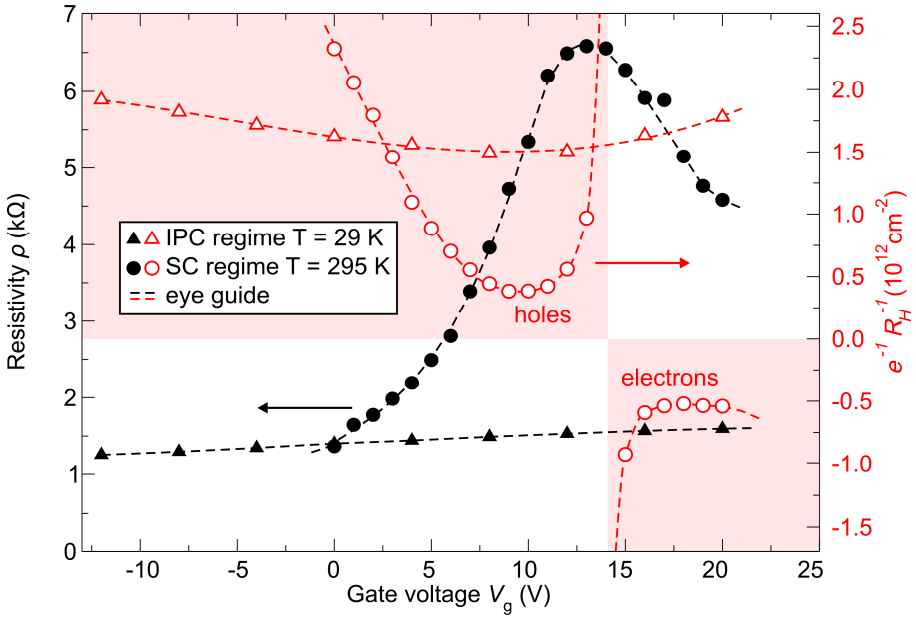

Figure 1: *Gate response of ρ and $1/eR_H$ of sample HD3 in the IPC (triangles) and the SC regime (circles). The capacitance is much higher in the SC than in the IPC regime. In addition the minimal measured charge carrier concentration $n_{min} = (1/eR_H)_{min}$ is much smaller in the SC than in the IPC regime indicating a higher homogeneity.*

MOLECULAR INTERACTIONS ON EPITAXIAL GRAPHENE

Andrew T.S. Wee, Wei Chen, Han Huang, Yuli Huang, Jiatao Sun, Xingyu Gao

Departments of Physics, National University of Singapore, 2 Science Drive 3, Singapore 117542
phyweets@nus.edu.sg

The growth of high quality epitaxial graphene will facilitate the development and commercialization of graphene nanoelectronics devices, and the main substrate-based approaches are chemical vapour deposition (CVD) on metal catalytic thin films and thermal decomposition of silicon carbide (SiC). We have performed detailed studies using in situ scanning tunnelling microscopy (STM), synchrotron photoemission (PES) and density functional theory (DFT) calculations to investigate the structure of the various reconstructions of 6H-SiC(0001) prior to its thermal decomposition to form epitaxial graphene (EG) [1-3] (Fig. 1). We show that the transition from monolayer EG to trilayer EG adopts a bottom-up growth mechanism [4], and x-ray absorption fine structure studies indicate an increase in disorder of Si atoms in the SiC substrate beneath the surface and the formation of Si clusters [5,6].

A major challenge in graphene-based devices is opening the energy band gap and doping. Molecular functionalization of graphene is one approach to modifying its electronic properties. Surface transfer doping by surface modification with appropriate molecular acceptors represents a simple and effective method to non-destructively dope graphene [7-9]. Surface transfer doping relies on charge separation at interfaces, and represents a valuable tool for the controlled and non-destructive doping of semiconductors and nanostructures at relatively low cost, thereby facilitating the development of hybrid organic-graphene nanoelectronics. Molecular self-assembly of bimolecular systems on epitaxial graphene and HOPG is demonstrated [10,11] (Fig. 2). Surface transfer hole doping of epitaxial graphene using oxide thin films is also discussed [12].

References:

[1] W. Chen, H. Xu, L. Liu, X. Y. Gao, D. C. Qi, G. W. Peng, S. C. Tan, Y. P. Feng, K. P. Loh, A. T. S. Wee, Surf. Sci. 596 (2005) 176.
[2] S. W. Poon, W. Chen, E. S. Tok, A. T. S. Wee, Appl. Phys. Lett. 92 (2008) 104102.
[3] S. W. Poon, W. Chen, E. S. Tok, A. T. S. Wee, Phys. Chem. Chem. Phys. 12 (2010) 13522.
[4] H. Huang, W. Chen, S. Chen, A. T. S. Wee, ACS Nano 2 (2008) 25.
[5] X. Y. Gao, S. Chen, T. Liu, W. Chen, A. T. S. Wee, T. Nomoto, S. Yagi, K. Soda, J. Yuhara, Phys. Rev. B 78 (2008) 201404.
[6] X. Y. Gao, S. Chen, T. Liu, W. Chen, A. T. S. Wee, T. Nomoto, S. Yagi, K. Soda, J. Yuhara, Appl. Phys. Lett. 95 (2009) 144102.
[7] W. Chen, S. Chen, D. C. Qi, X. Y. Gao, A. T. S. Wee, J. Am. Chem. Soc. 129 (2007) 10418.
[8] J. T. Sun, Y. H. Lu, W. Chen, Y. P. Feng, and A. T. S. Wee, Phys. Rev. B 81 (2010) 155403.
[9] W. Chen, D. C. Qi, X. Y. Gao, A. T. S. Wee, Prog. Surf. Sci. 84 (2009) 279-321.
[10] H. Huang, S. Chen, X. Y. Gao, W. Chen, A. T. S. Wee, ACS NANO 3 (2009) 3431-3436.
[11] Y.L. Huang, W. Chen, H. Li, J. Ma, J. Pflaum, A. T. S. Wee, Small 6 (2010) 70–75.
[12] Z.Y. Chen, I. Santoso, R. Wang, L.F. Xie, H.Y. Mao, H. Huang, Y.Z. Wang, X.Y. Gao, Z.K. Chen, D.G. Ma, A.T.S. Wee, W. Chen, Appl. Phys. Lett. 96 (2010) 213104.

Figures:

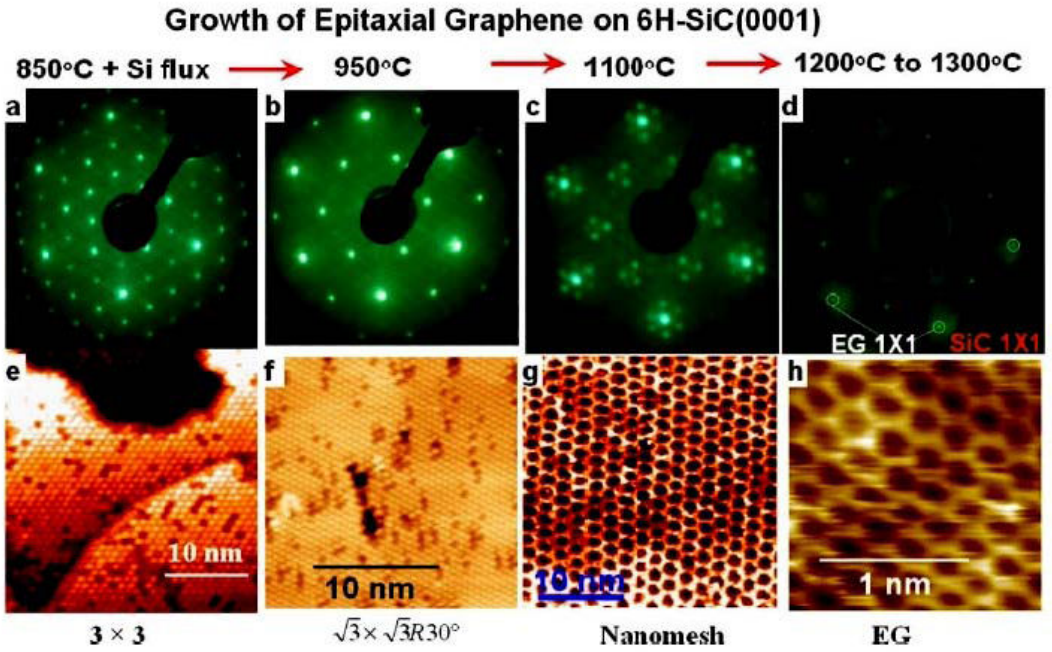

Figure 1: *LEED and corresponding STM images showing the evolution of various superstructures on 6H-SiC(0001) as a function of annealing temperature: 3×3 (panels a and e); (panels b and f); nanomesh (panels c and g); graphene (panels d and g). Incident electron beam energies (LEED) of 100 eV for panels a, b and c, and 175 eV for panel d. Adapted from Ref [9].*

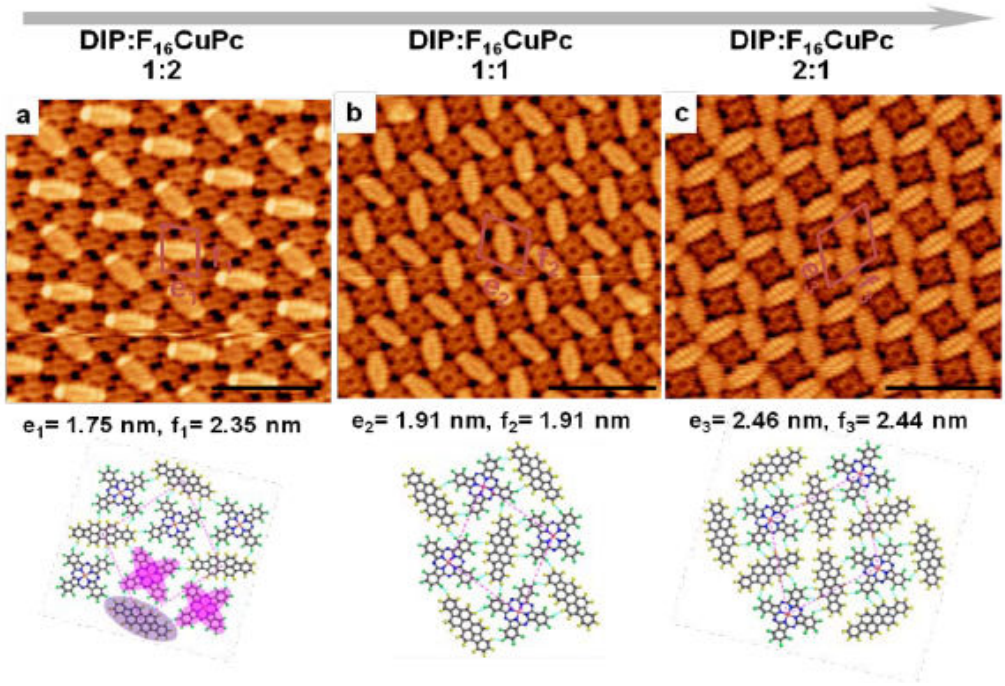

Figure 2: *Molecularly resolved 15x15 nm^2 STM images (top) and DFT simulated molecular models (below) of the F16CuPc molecular dot arrays with tunable intermolecular distance controlled by DIP molecular coverage. The scale bar in each STM image represents 5 nm. (from Ref [11])*

HALL EFFECT IN GRAPHENE NEAR THE CHARGE NEUTRALITY POINT

H. J. van Elferen[1], **S. Wiedmann[1]**, E. V. Kurganova[1], A. J. M. Giesbers[1], U. Zeitler[1], J. C. Maan[1], L. A. Ponamorenko[2], K. S. Novoselov[2], and A. K. Geim[2]

[1]Radboud University Nijmegen, Institute for Molecules and Materials, High Field Magnet Laboratory, Toernooiveld 7, 6525 ED NIJMEGEN, the Netherlands
[2]Department of Physics, University of Manchester, M13 9PL Manchester, United Kingdom
s.wiedmann@science.ru.nl

In single layer grapheme, when the carrier concentration through the charge neutrality point (CNP) is varied from hole-type to electron-type, the measured Hall resistivity ρ_{xy} close to the CNP shows a smooth zero crossing for magnetic fields up to 30 T. In contrast, ρ_{xy} diverges in a conventional semiconductor approaching the CNP from both the electron and the hole side. We explain our results in terms of a two-component carrier system where both electrons and holes with finite concentrations are present simultaneously around the CNP. The Hall resistivity is given by (supposing a similar mobility for electrons and holes) :

$$\rho_{xy} = \frac{n-p}{e(n+p)^2}B \qquad (1)$$

with n and p the charge carrier concentrations for electrons and holes, respectively, e is the electron charge and B the applied magnetic field.

Our samples are monolayer graphene devices deposit on Si/SiO_2 substrate using standard methods [1], and the charge carrier concentration is varied with a back gate from highly electron- to highly holedoped. Fig. 1(a) shows the low magnetic field data for one of our samples measured at T = 0.5 K where the Hall resistance does not yet show the quantum Hall effect (QHE). Knowing the total charge density q=n-p from the back-gate voltage, we have extracted the individual carrier concentrations n and p [Fig. 1(b)] as a function of the total charge with Eq. (1). We find that both types of charge carriers are present both above and below the CNP. For this sample, precisely at the CNP (q=0) we find $n = p = 4.2 \cdot 10^{14}$ m^{-2} only weakly dependent on the magnetic field in this non-quantized regime. Away from the CNP the system remains two-component and the minority carriers only disappear for $|q| > 2 \cdot 10^{15}$ m^{-2}.

When we increase the magnetic field into the quantum Hall regime at T = 4.0 K [2, 3] [Fig. 2(a)], we still observe a zero-crossing of ρ_{xy} and at the CNP in Fig. 2(b), we find that both n and p are present but their number increases with the magnetic field. Plotting charge carrier concentration as a function of *B*, n is found to be constant for $B < 5$ T after which it increases linearly as *B* increases. This behavior is attributed to transport dominated by electron-hole puddles for low magnetic fields evolving into a quantized density of states in high magnetic fields [4].

The observed presence of both electrons and holes near the CNP even deep into the quantized Hall regime may contribute to a better understanding of the nature of electronic states at the lowest Landau level in graphene [5]. In particular, in high magnetic fields it allows to distinguish between different splitting scenarios of the lowest Landau level: valley first where electrons and holes are separated and the Hall resistance is expected to diverge at the CNP, and spin-first where electrons and holes remain present above and below zero-energy and the Hall resistance crosses zero at the CNP [6].

References:

[1] A. K. Geim and K. S. Novoselov, Nat. Mater. 6 (2007) 183.
[2] K. S. Novoselov, A. K. Geim, S. V. Morozov, D. Jiang, M. I. Katsnelson, I. V. Grigorieva, S. V. Dubonos, and A. A. Firsov, Nature (London) 438 (2005) 197.
[3] Y. Zhang, Y. Tan, H. L. Stormer, and P. Kim, Nature (London) 438 (2005) 201.
[4] J. Martin, N. Akerman, G. Ulbricht, T. Lohmann, J. H. Smet, K. von Klitzing, A. Yacobi, Nat. Phys. 4, (2008) 144.
[5] S. Das Sarma and K. Yang, Solid State Commun. 149 (2009) 1502.
[6] A. J. M Giesbers *et al.*, Phys. Rev B 80 (2009) 201403(R).

Figures:

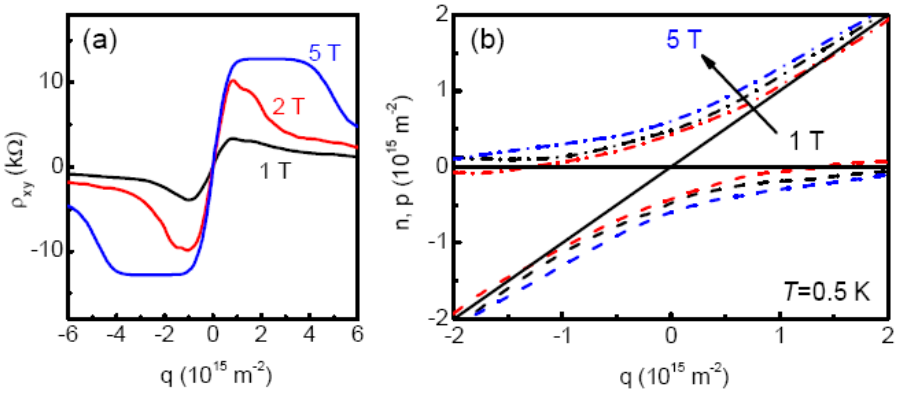

Figure 1: *(a) Low-field Hall resistivity and (b) extracted carrier concentration for electrons n and holes p according to Eq. (1) as a function of total charge q. Both types of charge carriers are present below and above the CNP for $|q| < 2 \cdot 10^{15}$ m^{-2}.*

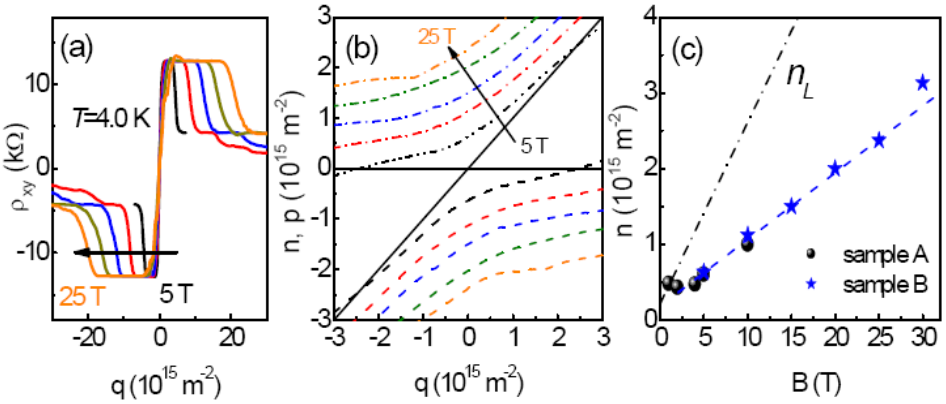

Figure 2: *(a) High-field Hall resistivity in the quantum Hall regime; (b) Extracted carrier concentration for electrons n and holes p according to Eq. (1) as a function of the total charge q; (c) Charge carrier concentration increases with B due to a quantized density of states. Most carriers are localized in the tails of the Landau level and only about 1/3 of the total carrier concentration is measured as free charge carriers.*

EDGE TRANSPORT CHANNEL ON A GRAPHENE NANORIBBON

Sungjong Woo, Young-Woo Son

KIAS Hoegiro 87, Dongdaemun-gu, Seoul 130-722, Korea
nl sjwoo@kias.re.kr

Recently, Scanning Gate Microscopy (SGM) experiment on a graphene nanoribbon by our collaborators has shown a clear evidence of the existence of an edge electronic transport channel; a remarkable SGM signal enhancement has been observed on the ribbon edge.
Charge accumulation on the edge of doped graphene nanoribbons has been studied by Silvestrov et.al.

For such a doped graphene nanoribbon, the effective local Dirac point deviates from the Fermi level depending on the local excess charge density, which is almost constant except the ribbon edge where charge is seriously accumulated.

We have investigated the electronic band structures and transport properties of such doped nanoribbons especially with zigzag edge structures and have further studied their responses to an additional local gate potential given by the SGM tip.
We have found that, once a graphene is doped, the energies of localized edge states of a zigzag graphene nanoribbon, which give a flat band for a neutral one, follow the shifted local Dirac point on the edge bending the corresponding flat band line.

Based on this, we have further showed that one can control the bent edge-state band line using SGM tip gating resulting in single-channel conductance enhancement that was seen in the expriment.
Our theory predicts that such conductance enhancement occurs when the polarity of the local tip potential is against the type of doping which is in good agreement with the experimental results. We have further confirmed that the phenomena persists on general edge structurs.

PROBING THE BANDGAP OF BILAYER GRAPHENE WITH THERMAL AND OPTICAL EXCITATIONS

J. Yan[1], M.-H. Kim[1], G.S. Jenkins[1], A.B. Sushkov[1], D.C. Schmadel[1], J. Melngailis[2], H.D. Drew[1] and M.S. Fuhrer[1]

[1]Center for Nanophysics and Advanced Materials
[2]Department of Electrical and Computer Engineering
University of Maryland, College Park, MD 20742, USA
juny@umd.edu

The opening of a tunable bandgap in bilayer graphene is an interesting problem that has attracted great recent attention. We study the bulk of dual-gated bilayer graphene using a Corbino-disk geometry which excludes the edge conductance channels. The temperature dependence of the maximum resistivity is found to be well described by simple thermal activation at high temperatures and variable range hopping at low temperatures, consistent with other transport studies, from which we conclude that edge transport is not significant [1]. The electric-field-dependent band gap extracted from thermal activation is found to be in good agreement with infrared spectroscopic studies [2, 3]. We further investigate the band gap effect by infrared photoconduction measurements in non-Corbino dual-gated devices. We have measured the photoconductive response as a function of band gap, temperature, incident wavelength, and power. We find that the response is proportional to the source-drain current and that it increases for larger band gap. Interestingly, the signal does not always vanish at zero source-drain voltage and it exists even when the average electric field is zero, corresponding to zero band gap in a disorder-free sample.

References:

[1] J. Yan and M. S. Fuhrer, Nano Lett. 10 (2010) 4521.
[2] Y. Zhang et al., Nature 459 (2009) 820.
[3] K. F. Mak et al., Phys. Rev. Lett. 102 (2009) 256405.

Figures:

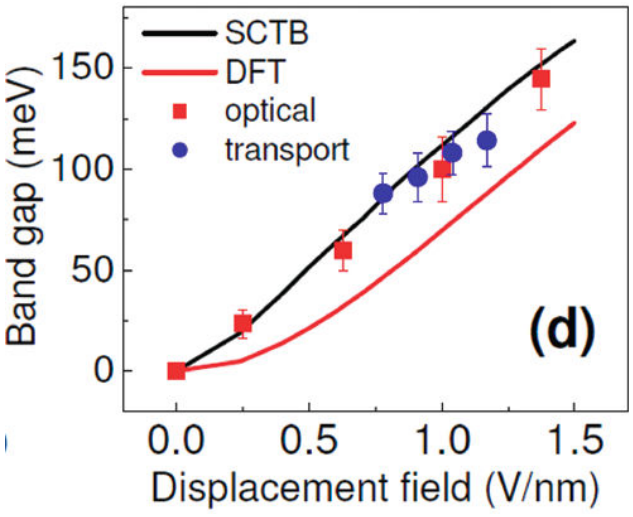

Figure 1: *Bandgap of dual-gated bilayer-graphene Corbino-disk. Transport measurements (blue dots) are from Ref.[1]. Optical data (red squares) and self consistent tight binding (SCTB) as well as density functional theory (DFT) calculations are taken from Ref.[2].*